5-2014

Increasing the Throughput of Liquid Chromatography

Joseph John Stankovich
University of Tennessee - Knoxville, jstankov@utk.edu

To the Graduate Council:

I am submitting herewith a dissertation written by Joseph John Stankovich entitled "Increasing the Throughput of Liquid Chromatography." I have examined the final electronic copy of this dissertation for form and content and recommend that it be accepted in partial fulfillment of the requirements for the degree of Doctor of Philosophy, with a major in Chemistry.

Georges A. Guiochon, Major Professor

We have read this dissertation and recommend its acceptance:

Michael J. Sepaniak, Sheng Dai, Robert N. Compton

Accepted for the Council:
Dixie L. Thompson

Vice Provost and Dean of the Graduate School

(Original signatures are on file with official student records.)

Increasing the Throughput of Liquid Chromatography

A Dissertation Presented for the
Doctor of Philosophy
Degree
The University of Tennessee, Knoxville

Joseph John Stankovich
May 2014

ACKNOWLEDGEMENTS

I want to start by thanking family: Joseph J. Stankovich Sr., Ana J. Stankovich, Joseph C. Stankovich, Edna Stankovich, Mary Sila, and Katie Stankovich for their support through years of schooling have made my education possible. They have been patient and generous and have shown me nothing but love throughout all the years of my life. I love you all greatly.

I also want to send my sincerest thanks to Dr. Georges Guiochon for accepting me as a student and teaching me how to compose proper scientific publications. Everything we wrote together was accepted into peer reviewed journals with relatively minor revisions. He has taught me that the human will can overcome all obstacles that life throws at you. Together with his wife, Lois Beaver, we traveled to many countries and they gave me opportunities that I would not have had otherwise. They both provided me emotional support when life gave me unexpected hardships.

I want to thank all my friends and colleagues who were there for me through some of the most difficult times of my life. The list includes Mark J. Schocke and his wife Amanda, Fabrice G. Gritti, Paul G. Stevenson, Peter Vajda and his wife Martina, Abjiht Tarafada and his wife Raqui, and Matthew J. Walworth. They all provided me guidance and emotional support throughout my graduate career.

I want to express my gratitude to my graduate committee: Dr. Michael J Sepaniak, Dr. Robert N. Compton, and Dr. Sheng Dai for their guidance through all the stages of my candidacy. They have all shown me true professionalism and have taught me how to improve my writing. UT personnel who helped me, including Mrs. Cathy Haggerty, and Mr. Gary Wynn who worked with me on prototyping two instruments; and Mr. William Gurley who helped out lab many times with computer issues.

Also a special thanks to Phenomenex, Agilent Technologies, and Waters Corporation; companies that provided our group with the instrumentation and the majority of the supplies we used to conduct our research.

ABSTRACT

In this manuscript the ramifications of operating very high pressure chromatographic (VHPLC) instruments at high linear velocities is discussed. Operating at higher inlet pressures causes thermal conditions inside the column to change to an extent that can alter the reproducibility and accuracy of the chromatograms produced. The experiments discussed in this dissertation were focused on the manner in which the mobile phase is eluted through the column; by either constant flow, constant pressure, operator controlled or programmed constant pressure, and conditions which keep the heat loss at the columns wall constant. Additional experiments included other practical considerations in system performance such as void spaces created from improper column connections. The results of these experiments showed that void volumes can be the leading cause of band dispersion. The metric used for all measurements were based on moment analysis, which provides a more rigorous analysis of chromatographic performance than the metrics used by the majority of the community.

TABLE OF CONTENTS

LIST OF TABLES

LIST OF FIGURES

Nomenclature

Roman Letters

Dm	bulk diffusion coefficient (m^2/s)
dp	average particle size (m)
Dp	average mesopore size (m)
$Fv(t)$	flow rate imposed to the column at the time t (m^3/s)
$Fv(tS)$	flow rate after the analyte has spent a time tS in the stationary phase
Fv,I	initial flow rate in the constant pressure gradient mode (m^3/s)
Fv,F	final flow rate in the constant pressure gradient mode (m^3/s)
F^*v	constant flow rate in the constant flow gradient mode (m^3/s)
$F(\lambda m)$	hindrance diffusion factor
$g(tS)$	function expressing the mobile phase composition as a function of the time tS
h	reduced plate height
H	column HETP (m)
$H(tS)$	local plate height after the analyte has spent a time tS in the stationary phase (m)
$k(t)$	retention factor of the analyte when it leaves the column at the time t
ki	retention factor of compound i
k_0	LSSM retention factor in pure water
k_1	zone retention factor
$k_{0,}I$	LSSM retention factor of compound i in pure water
K_0	specific permeability (m^2)
L	column length (m)
N	number of analytes in the sample mixture
P^0	atmospheric pressure (Pa)
P	local pressure (Pa)
PI	initial column inlet pressure in the constant flow gradient mode (Pa)

PI	final column inlet pressure in the constant flow gradient mode (Pa)
P^*	constant pressure in cP gradient mode (Pa)
Pc	peak capacity
Pc,exp	experimental peak capacity
Pf	heat power friction (W/m)
rc	column inner radius (m)
t	time variable (s)
ti	elution time of compound i (s)
t_0	hold-up column time (s)
tS	time spent by the analyte in the stationary phase (s)
tD	dwell time (s)
tF	gradient elution time of the most retained compound (s)
tG	gradient time (s)
S	slope of the LSSM plot
u	interstitial linear velocity (m/s)
V	total eluent volume delivered by the pumps (m^3)
V_0	column hold-up volume (m^3)

Greek Letters

αorg	empirical parameter in Eq. (5.4)
αw	empirical parameter in Eq. (5.4)
βv	linear gradient slope in volume unit (m^{-3})
βt	linear gradient slope in time unit (s^{-1})
εt	total porosity
εe	external porosity
εp	internal porosity for small molecules
$\varepsilon *p$	internal porosity for partially excluded molecules
γe	external obstruction factor
$\gamma *p$	internal obstruction factor for partially excluded molecules
λm	ratio of the analyte size to the average mesopore size

φ	volume fraction of the strong eluent in the mobile phase
φI	volume fraction of the strong eluent at the beginning of the gradient
φF	volume fraction of the strong eluent at the end of the gradient
μ_2'	second central time moment (s^2)
η	eluent viscosity of the mixture (Pa s)
ηorg	viscosity of the organic eluent (Pa s)
ηw	viscosity of water (Pa s)
Ω	ratio of the sample diffusivity across the particle to that in the bulk
$\omega_{1/2,}I$	half-height peak width of peak *i* (s)
v	reduced interstitial velocity
ξorg	empirical parameter in Eq. (5.4) (Pa^{-1})

CHAPTER I
Introduction and General Information

Liquid chromatography (LC) has been one the most utilized techniques for analyzing complex mixtures. LC involves the separation of chemicals dissolved in a liquid mobile phase. The mobile phase is percolated by means of a pump through a column which is packed with a bed of fine particles, known as the stationary phase. The compounds in the sample adsorb to the stationary phase and are retained with respect to the bulk. The compounds which are less strongly absorbed to the stationary phase are eluted through the column first.

Separation speed can be increased without changing the flow rate of mobile phase. The particle size can be decreased and shorter columns can be used. The drawback of doing this is that the inlet pressure increases when particle size is decreased. At pressures above 400 bar and flow rates exceeding 1.5 mL/min the friction of the mobile phase passing through the bed generates enough heat to effect the separation. The pumps on high pressure instruments also require more maintenance than the instruments of the 1980's and 1990's which operated at pressures less than 400 bar. The pumps seals tend to break down at higher pressures and require service every 6-12 months depending on use.

The heat produced by friction can alter the retention times and UV detector responses of analytes in Very High Pressure Liquid Chromatography (VHPLC). The primary focus of this manuscript is strategies for achieving rapid separations using liquid chromatography in situations where frictional heating occurs. Experimental approaches were used to assess the reproducibility of the chromatograms. Constant pressure based methods and methods which should theoretically produce a constant heat power at the column's wall were also examined here.

Since the speed limitations of linear chromatographic systems are quickly being realized by the community, there is also a discussion of possible alternatives for rapid multidimensional chromatography instruments in this manuscript. Currently the difficulties in their design and construction have hindered our efforts in producing a functional model. However they are a viable possibility provided that certain engineering obstacles can be overcome.

CHAPTER II
ORIGINS OF ANALYTICAL SEPARATIONS

The first publication involving the separation of mixtures was written in 1850 by Friedlieb Runge. His publications involved the separation of color dyes by spotting a substantial volume on paper and observing the resultant pattern. Runge noted that it was “Due to the power of its (the paper’s) hollow hairs, it was capable of separating drops of liquid into component parts according to their individual fluidity [1]. Runge was perhaps the first investigator in the separation field who used stationary phases. Runge was followed by Goppelsröder, who was the first to demonstrate the use of paper thin layer chromatography (TLC), although it was not referred as TLC in his publications. Figure 2.1 is a drawing from one of Goppelsröder’s publication. Importantly he identified the need for different solvent systems to be used as mobile phases to improve the separations. Planar surface separations preceded column separations.

In 1903 Mikhail Tswett, a botanist, published the first article on the topic of column chromatography [2]. He used a column packed with calcium carbonate to separate plant pigments, and named his technique chromatography since “chromate” means color in Greek and also means “Tswett” in Russian [2]. Over 100 years after the advent of column chromatography, biologists and analytical chemists still predominantly use linear methods of separating biological components. Substantial advances have been made in the liquid chromatography (LC) field, but the basic principal of eluting analytes through a one dimensional column is still employed. The greatest advances in liquid column chromatography were those made by the incorporation of a pressurized mobile phase and improving the stationary phases in packed columns.

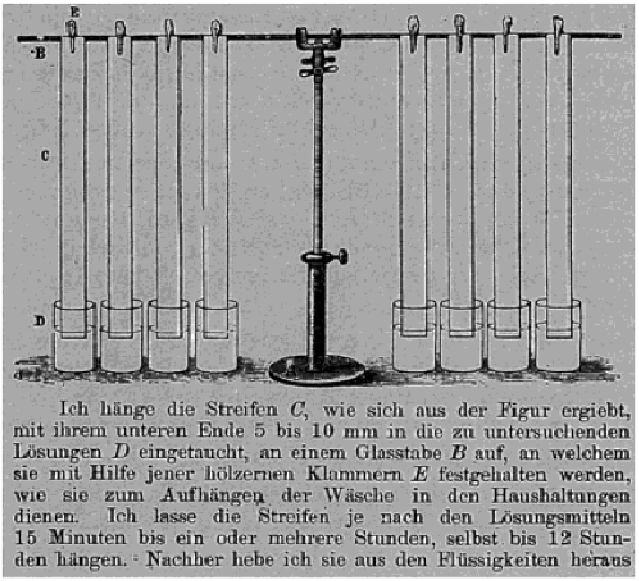

Ich hänge die Streifen *C*, wie sich aus der Figur ergiebt, mit ihrem unteren Ende 5 bis 10 mm in die zu untersuchenden Lösungen *D* eingetaucht, an einem Glasstabe *B* auf, an welchem sie mit Hilfe jener hölzernen Klammern *E* festgehalten werden, wie sie zum Aufhängen der Wäsche in den Haushaltungen dienen. Ich lasse die Streifen je nach den Lösungsmitteln 15 Minuten bis ein oder mehrere Stunden, selbst bis 12 Stunden hängen. Nachher hebe ich sie aus den Flüssigkeiten heraus

Figure 2.1. Goppelsröder's Diagram. The first use of paper separations. Reproduced from reference [2].

CHAPTER III
MODERN LIQUID SEPARATIONS

The first investigator in HPLC was Csava Horvath. His research in 1967, involved the use of packed ion exchange columns using coated glass beads of approximately 50 microns with column dimensions 0.4mm x 85mm. His HPLC was capable of running gradient elution separations using UV detection with solvent pressures as high as 275 bar. The optimum flow rate for his capillary column was found to be 0.4 mL/min at 75 bar [3]. Horvath's initial separations took 40-90 minutes to complete; this was due to the column and packing material used. Horvath's work was the impetus for most of the coming advancements in column chromatography, with many such advancements coming out of his lab. Using a pump to pressurize a separation allowed for the development of smaller particles and shorter columns to be used for HPLC.

The earliest particles used in chromatography had diameters on the order of 50 microns and were non-porous [4]. By today's standards these sizes are gigantic, but large particles were necessary so that pressure tolerances of early systems were not exceeded. As pumping technology improved, 10 μm particles had widespread use in addition to the incorporation of porous particles in columns [4]. Using porous particles greatly increased the surface area of stationary phases and resulted in increased efficiency's for columns. Eventually particle sizes proceeded down to the sub 2 micron level, however the pressures required for obtaining optimum flow rates for these columns often exceeded 1000 bar [4]. These tremendously high pressures led researches to coin the term ultra-high pressure liquid chromatography (UPLC or UHPLC). It should be noted that these high pressures also cause significant thermal gradients from the friction of the mobile phase flowing through the dense stationary phase, which is a major difficulty in the field.6 Another challenge became packing the columns so that there was minimal void volumes in the stationary phases. The process of how

columns are packed is often left out of more modern publications, due to the commercialization of column manufacturing. Importantly the analysis times and plate heights achieved by the sub 2 micron columns were improved by over 1 order of magnitude from the 10 micron particle columns [4].

In 1999, monolithic silica columns were commercialized [5]. Monolithic columns were unique due to the column being a solid piece of silica with both macropores (large through-pores approximately 2 µm) and mesopores (smaller interparticle pores of 130 Å) [5]. The substantial advantage of these columns was the low pressures they required to obtain optimal flow rates. Additionally the total surface area of these columns was not far from those of packed fully porous fine particle columns [4]. The greatest challenges in their production are ensuring that the monolith is highly homogeneous and that the monolithic rod is properly clad to the column wall. If the column in not highly homogeneous or well clad, there will be regions of higher flow velocity in the stationary phase relative to the rest of the column [4]. It has become a fairly well-known fact that the cladding processing appears to be the biggest challenge when preparing a monolithic column; void spaces along the wall of the monolith and column are difficult to eliminate. These regions of radial heterogeneity will ultimately increase band broadening and lower the column's efficiency. Also, pressure tolerances of these columns cannot be exceeded or the monolith will become irreparably damaged [4].

Some critical parameters, which are injection and detection based, are those associated with band broadening due to extra column contributions. Generally, smaller volumes of connective tubing used in HPLC and UPLC instruments reduce the band broadening effect. Importantly, the peak variance is the sum of all variance contributions, and include those contributions experienced in the column, the detector flow cell, the data acquisition rate of the detector, and the contributions caused from outlet column tubing [6]. These extra-column effects,

when using larger volume columns, are usually not substantial in relation to the sum of the terms of the peak variance. However, extra column effects with very small columns start to be the largest contribution to the total peak variance observed [6]. In any case, extra-column contributions should always be monitored to ensure the best possible instrument performance.

3.1 Detection in VHPLC

There have been numerous detection systems used in conjunction with liquid phase separations. Detectors such as ultra violet (UV) absorbance, refractive index light scattering, flowmetry, fluorescence detection, mass spectrometry (MS), and nuclear magnetic resonance (NMR) have all been coupled to liquid chromatography. The most common detector is the UV detector, since it is quantitative and relatively inexpensive to purchase and maintain. MS detection is also a popular detector, but quantitation can sometimes be difficult.

The UV detector measures the absorbance of analytes in the mobile phase after they are eluted from the column. The concentration of analytes can be determined based on the Beer-Lambert law.

$$A = \varepsilon * \mathrm{b} * \mathrm{c} \qquad \text{Eq. (3.1)}$$

Where A is the absorbance of the sample in miliabsorbance units (mAU), B is the path length the light travels through the cell in centimeters, and C is the concentration of the sample in mol L^{-1}, and ε is the molar extinction coefficient in L mol^{-1} cm^{-1}. The detector is quantitative generally from micromolar to low milimolar concentrations (which is dependent on the molar extinction coefficients of the analytes in the sample). The detector is susceptible to matrix effects from the mobile phase in addition to co-eluting compounds. Also the temperature of the sample can effect absorbance, as is discussed in following sections [7].

3.2 Modes of chromatography

There are numerous retention mechanisms in modern liquid chromatography. These mechanisms include entropic and adsorption based methods. For this manuscript reversed phase liquid chromatography (the most commonly used mode of liquid chromatography) is discussed. The other modes of liquid chromatography include normal phase, hydrophilic-interaction, hydrophobic-interaction, size exclusion, and ion exchange.

Normal phase liquid chromatography (NPLC) uses a polar stationary phase to and non-polar mobile phase to separate samples. Non-polar compounds elute first. The first columns used by Tswett fall into this category as he used calcium carbonate as his stationary phase. Generally nonaqueous mobile phases are used.

Reversed phase liquid chromatography (RPLC) uses a non-polar stationary phase and a polar mobile phase to separate samples. Polar compounds elute first. This has become the most common form of chromatography, because it provides robust separations and less hazardous solvent systems with respect to normal phase solvent systems.

Hydrophilic-interaction chromatography (HILIC) uses a similar retention mechanism to NPLC. In HILIC, mixtures of water and aprotic solvents are generally used. Water competes with the polar analytes for binding sites on the stationary phase and are eluted based on their hydrophilicity.

Hydrophobic-interaction chromatography (HIC) uses a similar mechanism to RPLC but is more suited to larger biomolecules using a salt gradient starting from a high salt concentration to a lower salt concentration. Generally a modified silica stationary phase is used, as the salt concentration is reduced analytes bind less strongly to the stationary phase and are facilitates the elution of the biomolecules

from the stationary phase.

Ion-exchange chromatography (IEC) uses ionic interactions from the analytes to bind them to the stationary phase. The stationary phase consists of either an anionic or cationically modified surface (generally silica based). Analytes are retained by forming ionic bonds to the stationary phase, as the solvent system becomes increasingly acidic or basic, depending on the charge of the stationary phase, analytes are eluted with weaker charged molecules being eluted before those of strongly changed analytes with opposite charges to the stationary phase. Neutral species and compounds with the same charge of the stationary phase are not retained.

Size-exclusion chromatography (SEC) is based on the principal of retaining analytes which are detained in the pours of a stationary phase. Larger molecules which cannot fit inside the pores of the stationary phase are eluted first. This is a mechanical separation rather than a chemical based separation method.

3.3 Metrics for analyzing separations (moment analysis)

The width of chromatographic bands (peaks) is characterized by the band variance (σ^2). The peaks in a chromatogram generally follow a Gaussian distribution where the peak encompasses 4σ. The variance relates to the perturbation caused to the eluted band by the instrument used to record and measure it. Columns cannot be used without an instrument. The considerable progress made these last ten years in column technology has resulted in the elution of narrower peaks having smaller variances, due to the use of finer particles and to the development of better packing methods, the column efficiency (*N*) is related to the variance of eluted bands. The general equation for column efficiency is shown below. Where t_r is the retention time and w is the peak width and is shown in Eq. (3.2).

$$N = 16 \left(\frac{t_r}{w}\right)^2 \qquad \text{Eq. (3.2)}$$

The accurate measurement of this characteristic is necessary to understand the relative contributions of the band broadening during analyte migration along the column and of the band broadening during its transit through the UPLC system. This transit includes the migration from the injection device to the column and from the column to the detector, including the detector cell.

Taking into account that separation performance has improved dramatically over the last decade, more rigorous metrics should be used for the assessment of chromatographic separations. The method used in the Guiochon Group is moment analysis. First, we present a brief summary of moment analysis, describe the moments up to the second one. In the following expressions, $C(t)$ is the record of the detector signal. In principle, it extends from $t = 0$ to infinity but for practical reasons, it must be limited to a finite time window of the order of a few SDs of the peak [8-9].

The zeroth moment (peak area)

In chromatography, the 0th order moment relates to the area underneath the band. It can be calculated by the following equation Eq. (3.3).

$$\mu_0 = \int_{t_0}^{t_f} C(t)dt \qquad \text{Eq. (3.3)}$$

Where μ_0 is the area underneath the band, t_0 is the time when integration is started, t_f is the time when integration is ended, and $C(t)$ is the function that corresponds to the absorbency of the band at time t. Experimentally $C(t)$ is comprised of the data points acquired by the detector. The starting and stopping

points of the integration should be chosen cautiously, so that the entirety of statistically relevant data is observed. It should be noted that errors in t_0 and t_f lead to increasingly large errors in higher moments [8-9].

The first moment (peak retention time)

The first moment relates to the average retention time of the analyte molecules comprising the peak. This moment (μ_1) is provided by Eq. (3.4).

$$\mu_1 = \frac{\int_{t_0}^{t_f} C(t) \times t \, dt}{\int_{t_0}^{t_f} C(t) \, dt} \qquad \text{Eq. (3.4)}$$

The first moment is a time but it is generally not the elution time of the apex of the peak, because the elution profiles of chromatographic bands are rarely symmetrical. Generally the first moment comes later than the apex because chromatographic peaks tend to tail.

The second central moment (peak variance)

The second central moment, μ_2 relates to the standard deviation (SD) of the retention time of the molecules of analyte in the eluted band and is shown in Eq. (3.5).

$$\mu_2 = \frac{\int_{t_0}^{t_f} C(t) \times (t - \mu_1) \, dt}{\int_{t_0}^{t_f} C(t) \, dt} \qquad \text{Eq. (3.5)}$$

The second central moment as expressed in Eq. (3.5) gives a result with units of seconds squared or minutes squared. However, since the flow rate had to be increased to study how the second central moment changes with the flow rate,

we expressed it in terms of μ_2, i.e., in volume squared. The conversion was done by multiplying μ_2 by the square of the flow rate used in the respective experiment.

Band variance is the only accurate way to measure band broadening [8]. It might be less precise than the result of the classical method of taking the peak width at half-height but it provides much higher accuracy. The classical method assumes that peak profiles are Gaussian, which is incorrect and, for this reason, most often provides wrong values. The variance derived from the second moment provides a good basis for comparison between different columns or the performance of one column under different conditions. Equation (3.5) yields the net variance of the band [9]. It is used to determine the true column efficiency when the contribution of band broadening due to the extra column volumes are taken into account.

In this manuscript the band variances were calculated from the digital records of the chromatograms using a program written in house, with Wolfram Mathematica 7 (Champaign, IL, USA) [8]. The program calculates the zeroth, first, and the second central moments using integration starting and stopping points that are user defined. The choice of relevant starting (t_0) and end points (t_f) of integration is critical for an accurate calculation of the second central moment [8,10-11]. We made every effort to encompass the entirety of statistically relevant data from the injections of uracil. The starting point is not difficult to define since peaks of nonretained compounds do not generally exhibit a high degree of asymmetry toward the front of the peak (fronting). The end points of integration were set to times corresponding to 5.5 peak widths at half-height away from the integration starting point. These parameters set the starting and ending points of integration sufficiently close to the baseline for most peaks, but in a few cases the bounds need to be shifted to account for the integration of the fronting or tailing sides of bands. The bounds of integration were then chosen by visual inspection from the

first chromatogram of each series. The goal was to start integration when the S/N of the peak baseline was approximately 250. We tried to code the program to automatically start and end the integration at a S/N of 250; however, this proved to provide only a poor reproducibility in practice since the baseline noise-level fluctuates significantly from chromatogram to chromatogram. The most reproducible method that we found was to set the integration window at 5.5 times the peaks width with manual adjustments to correct for any anomalies. Once the bounds were chosen for the first chromatogram in the series, the same constraints were used for the analysis of all replicate chromatograms to ensure that a relevant comparison could be made. It is also important to note that this method only works for peaks that are completely baseline resolved.

Several different phenomena contribute to the band variance. Besides the contributions to band variance originating inside the column and related to the chromatographic process, they include the injection process, the channels available to the transfer of the injected band to the column, then from the column exit to the detector flow cell (d.f.c), and this cell itself. All these parts used for the band transfer have to be connected and each one of these connections may bring its own contribution to the band variance. Other factors may also play a role in band broadening, like flow perturbations due to the operation of the pump or the presence of small bubbles of air in the mobile phase stream. These variance contributions are additive for all analytes whether they are retained or nonretained as long as the instrument operates under linear conditions. The most significant of these contributions are listed in the following Eq. (3.6).

$$\mu_2' = \sigma^2 = \sigma^2_{\text{injector}} + \sigma^2_{\text{channels}} + \sigma^2_{\text{column}} + \sigma^2_{\text{d.f.c}} + \sigma^2_{\text{connections}} + \sigma^2_{\text{others}} \qquad \text{Eq. (3.6)}$$

CHAPTER IV
BAND BROADENING

4.1 Band Broadening Due to Improper Column Connections

Eluted peaks in modern VHPLC instruments are narrower than those produced by HPLC instruments. The consequence of using very efficient short columns is that the instrument's contribution to band broadening (i.e. the extent in which the instrument broadens the peak) becomes a larger factor in dictating the peaks width than the column itself.

Voids or gaps in column connections create stagnant zones not flushed by the eluent stream. When an analyte band passes by these zones, a portion of the analyte molecules enters the stagnant zone, their velocities are slowed down or stopped. In these zones, the migration of molecules is governed by diffusion, which is not a fast mechanism but is controlled by the concentration gradient. Solute molecules enter when the band concentration increases and becomes high; when they leave, the axial concentration gradient along the column decreases, concentrations become low and their movement out of the void areas slows down, causing the band broadening, tailing, and peak asymmetry often observed. When short narrow-bore columns, generally preferred for providing short analysis times [4], are used, these void volumes contribute relatively more to band broadening than they do for longer wide-bore columns. The variance contributions from poor connections may be less noticeable for long, wide-bore columns because band broadening across the column becomes the largest contributor to band dispersion. Nevertheless, this broadening reduces peak height and separation resolution. For dilute analytes in the mobile phase, this signal reduction can lead to quantitation and detection problems. The presence of void volumes in connections decreases column performance in both liquid and gas chromatography [4,12-14]. Figure 4.1 illustrates where voids (Figure 4.1, marker (3)) can arise in column connections. Figure 4.1A shows how the

capillary tube in the Thermo Nanoviper connection is compressed against the column inlet. The metal capillary has a polyether ether ketone (PEEK) washer (Fig. 4.1 marker (1)), which prevents solvent from flowing backward toward the ferrule, because the fitting is tightened by the washer pressing up against the inlet walls, creating a seal. In contrast, Fig. 4.1B shows how a conventional metal capillary tube and a ferrule are married to the column. The capillary is held in position by the ferrule and a seal is created with the column by metal on metal contact. However, it is difficult to create reliable metal on metal seals at high pressures since the two surfaces are generally not fully parallel. Figure 4.1C depicts the capillary, and ferrule shown in Fig. 4.1B when connected to a different column. Column manufacturers do not use exactly the same specifications for their column inlets (and outlets). So, transferring the metal ferrule to another column cannot ensure the same low void volume as before. The transfer of column plumbing to different columns is common; it is the largest contributing factor to having unsatisfactory column connections. This problem is two-fold since the outlet endfitting of columns have voids like inlet ones and this further contributes to band broadening.

The most suitable metric to assess the degree of band broadening for the presence of void volumes in the column connections is the band variance, which has to be determined from the second central moment of a chromatographic peak [15]. Band variance is unfortunately ignored by most chromatographers although it offers the most accurate estimate of the extent of band broadening. Using moment analysis, instead of the obsolete United States Pharmacopeia (U.S.P.) protocols, permits evaluations of the entire zone of the chromatographic peak that are not based on the simplistic calculation of the peak width at half height. U.S.P. standards assume that peaks are nearly symmetrical, which is far from reality [8].

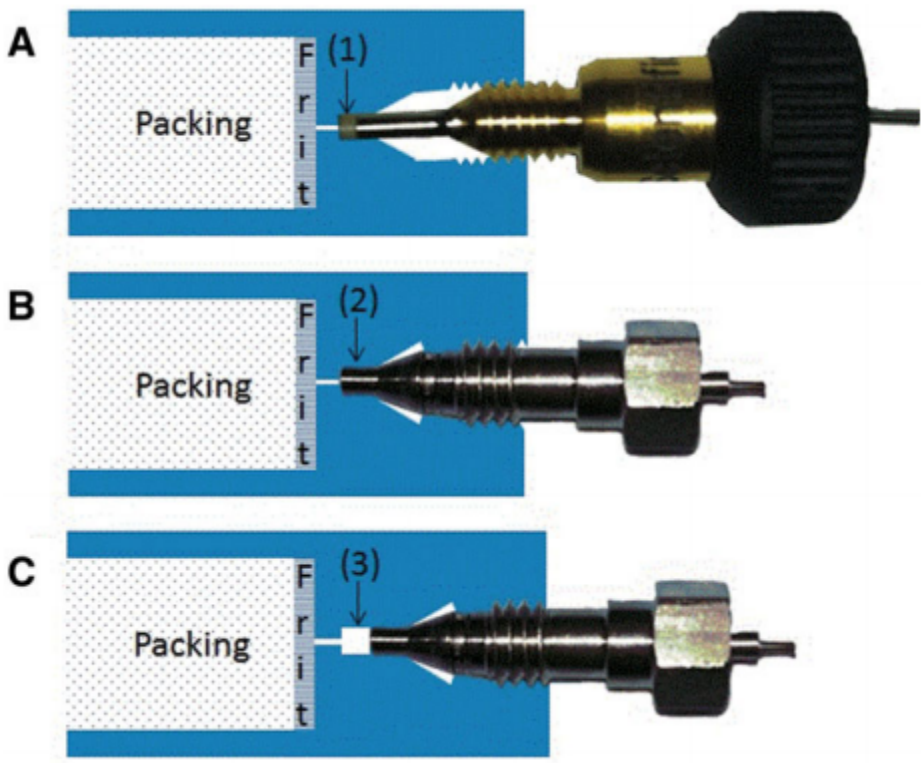

Figure 4.1. Column Connections. (A) Representation of a NanoViper connection. The 1.5875 mm (1/16 in.) od capillary presses up against the column inlet and ensures there will not be a significant void space. (B) Representation of a conventional metal end-fitting fitted to this column. The capillary length is set to match the column being used. (C) Representation of using a conventional metal end-fitting that has its capillary length fixed to a different column. Note that a void space is possible between the capillary and the column inlet.

Chromatographers record the elution profiles of the separated bands of the sample components. Using these recorded profiles they derive various parameters to characterize these bands, quantitate the amounts of the sample components from the band size, identify them from the band retention time, and estimate the efficiency of the column from the bandwidth. Resolution is proportional to the square root of efficiency. Low efficiency separations will yield peaks that have poor resolutions. In former times, the band size was estimated from the peak height, then from the product of the peak height and its width at

half-height, and finally from the peak area. This area was first measured with a planimeter. Finally, electronic integrators were developed. No analytical chemist would ever think now of using the product of peak height and peak width at half height: clearly this would not be accurate. Progressively, the capabilities of the data station of chromatographic instruments were expanded. Similarly and for the same reason, all other characteristics of the band should be related to the band moments, as described in Chapter III. Furthermore, data stations can be programmed to provide these band characteristics. Unfortunately, most data stations are not currently equipped with software that automatically calculates these metrics. The software only uses moment analysis to measure the areas of the peaks. Our efforts to use moment analysis require external software.

4.2 Materials and Methods

All experiments in this chapter were conducted on an Agilent 1290 Infinity System equipped with a low-volume (600 nL) detector flow cell (Agilent Technologies, Waldbronn, Germany) and an Agilent Ultra Low Dispersion Kit graciously supplied by the manufacturer. A Thermo NanoViper (75 µm id) column connection unit (Dionex-Fisher, Sunnyvale, CA, USA) was also used to connect different columns to the UPLC instrument. The NanoViper connections were selected because they have a universal fit to all modern chromatorgaphy columns. They can easily be removed without the use of wrenches. HPLC grade water and acetonitrile were purchased from Fisher Scientific (Fair Lawn, NJ, USA). Three columns were used for this work. The first was an Agilent Technology Zorbax Eclipse Plus C18 (2.1 × 50 mm; 1.8 µm particle size) that was supplied with the Agilent 1290. AWaters Acquity UPLC BEH C18 (2.1 × 50 mm; 1.7 µm particle size) was generously given by Waters (Milford, MA, USA). A Kinetex XB-C18 (2.1 × 50 mm; 1.7 µm) was generously gifted from Phenomenex (Torrance, CA, USA). All the experiments were conducted under ambient conditions, at around 25 ºC.

4.3 Experimental Conditions

Our objective was to measure the contribution to the band variance generated by the column connections to the instrument under ideal and unoptimized conditions. For this purpose, we connected the Agilent Zorbax column to the Agilent Ultra Low Dispersion capillaries by means of a conventional metal ferrule. The Agilent package came with PEEK ferrules and metallic ones. Experience proved the metallic ferrules to be more robust and less prone to leaks than the PEEK ones. Iwas rapidly observed that joining the capillary tube to the column through the metal ferrule caused the metallic capillary to be irreversibly fixed to the ferrule. The stress required to obtain a leak proof connection practically solders the ferrule to the capillary tube. The resultant connection is close to ideal for the column with which a given ferrule and capillary were initially used. However, different column manufacturers have different end fittings for their columns. This is not a critical issue if ferrules and capillaries were changed out for every new column used. The cost of replacing ferrules and capillary tubes that have been swaged (irreversibly fixed together) may not be practical for some labs. Attempting to reset the ferrule position on a swaged ferrule is not advisable. Attempting to replace a fixed ferrule may damage the capillary tube and cause leaks. Also, the use of adjustable ferrules (which do not swage to the capillary tubes), as provided by some manufactures, is not prudent. We found that these adjustable ferrules tend to leak. Furthermore, in certain situations with fixed ferrules, considerable empty spaces may appear between the column and the capillary tube and this causes a significant increase of the band variance.

4.4 Experimental Conditions with the Agilent Ultra Low Dispersion Kit

After swaging the Agilent Ultra Low Dispersion capillaries to the Agilent column, a series of injections of uracil (unretained) dissolved in water/acetonitrile (50:50 v/v) were conducted with a mobile phase of water/acetonitrile (50:50 v/v). The same sample of uracil was used for all experiments. The sample was diluted so that the maximum detector response for a 0.5 µL injection was less than 500

mA.U. (the upper boundary for linear detector response) when monitoring the eluent absorbance at 254 nm, at a flow rate of 100 µL/min. All injections were repeated five times, for flow rates ranging from 100–1400 µL/min, in increments of 100 µL/min. The data acquisition rate was set to the instrument maximum of 160 Hz and was kept constant for all flow rates and columns tested. Ambient temperature was used for all the experiments. A 5 min equilibration period was set between experimental sets to attempt to operate at thermal equilibrium. This is necessary to ensure that the consequences of the heat friction generated by flowing the mobile phase through columns packed with 1.7 µm particles at high pressures are the same for all replicate measurements. Periods of 2–3 h of column flushing with the mobile phase before the beginning of experiment sequences took place in an attempt to reduce the baseline drift, which could increase the errors associated with the calculation of the second central moment [10]. Although possible, baseline correction may skew the data since baseline drift is not linear. The same sequence conducted on the Agilent column was run with the Kinetex and the Waters columns, using the same Agilent capillary tubes, keeping the same Agilent capillary tubes and ferrules as those used in the previous experiments, parts which had been fitted to the Agilent column. afterwards the Kinetex column was replaced with the Waters BEH column and the same series of experiments was run again. However, the Waters BEH column cannot be operated at flow rates above 1200 _L/min with water/acetonitrile (50:50 v/v), since the inlet pressure would exceed 1000bar, the maximum pressure the column can tolerate. Consequently the flow rate range for the Waters BEH column was only 100–1200 µL/min. The Agilent capillary tubes were then connected to a union connector. A series of injections of uracil was performed for flow rates between 100 and 1200 µL/min, in increments of 100 µL/min with five replicates per data set.

4.5 Experimental Conditions with the NanoViper Column Connections

The capillary tubes leading from the injection valve to the column and the capillary tube from the column to the detector flow cell were replaced with finger-tightened NanoViper (75 µm id) capillary connections. The same sequences that were run on the Agilent Ultra Low Dispersion Kit were run using the NanoViper column connections, keeping all other experimental parameters the same.

4.6 Variance with the Union Connector

Figure 2 shows the results obtained for both the Agilent Ultra Low Dispersion Kit and the NanoViper column connections, when using a standard HPLC union connector. The same Agilent connections as used with the Agilent column were connected by a zero dead-volume union, which eliminates the variance contributions from the column packing. The NanoViper connections yield a degree of band broadening slightly lower than the one provided by the Agilent metal connections. The average band broadening contribution of the Agilent Ultra Low Dispersion Kit was 7.3% larger than that of the NanoViper connections. The difference between the contributions of both connections was most apparent at the highest flow rates tested. The zero dead-volume union allowed the measurement of the variance contribution of the system (the detector flow cell, tubing, injection mechanism, etc.). The union had a 130 µm through hole that skewed the measurement slightly. Knowing the variance contribution of the system allows the calculation of the variance contribution of the column. This was done by subtracting the variance measured for the column union from the different variances measured with the columns connected.

4.7 Apparent Variance with the Agilent Column

Figure 4.3(A) shows the results obtained when using the Agilent Ultra Low Dispersion Kit and the NanoViper column connections to connect the Agilent column to the Chromatograph.

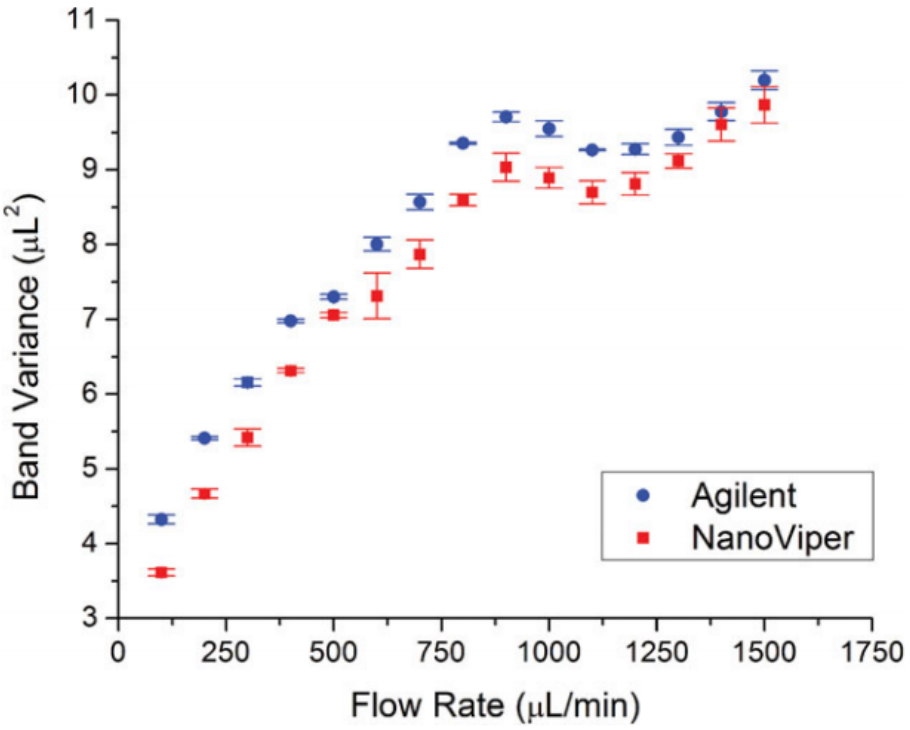

Figure 4.2. Variance vs. Flow Plot with Union Connector. The variance versus flow rate plot for NanoViper and Agilent column connections using a column union with a throughhole of 130 µm. The same Agilent fittings were used to connect a column union to Infinity 1290 UPLC system. The variance data variance data for the NanoViper connections is shown in red squares. Error bars shown as the SD of the five replicates for both scenarios.

As expected, there were only minor differences between the degrees of band broadening observed with the different two connections, since the Agilent capillary tubes and ferrules had been married to the Agilent column. At the highest flow rate tested, the performance obtained with the Agilent connections gives a larger degree of band spreading, which could be due to antiparallel metal-on-metal contact, creating small voids at pressures approaching 1000 bar. Metallic surfaces must be totally parallel and smooth to create a leak-proof seal, this is why most seals are created out of materials that can be compressed. As the flow rate was increased, there were greater deviations between the relative velocities of the molecules in the mobile phase (molecules that enter the voids or

cracks in the connections versus molecules in the bulk). The average band broadening observed is 3.8% larger with the Agilent Ultra Low Dispersion Kit than with the NanoViper connections. However, at a flow rate of 1.4 mL/min, the NanoViper gives a 19.9% smaller band variance than the Agilent Ultra Low Dispersion Kit. Figure 4.3(B) shows the difference between the variance contributions measured for the Agilent column connections and the NanoViper column connections (black squares). The green squares represent the variance contribution due to the Agilent column alone, which was calculated by subtracting the variance obtained with the NanoViper connections (when they are directly connected without a column) from the variance measured with the NanoViper connections and the Agilent column. This difference is a valid approximation as to the variance contribution of the column alone, since the union itself does not have a very large variance contribution.

Band broadening contributions due to migration through a packed bed and through the instrument plumbing are both inevitable. The goal of instrument manufactures should be to reduce the variance contributions of the plumbing as possible and certainly to a value much less than the contribution due to the packed bed alone. The average variance contribution due to the Agilent connections was 8.8% of the total column variance. At the highest flow rate examined (1.4 mL/min), however, the variance contribution from the column was only 32.0% of the total variance observed with the Agilent connections.

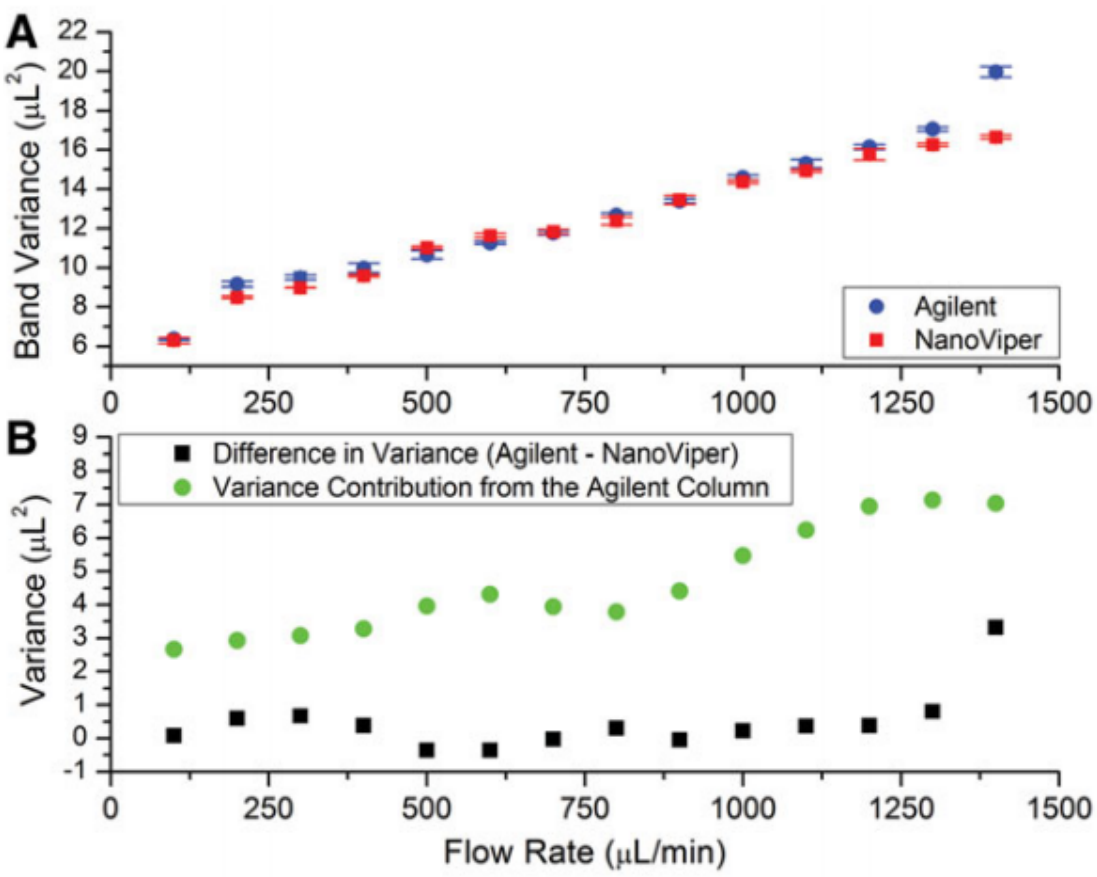

Figure 4.3. Variance vs. Flow Plot (Agilent Optimized). (A) The variance versus flow rate plot for NanoViper and optimized Agilent Low Dispersion column connections joined to Agilent Zorbax Eclipse Plus C18 column and Infinity 1290 UPLC. The variance data for Agilent connections are shown in blue circles. NanoViper connections were then used to join the same column to the system. The variance data for the NanoViper connections is shown in red squares. Error bars as shown as the SD of the five replicates for both scenarios. (B) The difference in variance from the Agilent and NanoViper connections (black squares) is plotted alongside the variance contribution from the column (green circles).

4.8 Apparent Variance with the Kinetex Column

Figure 4.4A shows the results for both the Agilent Ultra LowDispersion Kit and the NanoViper column connections using the Kinetex column. The Agilent connections had been joined to an Agilent column before these experiments

were conducted. The NanoViper connections consistently yielded a lower degree of band broadening than the Agilent connections. As observed with the previous set of experiments, there is an increase in band variance with the Agilent column connections at high pressures. The average band broadening with the Agilent Ultra Low Dispersion Kit is 28.7% larger than that observed with the NanoViper connections. At a flow rate of 1.4 mL/min the unoptimized Agilent connections yielded a band variance that was 41.5% greater than the variance contribution of the NanoViper connections.

Figure 4.4(B) shows the difference between the variance contributions due to the Agilent column connections and to the NanoViper column connections (black squares) for the Kinetex column. The green dots represent the variance contribution of the Kinetex column alone. To calculate the variance contribution of this column, the variance obtained with the NanoViper connections and the union was subtracted from the variancemeasured with NanoViper connections and the Kinetex column. The average variance contribution of the Agilent connections was 44.1% of the total variance. At the highest flow rate examined (1.4 mL/min) the variance contribution of the column is 52.8% of the total variance. On average, 44.1% of the band dispersion was generated at the connection sites when using unoptimized metal ferrules.

4.9 Apparent Variance with the Waters Column

Figure 4.5(A) shows the results obtained with both the Agilent Ultra Low Dispersion Kit and the NanoViper column connections using the Waters column. As with the previous two series of experiments, the Agilent connections had been fitted to an Agilent column before these experiments were conducted. The NanoViper connections yielded a much lower degree of band broadening the Agilent metal connections.

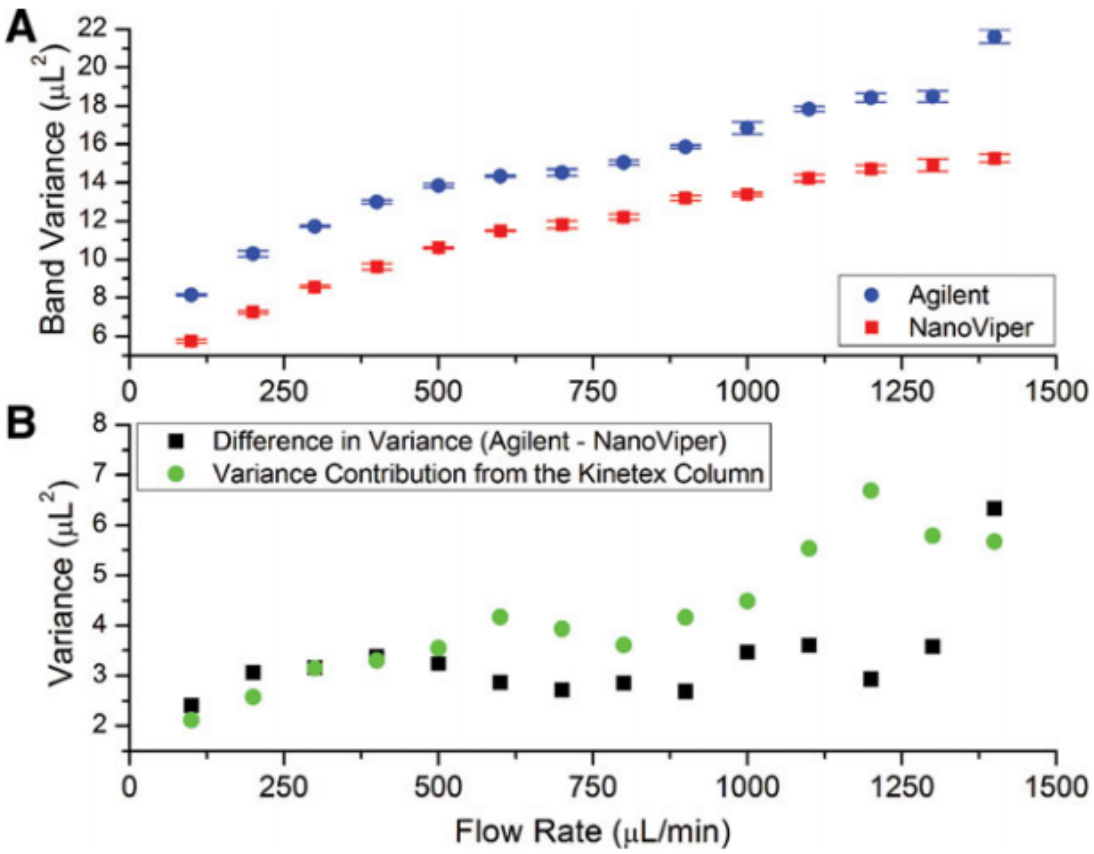

Figure 4.4. Variance vs. Flow Plot (Agilent Unoptimized 1). (A) The variance versus flow rate plot for NanoViper and unoptimized Agilent column connections using a Kinetex XBC18 column. Agilent column connections, previously used with an Agilent Zorbax column, were used to join a Kinetex XB-C18 column to an Infinity 1290 UPLC system. The variance data for Agilent connections are shown in blue circles. The variance data for the NanoViper connections is shown in red squares. Error bars as shown as the SD of the five replicates for both scenarios. (B) The difference in variance from the Agilent and NanoViper connections (black squares) is plotted alongside the variance contribution from the column (green circles).

The average band broadening with the Agilent Ultra Low Dispersion Kit was 53.9% larger than that observed with the NanoViper connections. The previous data sets show that a large increase in band variance occurs at a flow rate of 1.4mL/min. However, the Waters BEH column cannot be run at a flow rate as

high as the Agilent Zorbax or the Kinetex XB-C18 columns, due to pressure limitations. Consequently the variance at 1.4 mL/min could not be measured on our system.

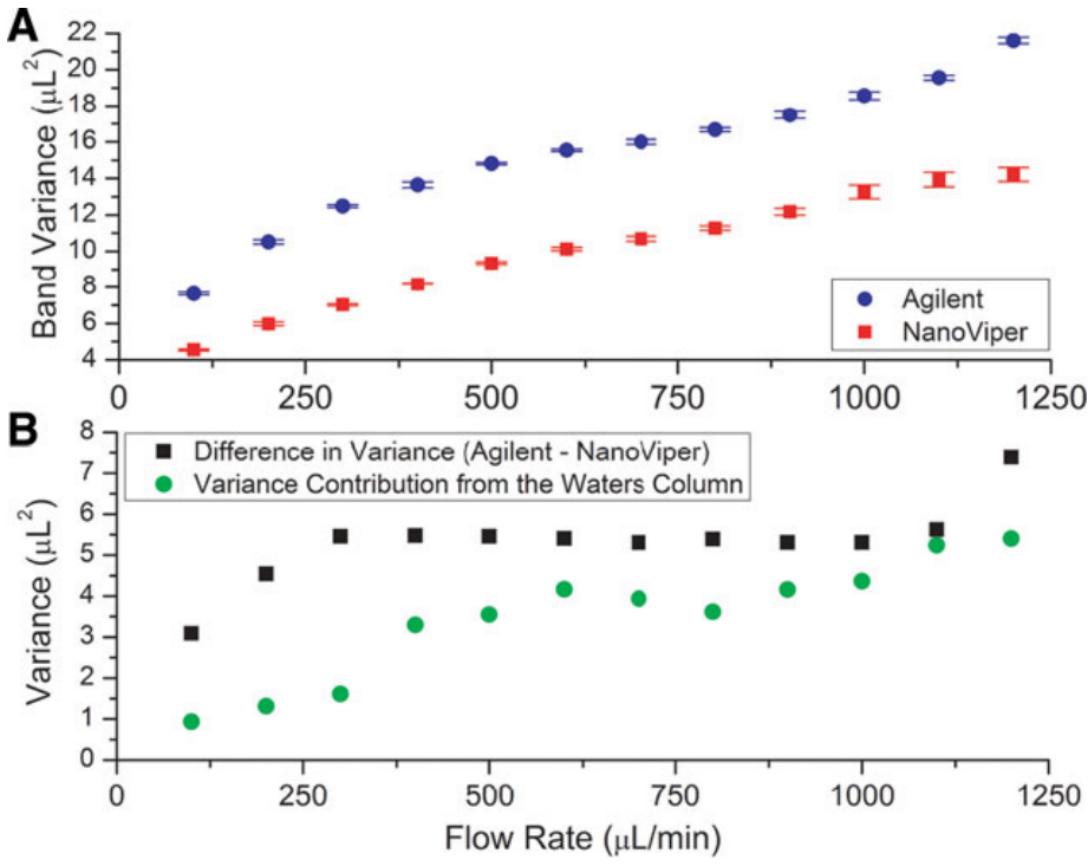

Figure 4.5. Variance vs. Flow Plot (Agilent Unoptimized 2). (A) The variance versus flow rate plot for NanoViper and unoptimized Agilent column connections using a Waters Acquity UPLC BEH C18 column. Agilent column connections, previously used with an Agilent Zorbax column, were used to join a Waters BEH column to an Infinity 1290 UPLC system. The variance data for Agilent connections are shown in blue circles. The variance data for the NanoViper connections is shown in red squares. Error bars as shown as the SD of the five replicates for both scenarios. (B) The difference in variance from the Agilent and NanoViper connections (black squares) is plotted alongside the variance contribution from the column (green circles).

Figure 4.5(B) shows the difference between the variance due to the Agilent column connections and to the NanoViper column connections (black squares) for the Waters column. The green dots represent the variance contribution of the Waters column alone. To calculate the variance contribution of the column alone, the variance obtained with the NanoViper connections and union were subtracted from the variances measured with the NanoViper connections and the Waters column at the same flow rate. The average variance contribution due to the Agilent connections was 60.5% of the total variance for this set of experiments. Therefore, 60.5% of the band dispersion is generated at the connection sites from unoptimized metal ferrules.

4.10 Comparison of the Chromatograms

Figure 4.6 shows sample chromatograms from the experiments performed at flow rates of 0.1 and 1.4 mL/min, respectively, for each of the columns tested, with the Waters column data from 0.1 and 1.2 mL/min, respectively. Inspection of the chromatograms shows that the peak width at half height is not drastically changed, even though the peaks show visible changes in both their heights and degree of tailing. For the experiments conducted with the Waters column at 1.2 mL/min the variance observed with the Agilent tubing is 52.0% larger than that provided by the NanoViper tubing. However, the U.S.P. standard ofmeasuring peak width at half height yields a result that shows that the unoptimized Agilent connections provide bands that are 8.8% less disperse than the NanoViper connections. Importantly, the peak recorded with the Agilent connection is shorter and tails more strongly than those recorded with the NanoViper connection for the Waters column. Situations like this one clearly demonstrate why the U.S.P. standard, which yields completely misleading results, is obsolete and must be abandoned while the measurement of the peak variance should be preferred.

4.11 Chapter Summary

We measured the differences between the variances of recorded chromatograms that are recorded when unoptimized and optimized column connections were used. The relative precision of these measurements is better than 2% for five replicate injections. We also demonstrated that the use of the second central moment provides accurate estimates of the band variance while the method suggested by the conventional U.S.P. protocols does not. Even if this U.S.P. method is more reproducible than the use of the second moment it is far less accurate and may lead to serious errors (see Fig. 6). In any case, we should always try and improve methods of data analysis, especially when we find potential flaws in commonly used techniques.

In gradient chromatography, moment analysis becomes more challenging, since there is baseline drift. We showed that using very narrow id plumbing may not suffice to record accurately the narrow peaks eluted from modern high efficiency columns and avoid the high degree of band broadening when voids or cracks take place in column inlet and outlet fittings. The differences in the band broadening observed can vary significantly depending on the experimental conditions. When the column diameter is decreased the relative degree of band broadening due to these voids becomes more noticeable. In VHPLC systems, this effect is especially significant. Although a column may provide excellent results, it may give broadened, tailing peaks when fitted to the same instrument with a different connection system. If this connection is made poorly, the consequences can be severe although the difference may appear unnoticeable to a skilled analyst who is using the U.S.P. method discussed. For example, in a very severe case we observed a 53.9% increase in the band variance when our control (NanoViper) connections were replaced with connections of a different design. Band broadening of this magnitude should not be ignored because it affects peak height and detection limits.

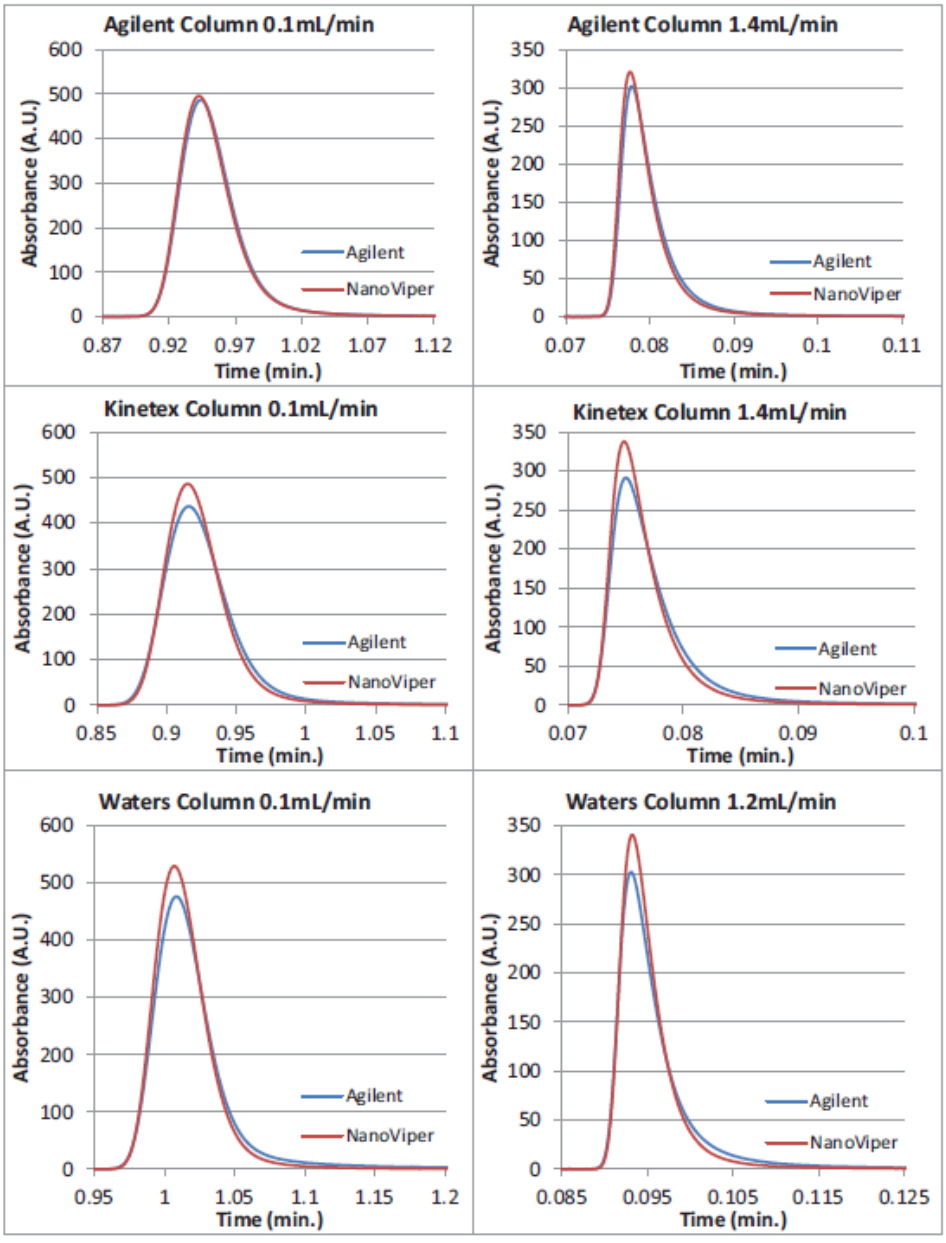

Figure 4.6. Sample Chromatograms with the Column Connectors. The elution times have been corrected so that the peaks start at the same time for easy comparison. Errors in injection volumes have also been corrected so that respective peaks have the same area.

Great care should be taken when connecting new columns to HPLC and UPLC systems. Actually, as we demonstrated, improper column connections can easily become the largest contributing factor to band broadening for nonretained compounds. Finally, small id tubings generate considerable backpressure. The reduction in band broadening achieved with the use of small id tubing may not warrant their use.

The variance contributions due to column connections increases at high flow rates. This trend is explained by the presence in these connections of stagnant pools into which mass transfer proceeds quickly when the band passes, due to its high concentration, but out of which mass transfer decreases rapidly with decreasing concentration when the band ends. With increasing flow rates, the difference between the rates of transfer of the molecules into and out of the void zones (a rate that is diffusion controlled) and the migration rate of the molecules that are in the bulk (which is flow rate controlled) becomes larger. The greater the velocity difference of the two regions, the greater the degree of band broadening. Analysts who wish to use narrow-bore columns must closely monitor the extra column variance contributions of their HPLC instrument so that separations are not compromised by the use of improper conditions (e.g., improper column connections) that could be corrected. Viper and NanoViper column connections are good options for a research laboratory in which many different columns are used and are often changed, possibly several times a week. NanoViper capillary tubes and connectors consistently yield peaks of lower variance at high pressures than conventional metal ferrules and capillary tubes. It is also worth noting that the more modern, adjustable ferrules that come with some modern instruments are prone to leaks. We did not experience any leak with the ferrules supplied with the Agilent connectors used in our experiment nor with the Viper series connectors either. Although most researchers are interested in compounds with high retention factors and the loss of efficiency for compounds with retention factors greater than 2 will be significantly less than those for

nonretained compounds. Analyte peaks with higher retention factors will have a larger variance contribution from the column than from column connections and instrument plumbing. Nevertheless, instrument variance contributions in linear systems are additive and will play a role in the efficiency of the separation.

CHAPTER V
CONSTANT PRESSURE VERSUS CONSTANT FLOW GRADIENT CHROMATOGRAPHY – THEORY AND APPLICATION

The conventional theory of gradient chromatography aims at predicting the elution time, the peak widths [16-17], and the column peak capacity in the time domain [18-20]. It is now well established. These gradients are operated under constant flow (cF) rate. As a consequence, the inlet column pressure changes continuously during the gradient time, in proportion to the average viscosity of the eluent over the column length. Recently, Choikhet et al. [21-23] presented a new concept, constant pressure (cP) gradient chromatography and the new operation mode of the Agilent 1290 binary pump requiring special Firmware that Agilent had provided to implement it. The instrument is modified to deliver (1) a constant inlet pressure during the gradient run, by adjusting the total eluent flow rate to the real time change of the column hydrodynamic resistance and (2) a ratio of the weak and strong eluent flow rate consistent with the required cF gradient. The volume gradient is kept identical in both the predefined cF and the cP gradients modes. For instance, if we consider a linear time gradient with a gradient slope βt at a constant flow rate, $F*v$, the same gradient slope in volume is fixed at $\beta v=\beta t/F*v$ in both gradient modes.

A recent paper extended the classical theory of gradient chromatography at constant flow rate to constant pressure gradient separations [24]. The prediction of the elution time, peak width, and peak capacity requires the knowledge of the viscosity of the binary eluent (usually acetonitrile–water or methanol–water mixtures) as a function of the composition, the temperature, and the pressure. The dependence of the reduced plate height on the reduced velocity, $h = f(v)$, and on the retention factor must also be known. Whereas retention volumes (controlled by thermodynamics) do not depend on the gradient mode, the volume peak widths and the volume peak capacities (controlled by mass transfer

kinetics) depend on whether the volume of the strong eluent is delivered at constant pressure or at constant flow rate [24]. Remarkably, for a constant analysis time, the peak capacity does not depend on the gradient mode, regardless of the nature of the analyte (small molecules, peptides, proteins) and of the amplitude of the gradients. This conclusion is valid if the eluent is incompressible, the HETP is independent of the mobile phase composition gradient along the bandwidth, the column remains isothermal, the gradient shape does not change during its migration along the column, and the pressure does not affect the retention of analytes. Then, the performance of cP gradients could potentially exceed that usually observed with cF gradient if the sole constraint imposed to the analyst is the maximum pressure that the column and/or the HPLC system can withstand. Indeed, in the cF mode, the maximum pressure is only attained when the average viscosity of the eluent along the column reaches its maximum. In contrast, in the cP mode, a constant maximum pressure is applied, providing the fastest possible separation. The question then arises, whether the peak capacity remains comparable to that expected in the cF mode, for which the gradient elution window in time coordinates is wider than that in cP gradients.

Thus, this work has two goals, (1) to experimentally confirm whether the peak capacity remains the same for a constant analysis time in either cF or cP gradient modes, at inlet pressures lower than 250 bar and (2) to compare theoretically and experimentally the gradient performances of cF and cP gradient modes when the sole constraint set by the analyst is a maximum pressure drop. A sample mixture containing twenty small molecular weight compounds will be analyzed on column packed with 3.5 µm BEH-C_{18} particles, eluted with a mixture of methanol and water. The maximum inlet pressure will be 250 bar. The relative advantages of cP and cF gradient chromatography will be discussed.

5.1 Theory

This section provides the expressions for the peak capacities is in the cF and cP modes.

5.1.1 Peak capacity

The standard definition of the peak capacity for a resolution of unity is given by [18-19,24] in equation 5.1.

$$P_c = 1 + \int_{t_D+t_0}^{t_F} \frac{1}{4\sqrt{\mu'_{2,t}(t)}} dt \qquad \text{Eq. (5.1)}$$

where *tD* is the dwell volume, *tF* is the gradient time of the last eluted compound, and t_0 is the column hold-up time, itself given by equation 5.2.

$$V_0 = \int_{t_D}^{t_D+t_0} F_v(t)dt \qquad \text{Eq. (5.2)}$$

where V_0 is the constant column hold-up volume, $Fv(t)$ is the flow rate at the time *t*, and μ'_2 is the peak variance in time units of the compound peak eluted at time *t*: equation 5.3.

$$\mu'_{2,t}(t) = \frac{V_0}{L}\frac{k(t)^2}{F_v(t)^2}\int_0^{t-t_D-t_0} F_v(t_S)H(t_S)\frac{(1+k[g(t_S)])^2}{k[g(t_S)]^3}dt_S \qquad \text{Eq. (5.3)}$$

where *k*(*t*) is the retention factor of the compound at the column outlet and at the time *t*, *L* is the column length, *H*(*tS*) is the plate height of the analyte after it has

spent a time tS in the stationary phase, and $g(tS)$ is the mobile phase composition delivered by the pump at the time tS.

5.1.2 Eluent viscosity

The variation of the viscosity, η, of the mixture of methanol and water at the temperature $T = 298$ K with the pressure, P, and the mobile phase composition, φ, is given by [24] and expressed as equation 5.4.

$$\eta(\varphi, P) = [\eta_{org}\varphi \exp([1-\varphi]\alpha_w) + \eta_w(1-\varphi)\exp(\varphi\alpha_{org})] \times [1 + \xi_{org}(\varphi)P] \quad \text{Eq. (5.4)}$$

For methanol–water mixtures at 298 K, the best empirical parameters are η_{MeOH}= 0.57 cP, ηw=0.89 cP,αw=1.9231, and α_{MeOH}=1.2183. The best cubic expression for $\xi_{MeOH}(\varphi)$ is given by [25] and expressed as equation 5.5.

$$\xi_{MeOH}(\varphi) = (6.88 - 33.80\varphi + 246.40\varphi^2 - 195.04\varphi^3) \times 10^{-10}\ \text{Pa}^{-1} \quad \text{Eq. (5.5)}$$

Figure 5.1 shows the plot of the viscosity of methanol–water mixtures as a function of the mobile phase composition ($\varphi = 0$–1) and the pressure ($P = 1$–1000 bar) at a constant temperature of $T = 298$ K.

5.1.3 Flow rate prediction

For linear volume gradients, the prediction of the flow rate, $Fv(t)$, in cP gradient mode is given by the solution of the following differential equation [24] and expressed in equation 5.6.

$$d\left[\frac{1}{F_v}\right] = \beta_v \frac{[\overline{\partial\eta/\partial\varphi}]_t}{[\overline{\eta}]_t} dt \quad \text{Eq. (5.6)}$$

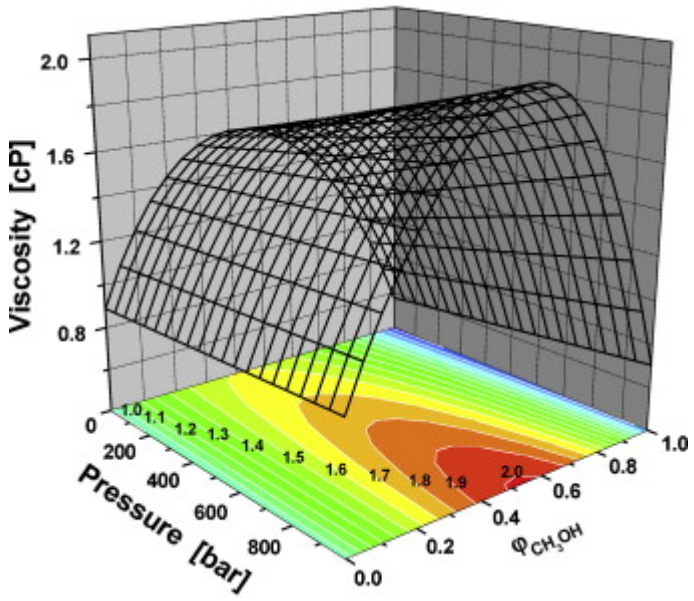

Figure 5.1. Viscosity Diagram (Methanol and Water). Three-dimensional graph (solid black lines) illustrating the variation of the viscosity of methanol–water mixtures as a function of the pressure (from $P^0 = 1$ bar to $P = 981$ bar) and the volume fraction of the organic eluent (from pure water, $\varphi = 0$, to pure methanol, $\varphi = 1$). The iso-viscosity lines are projected as thick solid white lines onto the (T, φ) plane.

In this equation, the average is taken over the full column length ($0 < z < L$). At $t = 0$ the initial flow rate, Fv,I, is a function of the initial mobile phase composition, φI, and of the desired constant column back pressure, ΔP^* and shown in equation 5.7.

$$\Delta P^* = \frac{\eta(\varphi_I)L}{K_0 \pi r_c^2} F_{v,I} \qquad \text{Eq. (5.7)}$$

Where K_0 is the column specific permeability and rc is the column inner radius.

5.1.4 Simulation of a sample mixture

Twenty one evenly distributed peaks along the gradient retention window from $t = t_0$ to $t = tF$ were generated in the constant flow-rate mode (t_0 and tF included). Nine different column lengths were considered for the construction of the theoretical gradient kinetic plot: L = 3.5, 7.0, 10.5, 14.0, 17.5, 21.0, 24.5, 35, and 45.5 cm. The pressure was fixed at a relatively low value of 250 bar, which permits neglecting the eluent compressibility and the thermal effects. For each eluted compound, the time domain was segmented into precisely 696 identical time increments of width dt. The program adjusted this increment so that each compound elutes exactly at the distance L (position at the column outlet). The column length was segmented into 150 identical space increments of length $dz = L/150$. The outlet pressure was the atmospheric pressure $P = P^0$.

For the sake of simplifying the calculations, the sample mixture was described by the distribution of the retention factors in pure water, $k_{0,i}$ of the different components i. The smallest and largest values for $k_{0,i}$ were $k_{0,1} = 0$ and $k_{0,21} = 300$, respectively. The retention factor of each compound was assumed to follow the linear strength solvation model (LSSM) and expressed in equation 5.8:

$$k_i(\varphi) = k_{0,i} \exp(-S\varphi) \qquad \text{Eq. (5.8)}$$

Where S was assumed constant for all the small molecules present in the sample mixture (S = 5).

According to the solution of the gradient equation and assuming linear, non-retained gradients, the retention time, ti of the component i ($1 \leq i \leq 21$) is given by [16] and shown in equation 5.9:

$$t_i - t_0 = \frac{1}{S\beta_t} \ln[1 + S\beta_t t_0 k_{0,i} \exp(-S\varphi_I)] = \frac{i-1}{20}(t_F - t_0) \qquad \text{Eq. (5.9)}$$

Where βt is the slope of the linear gradient in reciprocal time unit, t_0 is the hold-up time of the column under cF mode and is expressed in equation 5.10:

$$t_0 = \frac{\pi r_c^2 L}{F_v^*} \quad \text{Eq. (5.10)}$$

where F_v^* was the unique constant flow rate chosen so that the maximum pressure recorded in cF mode was equal to 250 bar.

Finally, in Eq. 5.9, tF is the gradient retention time of the most retained compound. tF depends on the gradient slope, βt, which was determined by imposing that $tF = t_0 + tG$ with tG the gradient time during which the mobile phase composition increases linearly from φI to φF. Accordingly, βt is given by [25] and shown in equation 5.11:

$$\beta_t = \frac{1}{Sk_{21}(\varphi)t_0}(e^{[S(\varphi_F - \varphi_I)]} - 1) \quad \text{Eq. (5.11)}$$

Since the parameters S, βt, t_0, φI, tF, and t_0 are fixed, the 21 solutes are evenly distributed along the retention window by choosing the nineteen ($2 \leq i \leq 20$) remaining retention factors, $k_{0,i}$, as follows [25] in equation 5.12:

$$k_{0,i} = \frac{1}{S\beta_t t_0 \exp(-S\varphi_I)} \left(\exp\left[\frac{S\beta_t (i-1)(t_F - t_0)}{20} \right] - 1 \right) \quad \text{Eq. (5.12)}$$

5.1.5 Theoretical column HETP

For all the small molecules, the same reduced plate height equation was considered and h was assumed to depend only on the retention factor, which affects both the B and C terms in the van Deemter equation. The column HETP

($H = hdp$) was that of a 4.6 mm × 150 mm column packed with 3.5 µm fully porous particles with an average mesopore size of 140 Å and a minimum reduced plate height of the order of 2.0. The external porosity was simply taken at $\square e = 0.4$ and the internal porosity was $\square p = 0.40$, so the total porosity was $\square t = 0.64$. The reduced plate height is simply given by [25-28] shown in equation 5.13:

$$h(\nu) = \frac{2(\gamma_e + ((1-\epsilon_e)/\epsilon_e))\Omega}{\nu} + \frac{0.003\nu}{1+0.004\nu} + \frac{0.11\nu}{1+0.31\nu} + \frac{0.54\nu}{1+0.27\nu} + \frac{1}{30}\frac{\epsilon_e}{1-\epsilon_e}\left[\frac{k_1}{1+k_1}\right]^2\frac{1}{\Omega} \quad \text{Eq. (5.13)}$$

In this equation, v is the reduced interstitial linear velocity is shown in equation 5.14:

$$\nu = \frac{ud_p}{D_m} \quad \text{Eq. (5.14)}$$

The value of the bulk molecular diffusion coefficient, Dm, in the expression of the reduced velocity was systematically adjusted for the local pressure and mobile phase composition in methanol–water mixtures shown in equation 5.15:

$$D_m(\varphi, P) = D_m(\varphi_I, P^0)\frac{\eta(\varphi_I, P^0)}{\eta(\varphi, P)} \quad \text{Eq. (5.15)}$$

Where $Dm(\varphi I, P^0) = 1.5 \times 10^{-5}$ cm^2/s is the reference diffusion coefficient at the initial mobile phase composition and under atmospheric pressure.

The value of the ratio, Ω of the sample diffusivity across the porous particle to the bulk molecular diffusion coefficient was adjusted semi-empirically to the data

collected in [29], which reported the variation of Ω as a function of the retention factor, k in equation 5.16:

$$\Omega(k) = \epsilon_p^* \gamma_p^* \left[F(\lambda_m) + 2.3k \exp\left(-0.141k\right)\right] \quad \text{Eq. (5.16)}$$

Where $\epsilon_p^* = \epsilon_p(1 - \lambda_m^2)$ is the internal porosity accessible to the analyte, $\gamma_p^* = 1 - (2/3)(1 + \epsilon_p^*)(1 - \epsilon_p^*)^{3/2}$ is the internal obstruction factor predicted by Pismen [30], $F(\lambda m)$ is the hindrance diffusion factor predicted by Renkin [31], and λm is the ratio of the size of the analyte molecule to that of the average mesopore size (Dp = 150 Å). Finally, the zone retention factor, k_1, is expressed as a function of the retention factor, k, given by [24] in equation 5.17:

$$k_1(k) = \frac{1 - \epsilon_e}{\epsilon_e}\left[\epsilon_p + (1 - \epsilon_p)\frac{\epsilon_t}{1 - \epsilon_t}k\right] \quad \text{Eq. (5.17)}$$

5.2 Experimental

5.2.1 Chemicals

The mobile phase was a mixture of methanol and water, both HPLC grade, purchased from Fisher Scientific (Fair Lawn, NJ, USA). The nineteen analytes were purchased from either Sigma–Aldrich (Milwaukee, WI, USA), Acros Organics (New Jersey, USA), Eastman Kodak (Rochester, NY), or Tokyo Chemical Industry (Tokyo, Japan). The origin and the level of purity of all these compounds are listed below:

01- Thiourea (Sigma, 99%)

02- Uracil (Sigma)

03- 3,5 Dihydroxybenzyl alcohol (TCI, >97%)

04- Theophylline (SA, Anhydrous)

05- Caffeine (SA, Reagent Plus)

06- Aniline (SA, 99.5+%)

07- o-Toluamide (SA, 98%)

08- Phenol (ACROS, Reagent ACS)

09- m-Toluamide (SA, 99%)

10- 3-Methylcatechol (SA, 99%)

11- o-Toluidine (ACROS, Reagent ACS)

12- 2-Nitroaniline (SA, 99%)

13- o-Nitrophenol (Eastman)

14- 4-Ethylphenol (SA, 99%)

15- Ethylbenzoate (SA, 99+%)

16- Phenetole (SA, 99%)

17- Propylbenzoate (SA, 99%)

18- Butylbenzoate (SA, 99%)

19- Butylbenzene (SA, 99+%)

5.2.2 Apparatus

All the measurements were performed on the 1290 Infinity HPLC system (Agilent Technologies, Waldbroon, Germany) liquid chromatograph equipped with prototype Firmware and prototype software utilities supporting non-constant flow gradient operation mode. The system includes a 1290 Infinity Binary Pump with Solvent Selection Valves and a programmable auto-sampler. The injection volume is drawn into one end of the 20 µL injection loop. The instrument is equipped with a two-compartment oven and a multi-diode array system. The

system is controlled by the Chemstation software. The sample trajectory in the equipment involves the successive passage of its band through the series of:

- A 20 µL injection loop attached to the injection needle. The design of the LIFO injection system is such that the volume of sample drawn into the loop only passes the part of the loop it has been drawn into before entering the seat capillary. So, the volume of sample actually injected into the column is the volume of sample drawn into the loop. This ensures an excellent injection repeatability.

- A small volume needle seat capillary (115 µm I.D., 100 mm long), ≃1.0 µL, located between the injection needle and the injection valve. The total volume of the grooves and connection ports in the valve is around 1.2 µL.

- Two 130 µm × 250 mm long Viper capillary tubes offered by the manufacturer (Dionex, Germering, Germany) were placed, one before, the second after the column. Each has a volume of 3.3 µL.

- A small volume detector cell, $V(\sigma)$ = 0.6 µL, 10 mm path.

The total dwell volume of this instrument was measured from step gradient experiments by the manufacturer at 170 µL. It includes the volume contributions of the connecting tubes (green tubings, I.D. = 254 µm, ≃75 µL), of the jet weaver V35 mixer (35 µL), of the loop (40 µL), and of the syringe (20 µL). No solvent heat exchanger has been used in the experiment. The extra-column volume is close to 10 µL and generate an extra-column peak variance which varies between 2 and 10 μL^2 when the flow rate is increased from 0.1 to 5.0 mL/min.

The particularity of this prototype instrument (hardware of the 1290 Infinity system unchanged with the additional functionality offered by the prototype Firmware and software utilities) is that it can operate under either constant flow (standard gradients) or constant pressure gradient mode. The switch between the two modes is simple; it is activated by running a pre-run macro in the

standard gradient method programmed in time units. In the constant pressure mode, it ensures that (1) the inlet pressure remains constant during the whole gradient run and (2) the variation of the mobile phase composition with the volume of eluent delivered by the pumps is strictly identical in the cF and the cP modes. Accordingly, if the unique slope of the linear gradient is βv in reciprocal volume unit (m^{-3}), the gradient slope βt in reciprocal time unit of the linear gradient in the cF mode (flow rate $F*v$) is then simply given by equation 5.18:

$$\beta_t = F_v^* \beta_v \qquad \text{Eq. (5.18)}$$

For a non-linear gradient, we have at any given time t in equation 5.19:

$$\frac{d\varphi}{dt} = F_v^* \frac{d\varphi}{dV} \qquad \text{Eq. (5.19)}$$

where the total volume, V, of eluent delivered by the pumps is:
equation 5.20:

$$V = F_v^* t \qquad \text{Eq. (5.20)}$$

In the cF mode, or in the cP mode equation 5.21:

$$V = \int_0^{t'} F_v(t')dt' \qquad \text{Eq. (5.21)}$$

where t' is the actual time elapsed during the cP gradient experiments.

5.2.3 Columns

Two 4.6 mm × 150 mm columns packed with 3.5 µm XBridge-C_{18} 140 Å particles (Waters, MA, USA) were used to measure the peak capacity and the analysis time in both the cF and the cP gradient modes. The hold-up volumes of the columns are both close to 1.6 mL, a volume much larger than the system dwell volume 170 µL) and the extra-column volume of the instrument (10 µL).

5.2.4 Experimental peak capacity

For both cF and cP gradients, the peak capacities were measured for at least $N = 17$ peaks, which were baseline separated with retention times as evenly distributed as possible along the retention window. For each compound, the half-height peak width, $\omega_{1/2,i}$, was measured (peaks in gradient are nearly Gaussian) and the experimental peak capacity, Pc,exp, was given by equation (5.22):

$$P_{c,exp} = 1 + N\frac{t_F - t_0}{\sum_i^N 2\omega_{1/2,i}} \qquad \text{Eq. (5.22)}$$

The peak widths at half-height were automatically calculated by the Agilent software after processing the output files.

5.3 Results and Discussion

In the first part of this section, the values predicted for the flow rate (which varies during the gradient run in the cP mode) and for the inlet pressure (which varies in the cF mode) by the model recently reported in reference [24] are compared to those recorded on the Agilent 1290 Infinity system.

In the second part of the section, we compared the peak capacities measured in the in cF and the cP gradient modes when the retention time of the last compound (butylbenzene) in ether mode is kept constant. Theory predicted that these peak capacities should be very similar.

In the last part of the section, these peak capacities are compared when the maximum pressure reached during the cF mode or the pressure at which the cP mode is run are ≃ 250 bar. For this purpose, we used a methanol and water solution as the binary eluent. The initial and final volume fractions of methanol in water,φI and φF, were 5 and 95%, respectively. As shown in Figure 5.1, the

viscosity of the eluent under the inlet pressure of 250 bar increases first from 1.0 to 1.6 cP (≃ 40% methanol), then decreases from 1.6 to only 0.6 cP.

5.3.1 Comparison between the recorded and the predicted inlet pressure and flow-rate curves

In the following calculations, we used the following parameters, measured for the column used: external porosity of the column, $\varepsilon_e = 0.36$, total porosity, $\varepsilon_t = 0.62$, particle diameter $dp = 3.5$ µm, column length $L = 15$ cm, inner column diameter $dc = 0.46$ mm, and column permeability $K_0 = 8.07 \times 10^{-15}$ m^2 (the Kozeny–Carman constant was $Kc = 173$ with respect to the hydraulic resistance to flow with methanol–water mixtures as the mobile phase). All the details regarding the calculations are given in [24]. In the cF gradient mode, the flow rate was fixed at $F_v^* = 0.76$mL/min. The predicted and experimental pressure profiles are compared in Fig. 5.2. The agreement between theoretical and experimental data is excellent, given the assumptions made in the calculations and the empirical expression for the viscosity of methanol–water mixtures at $T = 298$ K. Obviously, at constant flow rate, the ripple of the experimental pressure signal is very small (<0.5 bar); it results from the smooth variations of the average eluent viscosity over the column length. In the cP gradient mode, the column inlet pressure was fixed at $P^* = 197$ bar. The predicted and experimental flow rate profiles are compared in Fig. 5.2. Again, the agreement between calculated and recorded profiles is excellent, except during the beginning and end of the gradient, when the eluent viscosity is smallest and the errors are likely to be the largest. Overall, the flow and the pressure profiles predicted and measured are in excellent agreements, which validates the theory and renders relevant the program used to predict the gradient performances in both the cF and the cP gradient modes.

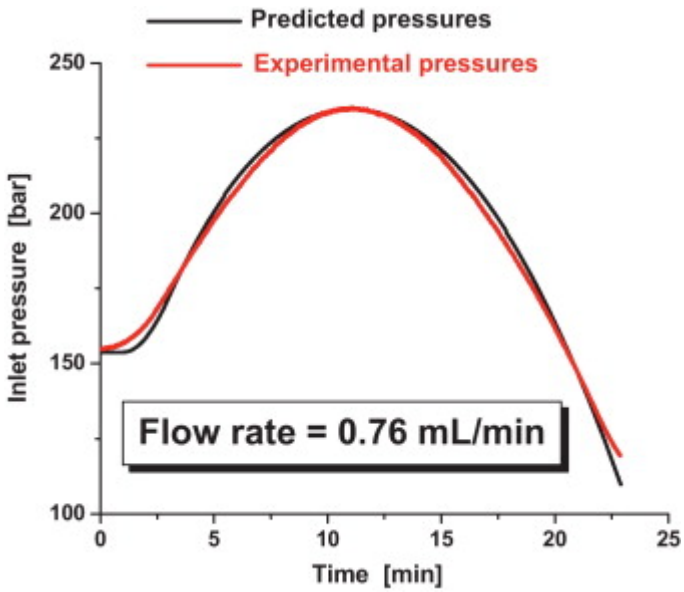

Figure 5.2. Predicted and Experimental Pressure Curves. Comparison between the predicted (black color) and the experimental (red color) profiles of the column inlet pressure (at constant rate 0.76 mL/min) *versus* time.

5.3.2 Comparison between the experimental peak capacities in constant flow-rate and constant pressure gradient chromatography at constant analysis time

A recent theoretical work [24] demonstrated that the peak capacity does not depend on the gradient mode (cF and cP gradients), provided that the analysis time is kept constant in both cF and cP gradient runs. It was assumed that the eluent is incompressible, the column is isothermal, the HETP is independent of the mobile phase composition gradient along the bandwidth, the shape of the gradient does not change during its migration along the column, and the retention is not affected by the local pressure inside the column. The conclusion was valid regardless of the nature of the gradient (whether the viscosity of the eluent increases, decreases, or increases and then decreases during the gradient run) and of the nature of the analytes considered (small molecules or peptides).

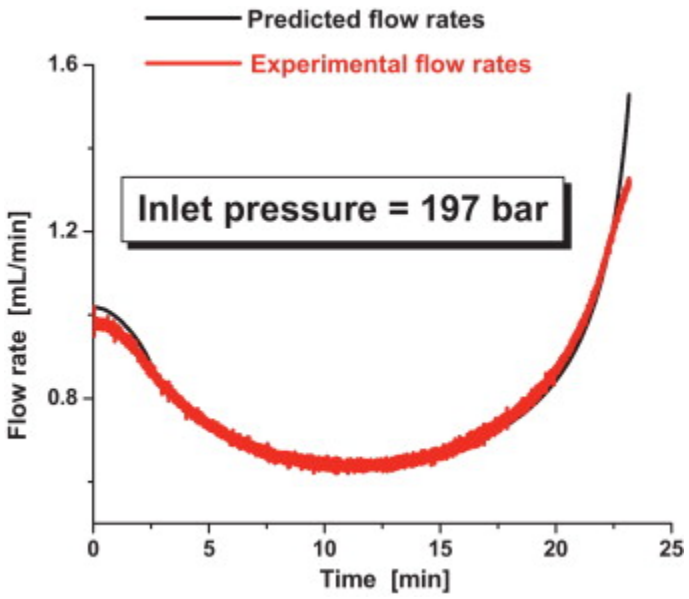

Figure 5.3. Predicted and Experimental Flow Curves. Comparison between the predicted (black color) and the experimental (red color) flow rate profiles (under constant column inlet pressure P^* = 197 bar) *versus* time. During the gradient, the methanol content increases linearly in volume from 5 to 95%. Note the relatively large experimental ripple of the flow rate.

In our experiments, three different flow rates were applied in the cF mode, in order to generate three maximum inlet pressures of about 240, 120, and 60 bar. The column length was L = 15 cm and its inner diameter 0.46 mm. The flow rates were set at 0.76, 0.38, and 0.19 mL/min, respectively. With such low back pressures and small flow rates, the power of frictional heating, *Pf*, is always smaller than 2 W/m, a value for which the variation of the temperature along the column is negligible [32] and the column efficiency remains constant [33]. Therefore, the column can be considered as isothermal. Small molecules were injected in order to minimize the effect of the pressure on their local retention factors inside the column. Methanol-water solutions were chosen as the eluent because methanol is weakly adsorbed onto silica-C_{18} stationary phases [34-35]. Therefore, the gradient is neither retained nor distorted during its migration along the column [36]. Below 250 bar, i.e., for an average column pressure lower than

125 bar, the compressibility of methanol–water mixtures is less than 1.5% [37]. The experimental gradient slope, βt, was adjusted so that the last eluted compound (butylbenzene) was eluted close to the time when the gradient ends at the column outlet. This slope was 0.041, 0.020, and 0.010 min^{-1} for the selected flow rates of 0.76, 0.38, and 0.19 mL/min, respectively. The analysis times were nearly the same (23.1 min *versus* *22*.8 min, 46.2 min *versus* 5.5 min, and 92.2 min *versus* 91.2 min) as observed in the cP mode when the pressures were set at P^* = 197, 99, and 50 bar, respectively.

The corresponding chromatograms measured under the cF and the cP gradient conditions are shown in Fig. 5.4, Fig. 5.5 and Fig. 5.6. The analysis times were about 23, 46, and 92 min. As expected, the hold-up times derived from the elution times of thiourea and uracil (the first and the second eluted compounds) are systematically smaller in the cP than in the cF gradient experiments, because the initial flow rate in the cP mode is larger than that in the cF mode (see Fig. 5.2 and Fig. 5.3). The peak capacities measured are Pc,exp = 326, 315, and 286 in the constant flow rate gradient mode for $F_0 = 0.76$, 0.38, and 0.19 mL/min, respectively. The peak capacities measured in the constant pressure gradient mode are Pc,exp = 313, 305, and 295 for P^* = 197, 99, and 50 bar, respectively. A slight decrease of the peak capacity is observed when the flow rate is decreased, a result consistent with the slight increase of the column HETP. The HETPs decreased slightly with decreasing reduced velocity below the optimum reduced velocity. At the highest flow rate of 0.76 mL/min, the largest local reduced velocity was 8.3; at flow rates of 0.38 and 0.19 mL/min, it decreased to only 4.1 and 2.0. In such a range of reduced velocities, the HETP is essentially controlled by longitudinal diffusion, so it is expected that the HETP increases with decreasing flow rate. Most importantly, the relative difference between the peak capacities in the cF and the cP gradient modes are +4.0%, +3.2%, and –3.1%, respectively. Given the magnitude of the relative error made on measurements of the peak capacities, such small differences are not significant. This series of

measurements confirms that the peak capacities measured in the cF and the cP gradient modes are virtually the same, provided that the analysis time is kept constant in both modes. These results validate the earlier theoretical work [24].

5.3.3 Comparison between the experimental peak capacities and the analysis times in constant flow-rate and constant pressure gradient chromatography at constant maximum inlet pressure

5.3.3.1 Theoretical predictions

For these calculations, we selected a virtual column with a typical external porosity $\varepsilon_e = 0.40$, a total porosity $\varepsilon_t = 0.64$, an average particle size $dp = 3.5$ μm, and a Kozeny–Carman constant $Kc = 180$. Accordingly, the column permeability is $K_0 = 1.21 \times 10^{-14}$ m^2.

The analysis times and the peak capacities were predicted for 9 columns differing only by their lengths (3.5, 7.0, 10.5, 14, 17.5, 21, 24.5, 35, and 45.5 cm). The maximum pressure drop was fixed at $\Delta P = Pinlet - 1 = 250$ bar. Table 1 lists the initial (PI) and final (PF) inlet pressures at the constant flow rates, F_v^*, in the cF mode, and the initial (Fv, I) and final (Fv, F) flow rates at a constant column back pressure $\Delta P = 250$ bar in the cP mode. Fig. 5.7 shows a typical example of the variations of the pressure and the flow rate in the cF and cP modes for a column 17.5 cm long.

In the constant flow gradient experiment $F_v^* = 1.04$ mL/min), the inlet pressure is expected to increase first from 164.1 to 251.0 bar (the maximum inlet pressure arbitrarily imposed) during the first 10 min of the gradient. This result is consistent with Fig. 5.1 and the viscosity dependence of methanol–water mixtures on the volume fraction of methanol from 5 (≃0.9 cP) to about 45% (≃1.6 cP).

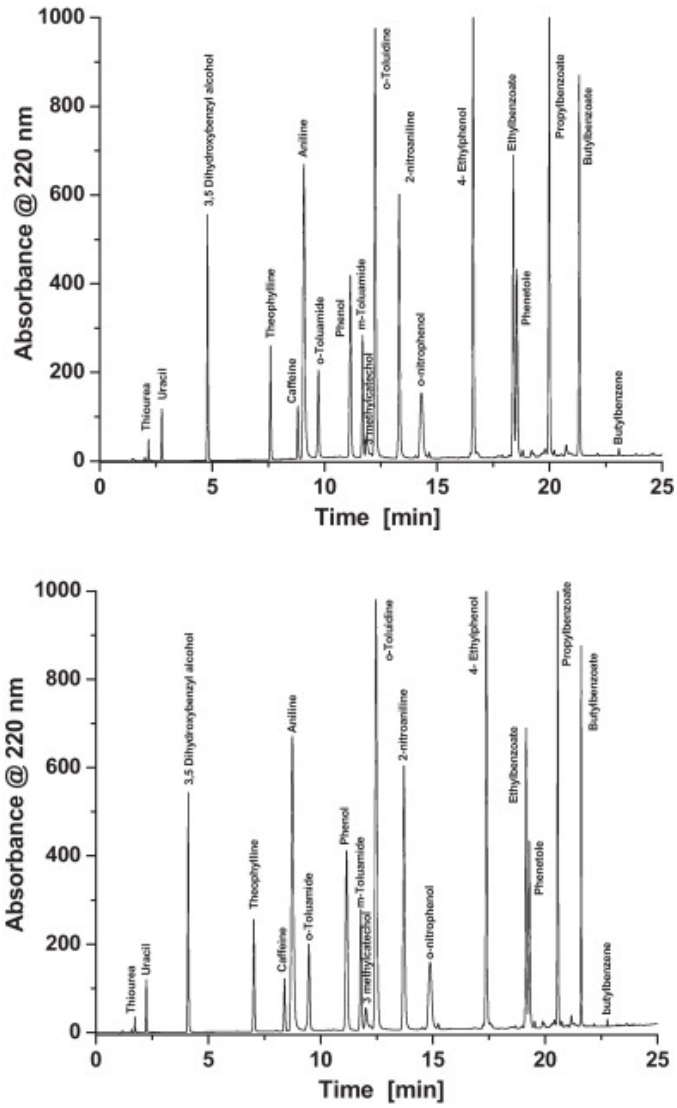

Figure 5.4. Chromatogram Comparison (Cf and Cp). Chromatograms of the nineteen small component mixture in the cF (top graph) and the cP(bottom graph) gradient modes. The column length is L = 15 cm. The constant flow rate and inlet pressure were set at 0.76 mL/min and 197 bar, respectively. The analysis time was about 23 min in both gradient modes. The slope of the linear volume gradient is 0.054 cm^{-3} in both gradient modes. The names of the compounds are indicated in the graph close to their respective peaks. The methanol volume fraction increased from 5 to 95%. T = 298 K. The measured peak capacities are 326 (in cF mode) and 313 (in cP mode).

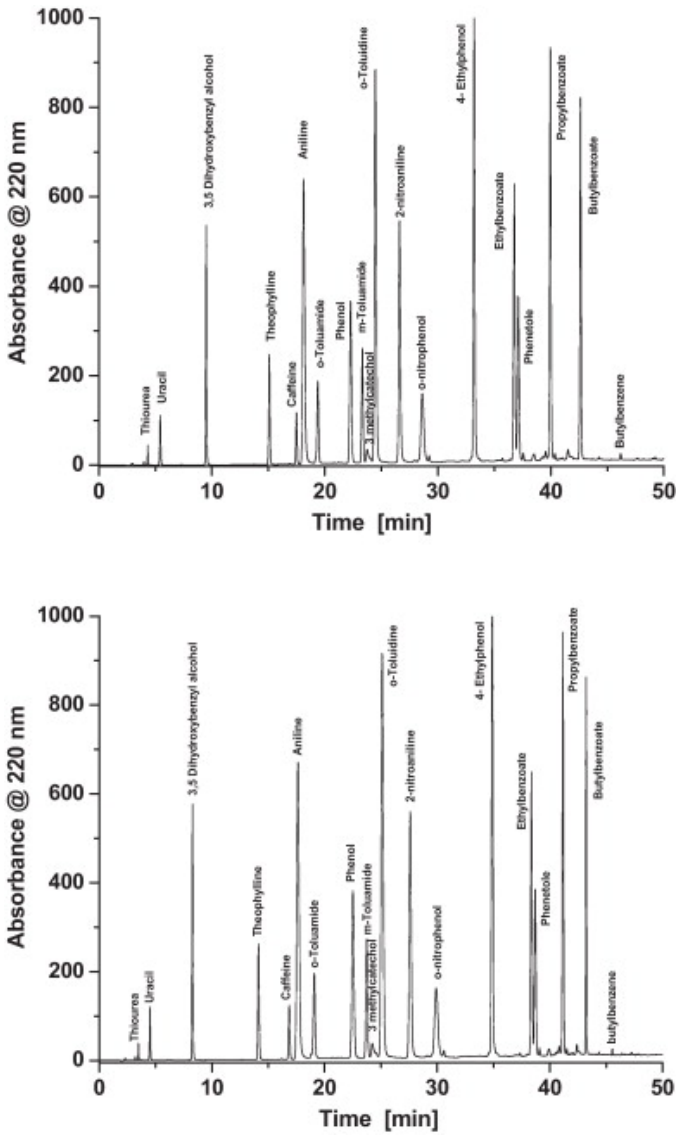

Figure 5.5. Chromatogram Comparison (Cf and Cp 2). Chromatograms of the nineteen small compounds in the cF (top graph) and the cP (bottom graph) modes. The column length is $L = 15$ cm. The constant flow rate and inlet pressure were set at 0.38 mL/min and 99 bar, respectively. The analysis time was about 46 min in both gradient modes. Same linear volume gradient as in Fig. 5.4. The names of the compounds are indicated in the graph close to their respective peaks. The methanol volume fraction increased from 5 to 95%. $T = 298$ K. The measured peak capacities are 315 (in cF mode) and 305 (in cP mode).

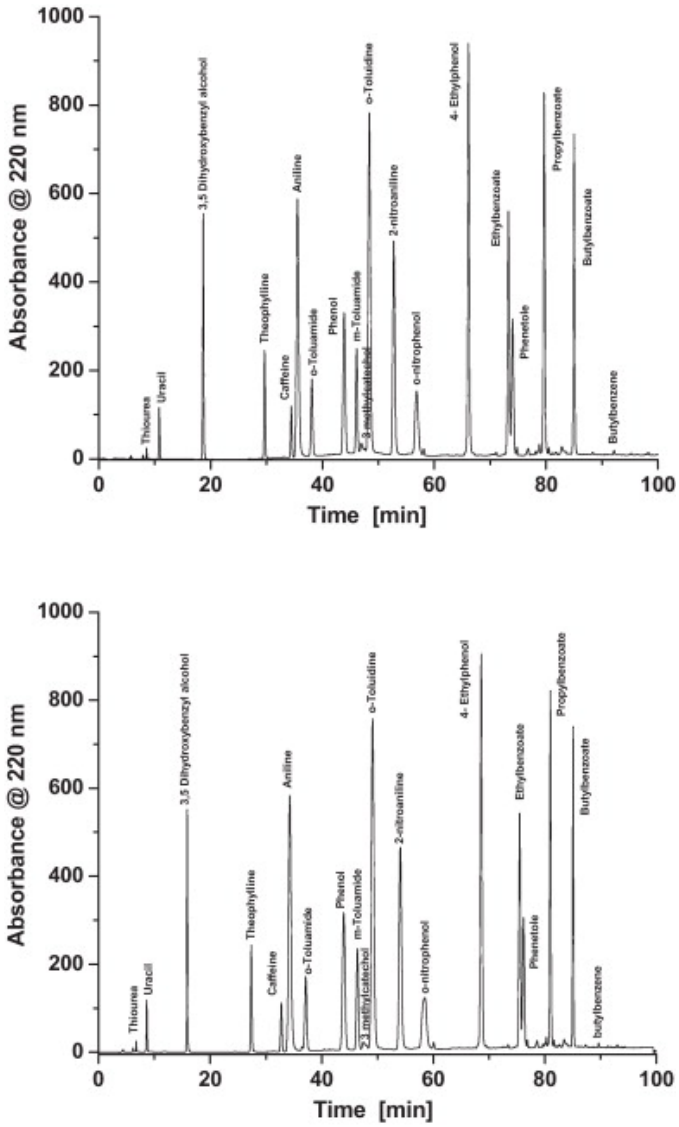

Figure 5.6. Chromatogram Comparison (Cf and Cp 3). Chromatograms of the nineteen small compounds in the cF mode (top graph) and in cP mode (bottom graph). The column length is L = 15 cm. The constant flow rate and inlet pressure were set at 0.19 mL/min and 50 bar, respectively. The analysis time was about 92 min in both gradient modes. Same linear volume gradient as in Fig. 5.4 The names of the compounds are indicated in the graph close to their respective peaks. The methanol volume fraction increased from 5 to 95%. T = 298 K. The measured peak capacities are 286 (in cF mode) and 295 (in cP mode).

In the second part of the cF gradient, the inlet pressure decreases from 251 to 94.2 bar because the eluent viscosity drops down to only about 0.6 cP when the volume fraction of methanol reaches 95%. In the constant pressure gradient experiment, the inverse trend is obviously expected for the variation of the flow rate, which first decreases from 1.79 to 1.04 mL/min (exactly the unique flow rate in the cF mode) and then steadily increases up to 2.75 mL/min.

Table 5.1. Initial and Final Column Inlet Pressures. Initial (*PI*) and final (*PF*) column inlet pressures at constant flow rate (F_v) in cF gradient mode for a maximum pressure drop of 250 bar and initial (Fv, I) and final (Fv, F) flow rates at constant pressure drop (ΔP = 250 bar) in cP gradient mode. The gradient starts with 5% methanol and ends with 95% methanol in water.

Initial and Final Column Inlet Pressures					
Column length [cm]	*PI* [bar]	*PF* [bar]	F_v [cm^3/min]	Fv, I [cm^3/min]	Fv, F [cm^3/min]
3.5	164.1	94.1	5.22	8.97	13.77
7.0	164.1	94.1	2.61	4.48	6.88
10.5	164.1	94.2	1.74	2.99	4.59
14.0	164.1	94.1	1.31	2.24	3.44
17.5	164.1	94.2	1.04	1.79	2.75
21.0	164.1	94.2	0.87	1.50	2.30
24.5	164.1	94.1	0.75	1.28	1.97
35.0	163.7	93.8	0.52	0.90	1.38
45.5	163.2	93.6	0.40	0.69	1.06

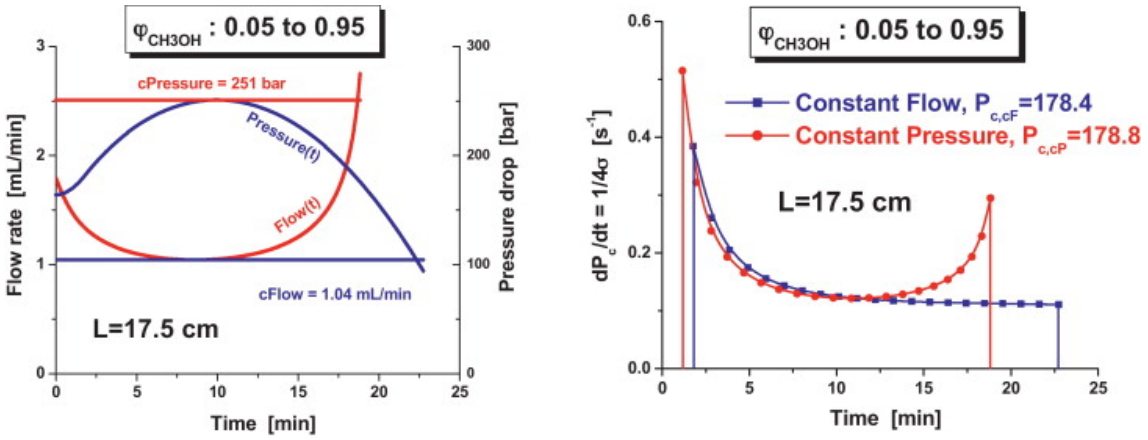

Figure 5.7. Flow Curves and Peak Capacity (Cf and Cp). **Left graph**: Plots of the variable flow rate (at constant pressure, red color) and pressure (at constant flow rate, blue color) *versus* time. The methanol content increases linearly in volume from 5 to 95%. The slope of the linear gradient was set at 0.041 cm^{-3} in order for the last retained compound (LSSM parameter $S = 5$ and $k_{0,21} = 300$) to elute when the end of gradient reached the column outlet. In both cases, the maximum pressure reached during the gradient was 250 bar. **Right graph**: Plots of the derivative of the peak capacity with respect to time obtained from the bandwidths of 21 eluted small compounds ($0 < k_{0,}i < 300$, $S = 5$) evenly distributed across the gradient elution window. The integral of these curves provide the peak capacity (178.4 for the cF gradient and 178.8 for the cP gradient). Note the relative decrease of the analysis time by about -17% from the cF to the cP mode.

Eventually, the calculations showed that the elution times of the least and most retained sample components expected in the cP gradient experiments are 35% (1.16 min *versus* 1.77 min) and 17% (18.83 min *versus* 22.75 min) smaller than those in the cF gradient experiments. This result is consistent with the larger average flow rate during the cP gradient mode, 1.26 mL/min or 21% larger than the constant flow rate in the cF gradient mode (1.04 mL/min), because the column is then operated at the maximum pressure of 250 bar. Figure 5.8 shows the expected variation of the peak capacity per unit time, $\frac{dP_c}{dt}$ or $\frac{1}{4\sigma}$, with the elapsed time t for the same column length $L = 17.5$ cm. Remarkably, despite a

shorter analysis time, the peak capacities or the area underneath the red (cP) and the blue (cF) curves are barely different, at 178.8 and 178.4, respectively.

The advantage of the cP gradient mode takes place with the early eluted, weakly retained analytes and with the last retained ones, which are eluted when the flow rate is significantly larger in the cP gradient mode than the average flow rate in the cF mode. Because the peak widths are inversely proportional to the flow rate at elution and the HETP of small molecules vary little with increasing flow rate, the peak capacities per unit time at the beginning and at the end of the cP gradient are larger than those in the end of the cF gradient. These effects compensate for the gradient time window being narrower in the cP gradient mode than in the cF mode (17.70 min *versus* 20.98 min).

Fig. 5.8 represents the theoretical kinetic plot in the cP and the cF gradient modes when the maximum pressure drop reached during the gradient is 250 bar, for column length increasing from 3.5 to 45.5 cm, as listed above. The plot is provided in a double logarithm scale. Regardless of the column length, the gradient performance in the cP mode is always superior to that in the cF mode. Nearly the same peak capacity is achieved, for a gain in analysis time close to 17%, at all the column lengths.

5.3.3.2 Experimental results

The previous section predicted that when a given separation is made with a given column, the maximum inlet pressure reached during the analysis and the initial and final mobile phase compositions are the same, a cP gradient analysis will provide a 17.3% shorter analysis time than a cF gradient while providing nearly the same peak capacity (±3%). To test the validity of this prediction, we used two identical columns (length L = 15 cm, inner diameter 0.46 cm) packed

with 3.5 µm BEH-C_{18} particles. In the first series of experiments, only one column was used, at the maximum pressure of 250 bar, in the cF gradient mode.

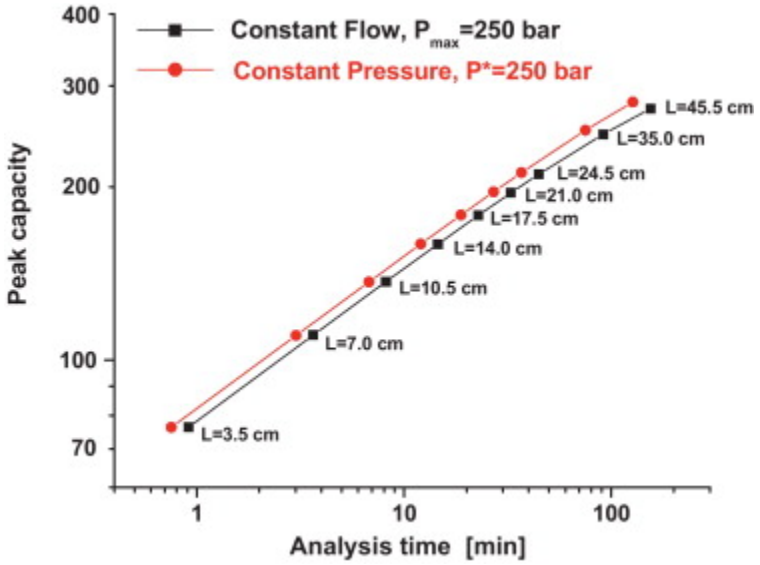

Figure 5.8. Peak Capacity vs. Analysis Time. Theoretical gradient kinetic plots at a maximum constant pressure of 250 bar or the plot of the peak capacity *versus* the analysis time in cF (full black square symbols) and cP (full red circle symbols) modes. The sample is a solution of 21 small molecules ($Dm \simeq 1.5 \times 10^{-5}$ cm^2/s). The column is packed with 3.5 µm fully porous particles. The analysis time is decreasing by about 20% from cF to cP gradient runs while the peak capacity remains about the same.

The corresponding flow rate was $F_v^* = 0.80$ mL/min. The gradient time was set at 22 min. The same volume gradient was then run in the cP mode by setting the pressure (now constant) at P^* = 250 bar. The elution times of the most retained compound (butylbenzene), hence the analysis time were measured at 22.88 min (in the cF mode) and 18.85 min (in the cP mode). Accordingly, the relative decrease of the analysis time was 17.6%, a result in excellent agreement with the theoretical predictions. The peak capacities were measured with Eq. (5.22) at 298 (in the cP mode) and 286 (in the cF mode), e.g., a relative decrease in the peak capacity of –4%. Given that the distribution of the elution times of the real

analytes differ somewhat from those simulated in the theory section (all the simulated peaks were equally distant from each other), the difference between these two results borders on being insignificant.

In the second series of experiments, two identical columns were placed in series (Fig. 5.10). The columns were connected by a 130 µm × 70 mm Viper tubing, which provides the smallest column-connection band broadening available [25]. The maximum pressure during the gradient analyses was also set at 250 bar. The constant flow rate was set at 0.443 mL/min. The experimental analysis times were 47.75 min (in the cF mode) and 37.86 min (in the cP mode), a relative difference of 20.7%. The peak capacities were slightly increased and were measured at 328 (in the cF mode) and 315 (in the cP mode). Again, the relative difference observed is practically insignificant (–4%), which is in good agreement with the theoretical prediction.

5.4 Chapter Summary

The experimental results of this work confirm that gradients performed under constant pressure provide the same peak capacity as those performed under constant flow rates, at constant analysis time or elution time of the most retained sample component provided that the volume gradient is kept the same in both gradient modes. However, this result is so far valid only for non-retained gradients, incompressible eluents, and retention patterns that are not affected by the local pressure.

In practice, this corresponds to gradients carried out under *classical* conditions, with flow rates lesser than 1.0 mL/min and under pressure drops smaller than 250 bar. Under such conditions, the experimental data that we report fully support the recent extension of the classical theory of gradient chromatography in the cF mode to that in the cP mode.

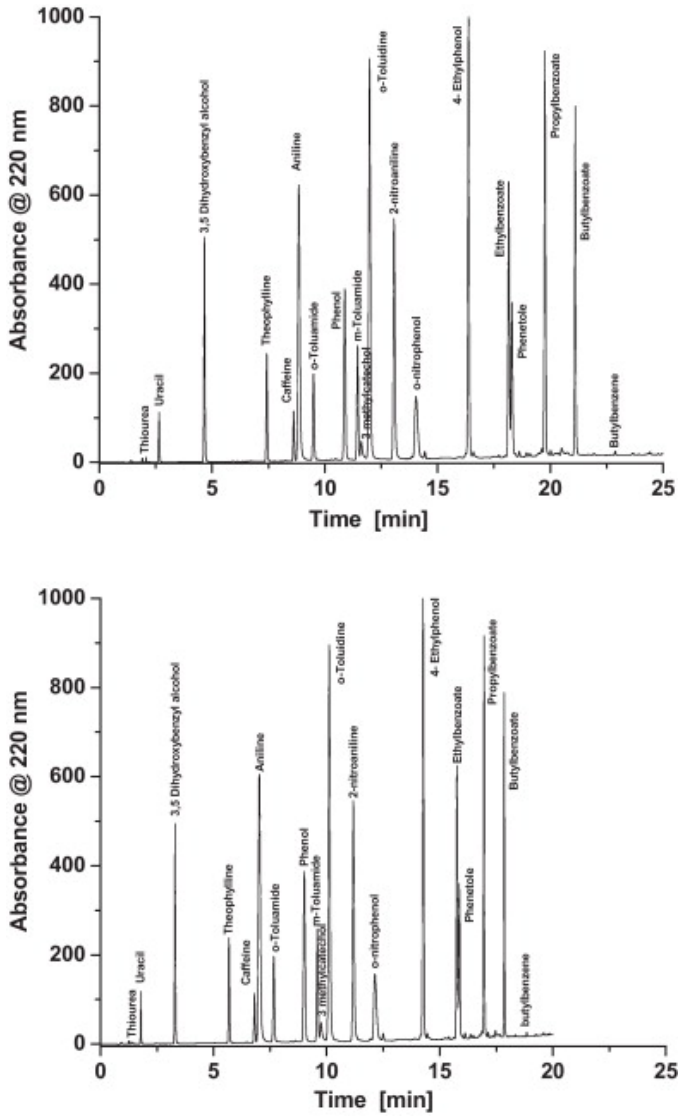

Figure 5.9. Chromatogram Comparison (Cf and Cp 4). Chromatograms of the nineteen small compounds in the cF (top graph) and the cP (bottom graph) gradient modes. The constant flow rate is 1.04 mL/min. Column length L = 15 cm. The maximum inlet pressure was set at 250 bar in both cF and cP modes. Same linear volume gradient as in Fig. 5.4. The names of the compounds are indicated in the graph close to their respective peaks. The methanol are indicated in the graph, close to their respective peaks. The methanol volume fraction increased from 5 to 95%. T = 298 K. The peak capacities are 298 (in cF mode) and 286 (in cP mode).

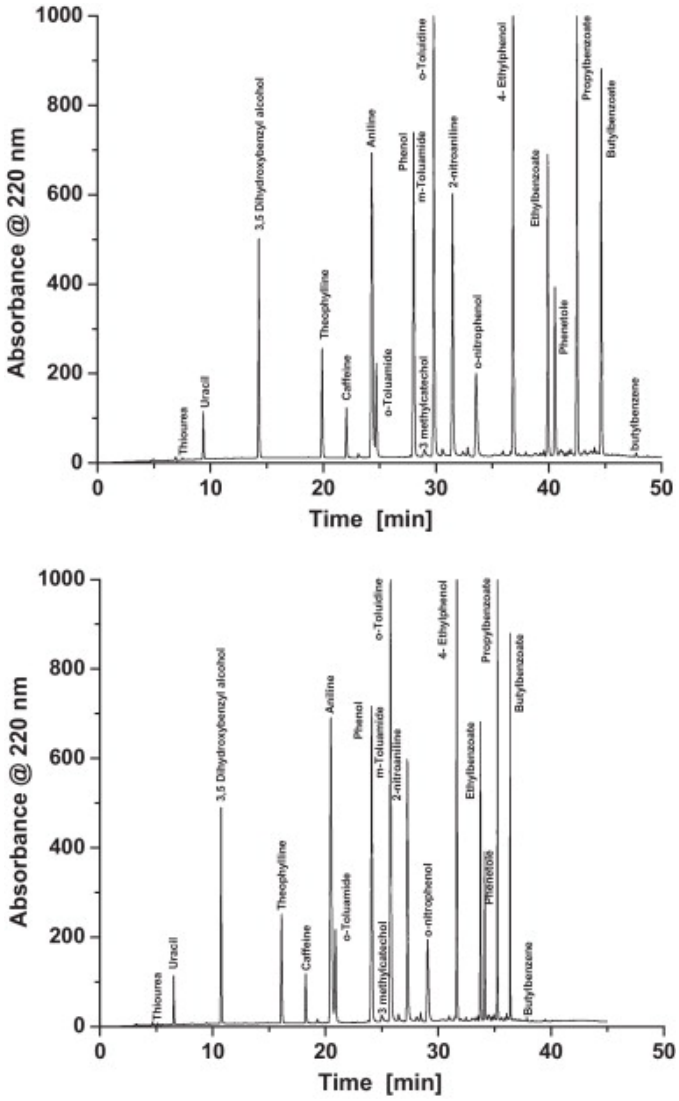

Figure 5.10. Chromatogram Comparison (Cf and Cp 5) Chromatograms of the nineteen small compounds in the cF (top graph) and the cP (bottom graph) gradient modes. The constant flow rate is 0.52 mL/min. Column length L = 30 cm. The maximum inlet pressure was set at 250 bar in both the cF and the cP modes. Same volume gradient as in Fig. 5.4. The names of the compounds are indicated in the graph close to their respective peaks. The methanol volume fraction increased from 5 to 95%. T = 298 K. The peak capacities are 328 (in cF mode) and 315 (in cP mode). In contrast to Fig. 5.9, note the co-elution of phenol and m-toluimide at $t \simeq$ 28 min (in cF mode) and 24 min (in cP mode) and the full baseline resolution of ethylbenzoate and phenetole at $t \simeq$ 40 min (in cF mode) and 34 min (in cP mode).

The predictions of the pressure (for cF gradients) and flow rate (for cP gradients) profiles observed are in excellent agreement with the experimental results for linear volume gradients starting and ending with volume fractions of methanol of 5 and 95%, respectively, the most general case, for which the eluent viscosity first increases (from 0.9 to 1.6 cP, + 80%) then decreases (from 1.6 to 0.6 cP, –60%) during the gradient run.

One potential advantage of the constant pressure mode over the constant flow mode gradients run under low pressures (<250 bar) takes place when the main separation constraint is not the analysis time but the maximum pressure under which the column and/or the HPLC system can be run. For the same linear volume gradient, βv, of methanol in water (from 5 to 95% methanol in volume) and for small molecules, the extended theory of gradient chromatography and the experimental data agree well, showing that the analysis time is about 20% shorter in the cP than in the cF mode while the peak capacity is virtually unchanged. The cP gradient mode benefits from an average flow rate during the gradient run that is larger than the constant flow rate in the cF mode. Since the peak width is inversely proportional to the flow rate (Eq. (5.3)) and the HETP of small molecules varies little or even decreases with increasing flow rate in the low reduced velocity range ($2 < v < 8$, within which the overall HETP is controlled by the longitudinal diffusion HETP term), the peak capacity in the cP mode is comparable to that in the cF mode, despite a 20% smaller gradient elution window.

Obviously, gradient separations are not restricted to the use of long columns and to large analysis times at low back pressures. Most gradients are now performed above the optimum velocity, where the HETP usually increases with increasing flow velocity. Therefore, the conclusions of a more general comparison between the performance of the cP and the cF gradient mode separations performed with

short modern columns packed with fine particles could be different. It remains possible that cP gradients would not always outperform cF gradients performed under inlet pressures as high as 1 kbar, with short columns and large molecules. Further experimental investigations are currently under way in order to explore the relative performance of cP and cF mode gradients in vHPLC, with higher molecular weight compounds than those used here, such as peptides and proteins. Under these more complex conditions, no model is yet available to predict the kinetic performance of the cP and the cF modes because neither the compressibility of eluents nor the influence of the pressure on their viscosity can be neglected any longer, the column is no longer isothermal, the gradient is retained with modifiers like acetonitrile, and the effect of the pressure on the retention factors of peptides and proteins can no longer be neglected in RPLC.

CHAPTER VI
REPRODUCIBILITY OF ANALYTICAL DATA AND INFLUENCE OF DELAY BETWEEN SUCCESSIVE RUNS

6.1 Introduction

Chromatographic separations are often performed in gradient elution when the sample is complex and contains compounds with properties leading to a wide range of retention times. Such separations are often performed in the pharmaceutical, biochemical and food industries where the analysis time is important and analysts are trying to minimize it. Because large batches of samples are often analyzed under similar conditions, the re-equilibration time between successive analyses affects the throughput.

For over forty years, the general trend to limit analysis time has been to reduce the column length while maintaining efficiency. This was achieved by packing the columns with finer particles using improved packing procedures. In the process, the optimum flow rates at which columns are operated is increased, contributing to reduced analysis times. However, this approach is now reaching its limits. The permeability of columns decreases with decreasing particle size and the pressure needed to force the required flow through the columns now exceeds 1000 bar with the finest particles currently used. This led to the modern method of very high pressure liquid chromatography (VHPLC).

Unfortunately, operating columns with high inlet pressures comes with a consequence. The mobile phase stream expands endothermally during its migration along the column but friction against the particles of the bed through which it percolates generates heat. The heat power generated by the eluent flow is proportional to the product of the flow rate and the pressure gradient. While this power was negligible with the columns used ten years ago, it is now potent enough to affect the column efficiency.

An issue that arises in VHPLC is that an increased heat power is generated by the mobile phase flowing through densely packed columns at pressures exceeding 300 bar [33,38]. Raising the pressure to increase the separation speed may impact the thermal equilibrium throughout the column, endangering the reproducibility of measurements and slowing the throughput by increasing the time required to return to thermal equilibrium. The equilibration time between injections is as important as the net time of the separation [12-14]. Decreasing the analysis time by increasing the flow rate of the separation beyond the optimal flow rate of the column, decreases the net peak capacity. An overview of the theoretical and practical advantages of constant pressure gradient elution mode VHPLC was presented by Verstraeten et al. who confirmed retention time shifts due to viscous heating and pressure effects. They applied a volume-based reconstructed time scale to demonstrate repeatability between constant pressure and constant flow modes [39].

Based on the theory and potential advantages of gradient separations performed under steady state temperature [40-41], the goal of this work is to demonstrate an approach that optimizes column efficiency in VHPLC and produces fast reproducible separations with minimal equilibration time. Column efficiency is determined by monitoring changes in the band variance [42] and demonstrated by time based chromatograms. Cabooter et al. and Clicq et al. presented works regarding the performance of high temperature liquid chromatography systems, using kinetic plots [43-44]. Other important findings regarding column equilibrium times with buffered eluents were discussed by Schellinger et al. [45-46].

6.2 Theory

To permit a critical analysis of the data, moment analysis was used to determine column efficiencies and to interpret chromatograms. Common metrics used in chromatography to evaluate the quality of separations are based on the use of the peak height, the peak width at half-height, the retention time, and the peak

area. Peak height is rarely used to estimate concentrations, since the height of a band can vary greatly with the linear velocity of the separation and the column temperature. The use of the peak width at half height is misleading since calculating the column efficiency from a single measurement of the band width made at a considerable distance above the baseline does not provide an accurate estimate of the degree of band broadening [15]. Cracks or small gaps in the column bed or in connections contribute to band variance due to diffusion and eddies and affect the peak base far more than its width. A recent work shows the influence of connections on apparent efficiency [47].

6.2.1 Determination of the concentrations of sample components

The purpose of most analyses involving gradient elution is to measure the composition of a sample. For these measurements to be accurate and precise, the amount of each compound is determined from the area of the peak recorded using a calibration curve. If the response of the detector used is proportional to the mass flow rate of the sample component at the column exit (e.g., in mass spectrometry), the peak area is independent of the mobile phase flow rate [48]. If the detector responds to the component concentration in the mobile phase (e.g., with spectrophotometric detectors), the peak area is inversely proportional to the flow rate [48-51]. As indicated later, the volume flow rate of the mobile phase varies in gradient elution, unless this flow rate is kept constant. Even in this case, if the heat power generated by the mobile phase stream is significant, the thermal expansion of the mobile phase may cause the flow rate to increase. The flow rate during gradient elution analyses may change because the mobile phase composition varies widely (e.g., 50–95% acetonitrile in water).

For a detector responding to component mass flow rate, one calibration curve will remain valid for all gradient conditions, since the areas measured are independent of the mobile phase flow rate. Ideally, detection by mass spectrometry would apply. For the UV detector frequently used in HPLC [48-51], the peak area, A, is given by equation 6.1:

$$A = \frac{Sm}{F_v} \qquad \text{Eq. (6.1)}$$

where *m* is the mass of compound eluted, *Fv* is the volume flow rate of the mobile phase and *S* is a response factor that depends on the component spectrum, the detection wavelength and the data station characteristics. Analysts may determine calibration data by injecting solutions of the analytes and running gradient elution under the same conditions or they may measure the product *AFv* and use it for calibration. The advantage of the first approach is that the variation of the flow rate during a gradient measurement is slow and does not deviate much from a linear variation. The second method corrects for variations of the flow rate but it requires accurate measurements of that flow rate, which is recorded by the data station.

The Chemstation software of the Agilent instrument includes a command macro that allows the analyst to export data to other software with the chromatogram expressed as a function of the volume of mobile phase eluted. This volume based chromatogram can be integrated. The Chemstation provides chromatograms in units of minutes, the output of the macro being a volume based chromatogram where 1 min is equivalent to 1 mL. When the volume based chromatogram is integrated by the Chemstation, the peak area is expressed in mAU × min (milliabsorbance units × min), but it can be converted to mAU × mL by dividing the area by 60. This series of separations was conducted using a fixed volume of sample for all the experiments, with a presentation of the response factors obtained in each method.

6.3 Experimental

6.3.1 Instruments

The experiments were conducted in a 24 ℃ laboratory, using an Agilent 1290 Infinity System (Agilent Technologies, Waldbroen, Germany). This instrument was equipped with a diode-array UV detector having a low flow cell volume (600 nL) and an Agilent Ultra Low Dispersion kit. The Agilent 1290 comes equipped with a programmable auto-sampler and is controlled by the Chemstation Software.

6.3.2 Columns

A Thermo Viper (130 µm I.D.) column connection unit (Dionex-Fisher, Sunnyvale, CA, USA) was used to connect the Agilent Technology Poroshell 120 EC-C18 (4.6 × 100 mm; 2.7 µm particle size) and the Waters Xbridge BEH C18 XP (4.6 × 100 mm; 2.5 µm particle size) columns to the instrument. The columns were insulated with 2 layers of paper towels, which act as a buffer between the ambient air in the laboratory and the column wall. The Thermo Viper connection unit provides low volume connections and small dispersion induced extra-column band broadening contributions [47]. Unfortunately, the size of these connections does not allow the door of the instrument to be closed and the column must rest outside the oven.

6.3.3 Reagents

Fisher Scientific (Fair Lawn, NJ, USA) HPLC grade water and acetonitrile were used. The test samples for all experiments were the components in a 1 µL of the Agilent RPLC checkout sample injected at post run times of 0, 1, 3, 5, 8, 11 and 15 min (n = 6 for each of the post run times).

6.3.4 Procedures

Our objective was to estimate how much the equilibration time between consecutive gradient separations affects the reproducibility of the separations. We presumed that the heat gained or lost by the column bed during the gradient and the steps under isocratic conditions following the gradient, during which the column is regenerated and the next sample injected, might impact the reproducibility of subsequent separations. Conducting gradient analysis under constant flow rate or constant pressure conditions changes the extent of the heating/cooling of the column. Therefore the equilibration time required to achieve reproducible results differ for different modes of analysis. Also columns packed with fully porous and with core–shell particles dissipate heat at different rates [52-54].

A series of similar measurements were performed with two columns, one packed with core–shell particles, the other with fully porous particles. Both columns were operated under the same gradient conditions. All the experiments were conducted at room temperature, approximately 24 ℃. Five procedures were used for each column. The first series of measurements was conducted under constant flow rate. This flow rate was chosen to yield a maximum inlet column pressure just below the highest operating pressure recommended for the column by its manufacturer.

A second series of experiments was performed under a constant inlet pressure chosen to provide a net analysis time equivalent to that achieved in the previous series. A third series of experiments used a constant inlet pressure just under to the maximum pressure recommended by the manufacturer.

For the fourth series of measurements, the gradient parameters based on the flow rate and solvent composition recorded during the third series of

measurements were put into the instrument software. This was done in order to keep the column maximum operating pressure close to the value set in the third series. For these measurements, neither the flow rate nor the inlet pressure was kept constant. Instead, the instrument set the mobile phase flow rate as based on the flow rates and mobile phase compositions input provided by the method.

The gradient parameters for the fifth series of measurements were calculated to maintain the net amount of heat lost by the column wall during the gradient and the post run times. For this purpose, a program was written in Microsoft Excel to implement the method described by Gritti and Guiochon [41]. The program requires many physicochemical properties of the column and mobile phase, the column inner and outer radii, the mobile phase temperature at the column inlet and outlet, the columns permeability, the dwell volume, the column hold-up volume, the viscosity, the density, the expansion coefficient of the mobile phase as a function of the mobile phase composition during the gradient, and the ambient temperature. A detailed explanation of this method is provided in reference number 8. This method is a refinement of a previous work [40].

6.3.5 Experiments performed using the Agilent Poroshell column (core–shell column)

The constant flow conditions used a solvent gradient consisting of 50–95% (water/acetonitrile) delivered over 2.1 min at a flow rate of 2.8 ml/min. This flow rate was selected so that the inlet pressure at the start of the gradient was 530 bar (safely under the maximum recommended operating pressure for the column). Six consecutive 1 µL injections of the Agilent RPLC checkout sample were performed. The wavelength monitored was 245 nm with a bandwidth of 4.0 nm and a sampling rate of 160 Hz. Analyses were carried out using successively each of the following wait times: 0, 1, 3, 5, 8, 11, and 15 min for all the experiments described. There was a 15 min wait period between experimental series (i.e., there was a 15 min post run time after the six injections

had been made with the same equilibration time) to bring the column back to a stable initial temperature.

The constant pressure gradient conditions were based on the volumetric gradient conditions, with the volume of the mobile phase eluted dictating the mobile phase composition. For this first series of experiments made under moderate constant pressure, the back pressure was maintained at 435 bar. This yielded chromatograms providing almost the same analysis times as those observed under constant flow rate conditions. The third series of experiments was carried out under constant pressure at the maximum operating pressure allowed by the column and the instrument. The Agilent column can safely withstand inlet pressures of 600 bar. The limiting parameter of this analysis was determined by the instrument pump, which cannot deliver solvent at flow rates above 5 mL/min. The maximum constant pressure separations were done at 510 bar, which kept the mobile phase flow rates below 5 mL/min. The fourth series of experiments involved the programming of semi-constant pressure measurements (flow programmed constant pressure analysis) run with a flow controlled method. This was done by manually inputting the flow rates and solvent compositions parameters measured during the 510 bar constant pressure gradient run. These parameters include the gradient composition and the flow rates which are input into the Chemstation, as a new method file in 3 s increments to mimic the experiments in which the instrument is operated under constant pressure. This approach was devised in an attempt to increase the reproducibility of the constant pressure separations, since the flow rates in each experiment would not be altered by the column permeability, which may not always be constant. The fifth series of experiments were constant heat loss experiments with the parameters selected to run at the fastest possible flow rates the instrument and column could tolerate.

6.3.6 Experiments performed using the Waters BEH XP (fully porous) column

The constant flow rate conditions included a solvent gradient consisting of 50–95% (water/acetonitrile) delivered over 2.45 min at a flow rate of 2.3 ml/min. This flow rate was selected so that the inlet pressure at the start of the gradient was 550 bar (safely under the maximum recommended operating pressure for the column of 620 bar). Six consecutive 1 µL injections of the Agilent RPLC checkout sample were performed successively. These analyses were carried out with the following wait times: 0, 1, 3, 5, 8, 11, and 15 min for all the experiments described. There was a 15 min wait period between experimental series (i.e., there was a 15 min post run time after the six injections had been made with the same equilibration time) to bring the column back to a stable initial temperature.

For the second series of experiments, the inlet pressure was maintained at 433 bar (constant pressure analysis under moderate pressure); this yielded chromatograms with analysis times similar to those achieved in the constant flow rate experiments. The third series of experiments was also carried out under constant pressure but at 550 bar (constant pressure analysis at maximum pressure). The fourth series of experiments involved the programming of semi-constant pressure measurements run with a flow controlled method (flow programmed constant pressure analysis). This was done by manually inputting the flow rates and the solvent compositions parameters measured during the 550 bar constant pressure gradient run. These parameters include the gradient composition and the flow rate in 3 s increments to mimic experiments during which the instrument is operated under constant pressure. This approach was devised in an attempt to increase the reproducibility of constant pressure separations, since the flow rates in each experiment would not be affected by the column permeability, which is not always constant. The fifth series of experiments were constant heat loss experiments with the parameters selected

to run the instrument and column at the fastest possible flow rates they could tolerate.

6.4 Results and Discussion

Figures 6.1-6.5 (A) and (B) show how the average peak width shifts for injections with different post run times. Peak widths relate to the peak capacity of separations and govern the limits of detection. Parts C and D are of interest in assessing the reproducibility of peak widths for a given post run time. If the RSDs of the second moment are under 2.5%, the column is operating at a highly reproducible thermal state with the set of equilibration times considered. The RSDs of the retention times vary depending on the method of delivering the gradient, as shown in Figures 6.1-6.5 (E) and (F). Analysts interested in quantitative analysis will find differences in the response factors, displayed in Figures 6.4 and 6.5 as perhaps the most critical metrics discussed, since they may impact the accuracy of quantitation.

6.4.1 Constant flow analysis

Figure 6.1 shows the average values of the second central moments of the nine analytes in the Agilent RPLC checkout sample for the Agilent Poroshell column (Fig. 6.1A) and for the Waters column packed with fully porous particles (Fig. 6.1B). In conventional solvent gradients, if the concentration of the mobile phase modifier increases beyond 25% acetonitrile, the mobile phase viscosity decreases and the frictional heat generated decreases. Increasing the column equilibration time causes the column to progressively warm up since more time is spent operating the column under a higher pressure. The eluted peaks of analytes in the RPLC checkout sample are sharper since the column temperature is higher, and a downward shift of the second moment is observed as the equilibration time increases.

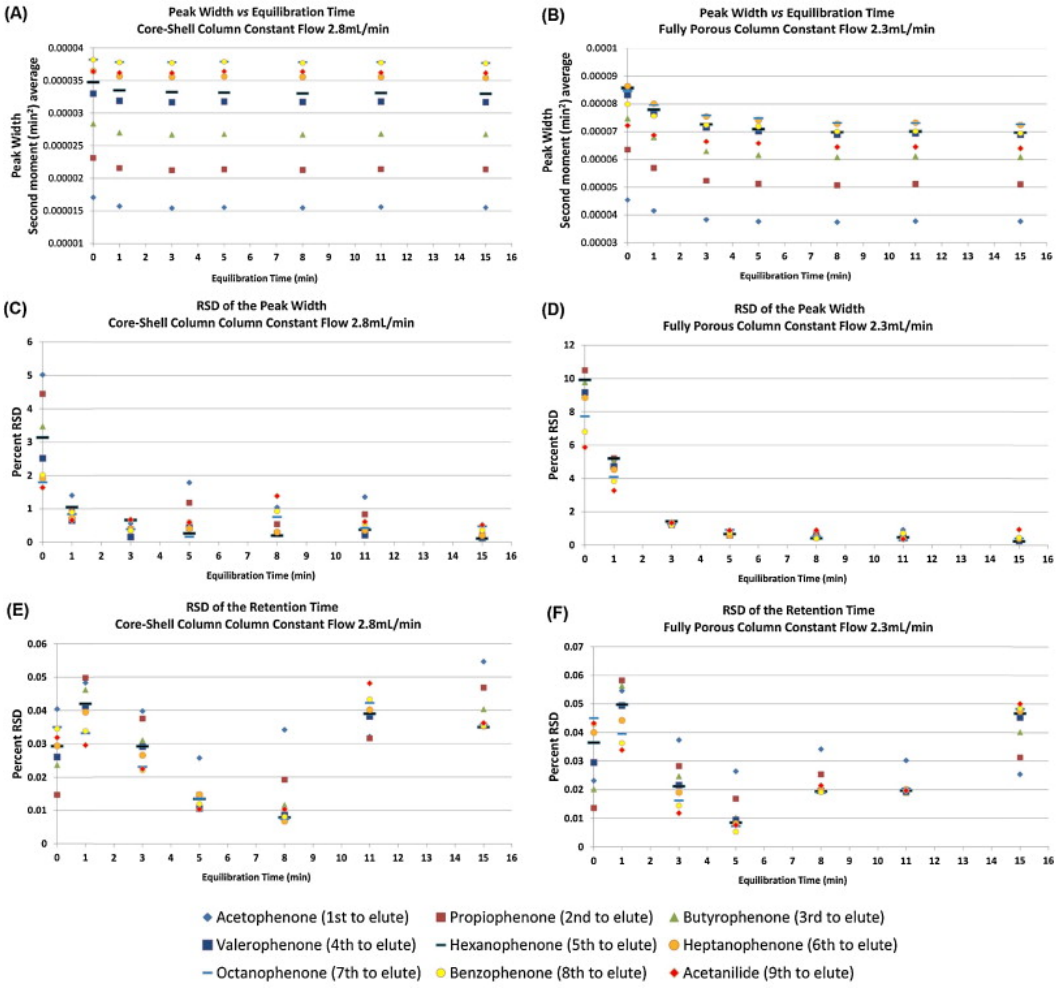

Figure 6.1. Constant Flow Moment Analysis. Part (A): the average second central moment vs equilibration time for the Poroshell column at a flow rate of 2.8 mL/min with $n = 6$. Part (B): the average second central moment vs equilibration time for the BEH column at a flow rate of 2.3 mL/min with $n = 6$. Part (C): the percent relative standard deviation for the second moment vs the equilibration time for the variance values using the Poroshell column at a flow rate of 2.8 mL/min. Part (D): the percent relative standard deviation for the second moment vs the equilibration time for the variance values using the BEH column at a flow rate of 2.3 mL/min. Note that overall the Poroshell column demonstrates a higher degree of reproducibility for variance values, due to its core–shell particles being able to dissipate heat at a faster rate than the BEH column with fully porous particles.

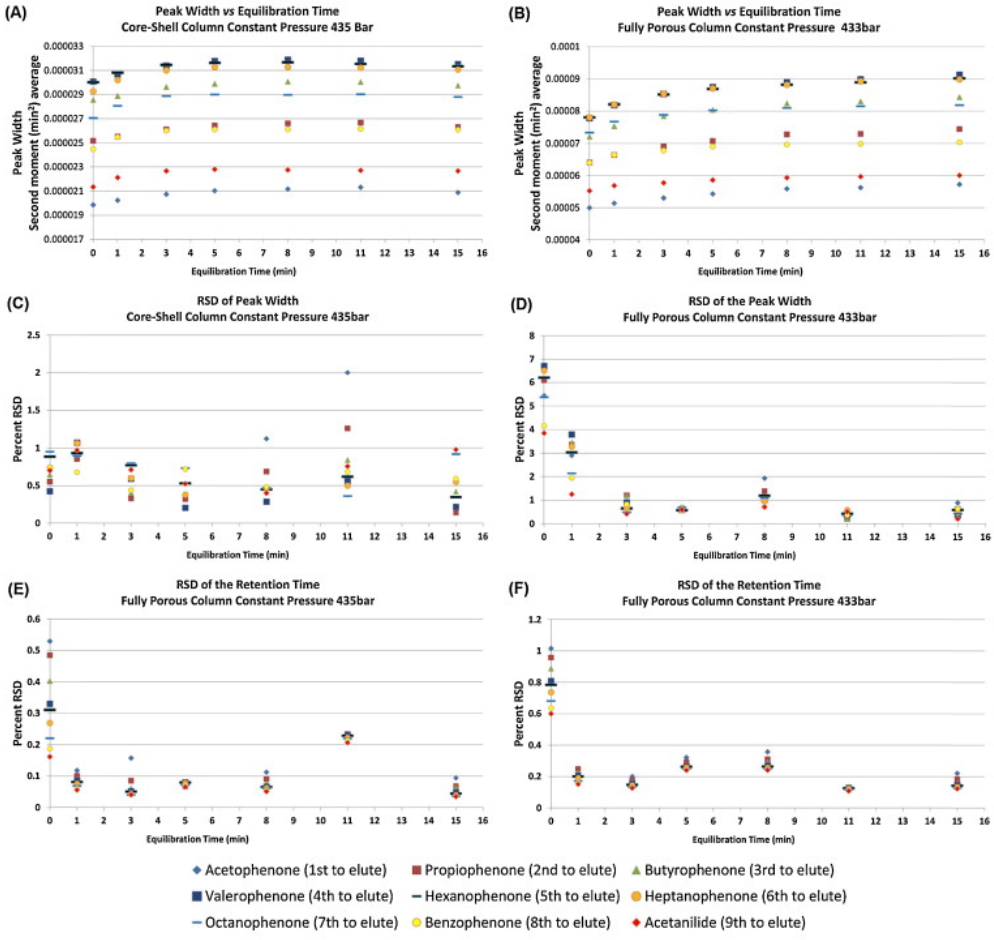

Figure 6.2. Constant Low Pressure Moment Analysis. Part (A): the average second central moment vs equilibration time for the Poroshell column using constant pressure conditions of 435 bar with $n = 6$. Part (B): the second central moment vs equilibration time for the BEH column using constant pressure conditions of 433 bar with $n = 6$. Part (C): the percent relative standard deviation for the second moment vs the equilibration time for the variance values with the Poroshell column using constant pressure conditions of 435 bar with $n = 6$. Part (D): the percent relative standard deviation for the second moment vs the equilibration time for the variance values with the BEH column using constant pressure conditions of 435 bar with $n = 6$. Part (E): the average first moment values for the same series of experiments as (A) and (C). Part (F): the average first moment values for the same series of experiments as (B) and (D). The BEH column suffers from poor precision when there is an insufficient post run time.

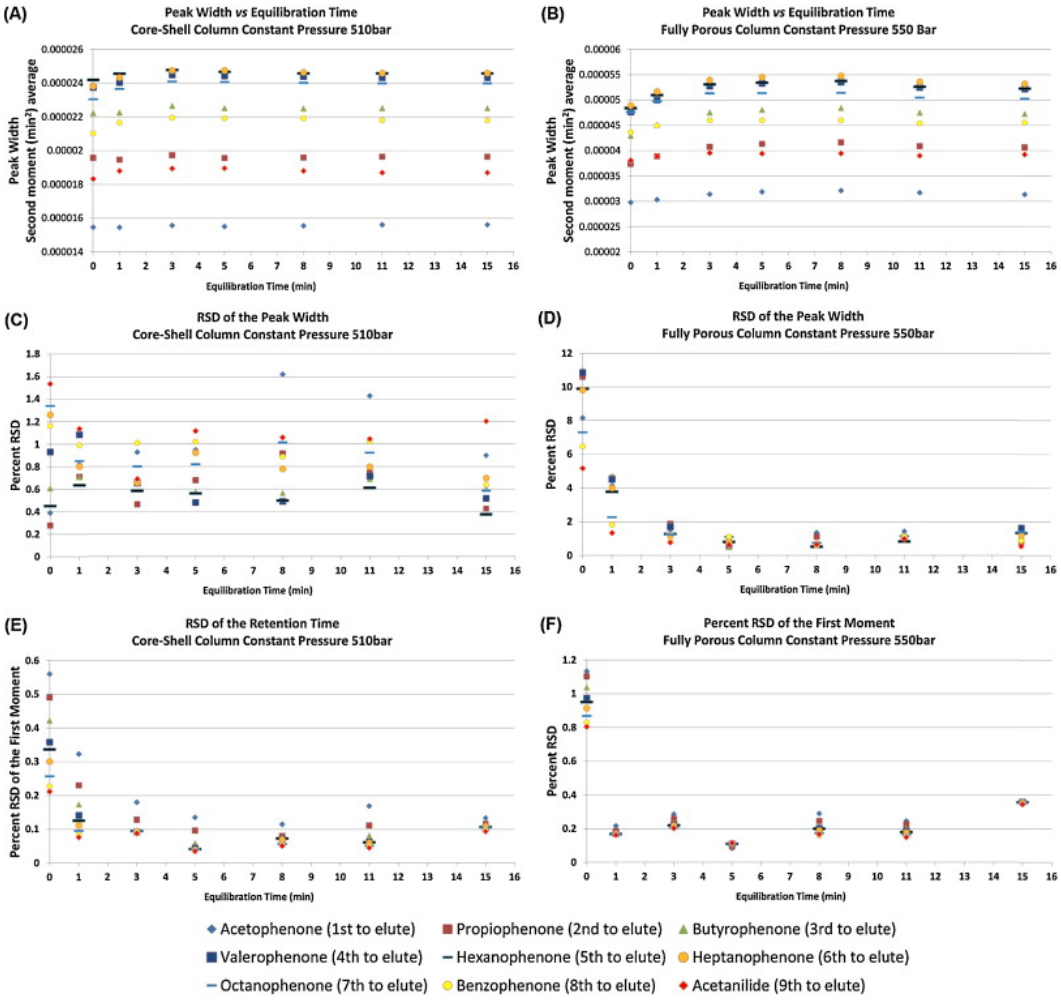

Figure 6.3. Constant High Pressure Analysis. Part (A): the average second central moment vs equilibration time for the Poroshell column using constant pressure conditions of 510 bar with $n = 6$. Part (B): the second central moment vs equilibration time for the BEH column using constant pressure conditions of 550 bar with $n = 6$. Part (C): the percent relative standard deviation for the second moment vs the equilibration time for the variance values with the Poroshell column using constant pressure conditions of 510 bar with $n = 6$. Part (D): the percent relative standard deviation for the second moment vs the equilibration time for the variance values with the BEH column using constant pressure conditions of 550 bar with$n = 6$. Part (E): the average first moment values for the same series of experiments as (A) and (C). Part (F): the average first moment values for the same series of experiments as (B) and (D).

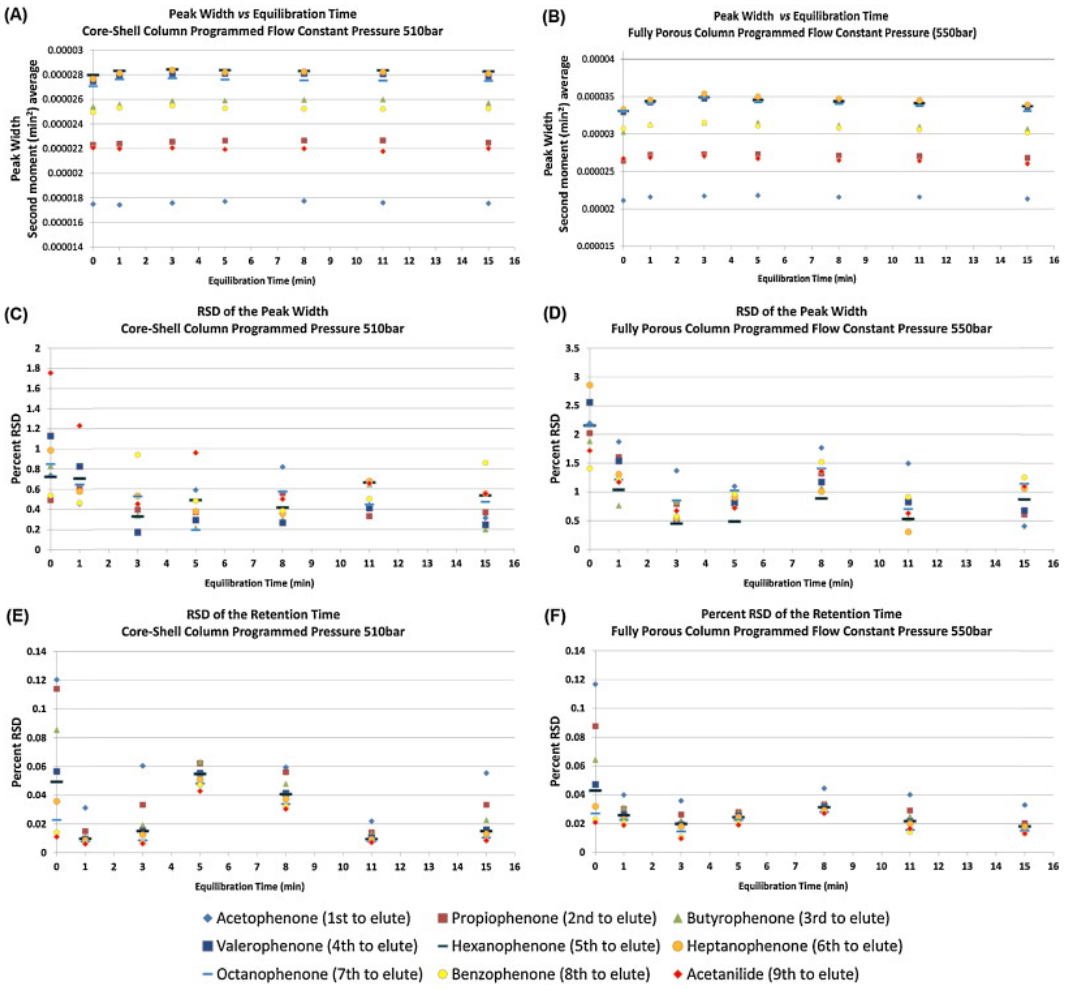

Figure 6.4: Programmed Flow Constant Pressure Moment Analysis. Part (A): the average second central moment vs equilibration time for the column packed with core–shell particles, using programmed flow constant pressure conditions of 510 bar with $n = 6$. Part (B): the average second central moment vs equilibration time for the column packed with fully porous particles using programmed constant pressure conditions of 550 bar with $n = 6$. Part (C): the relative standard deviation for the second moment for the data in (A). Part (D): the relative standard deviation for the second moment for the data in (B). Part (E): the average first moment values for the same series of experiments in (A) and (C). Part (F): the average first moment values for the same series of experiments as (B) and (D). Programming the instrument to deliver a dynamic flow rate in time appears to be a much better strategy for performing reproducible VHPLC separations under pseudo constant pressure conditions.

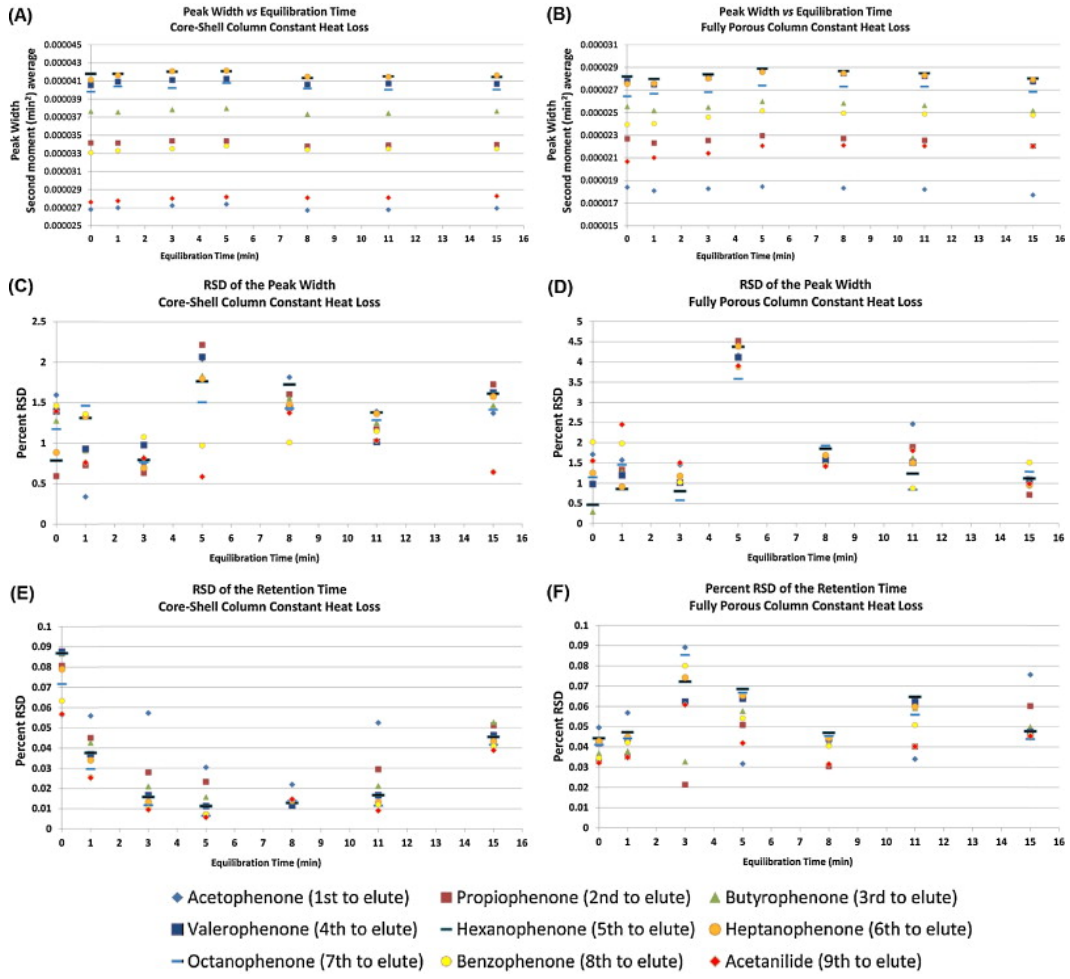

Figure 6.5. Constant Heat Loss Moment Analysis. Part (A): the average second central moment vs equilibration time for the Poroshell column using the constant heat loss method with $n = 6$. Part (B): the second central moment vs equilibration time for the BEH column using the constant heat loss method with $n = 6$. Part (C): the percent relative standard deviation for the peak width vs the equilibration time for the data obtained in part (A). Part (D): the percent relative standard deviation for the peak width vs the equilibration time for the variance values for the data collected in part (B). Part (E): the average first moment values for the same series of experiments as (A) and (C). Part (F): the average first moment values for the same series of experiments as (B) and (D).

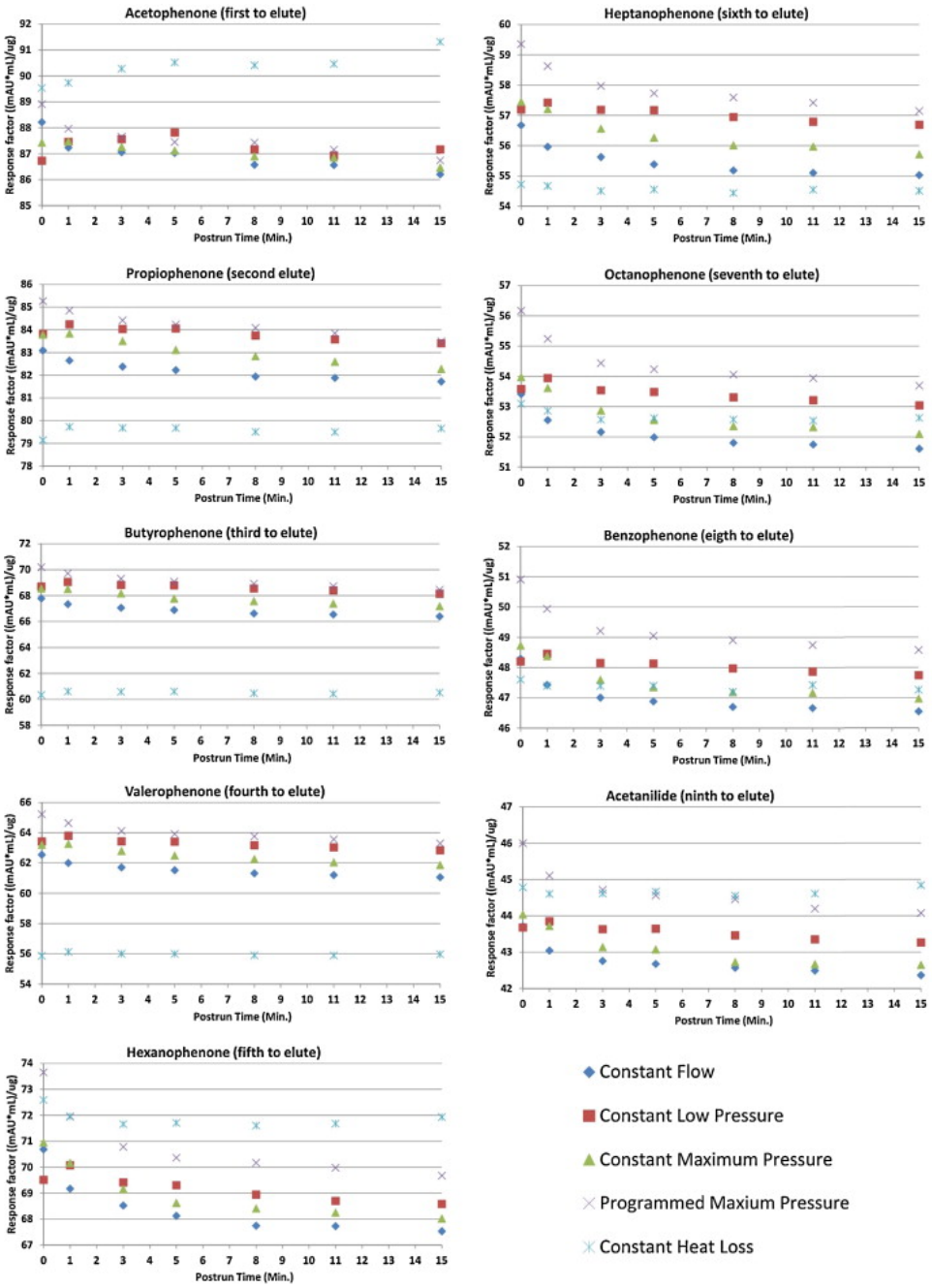

Figure 6.6. Response Factors Core–shell Column. Response factors for the nine sample components for the core–shell column (Agilent) using the discussed methods (n = 6).

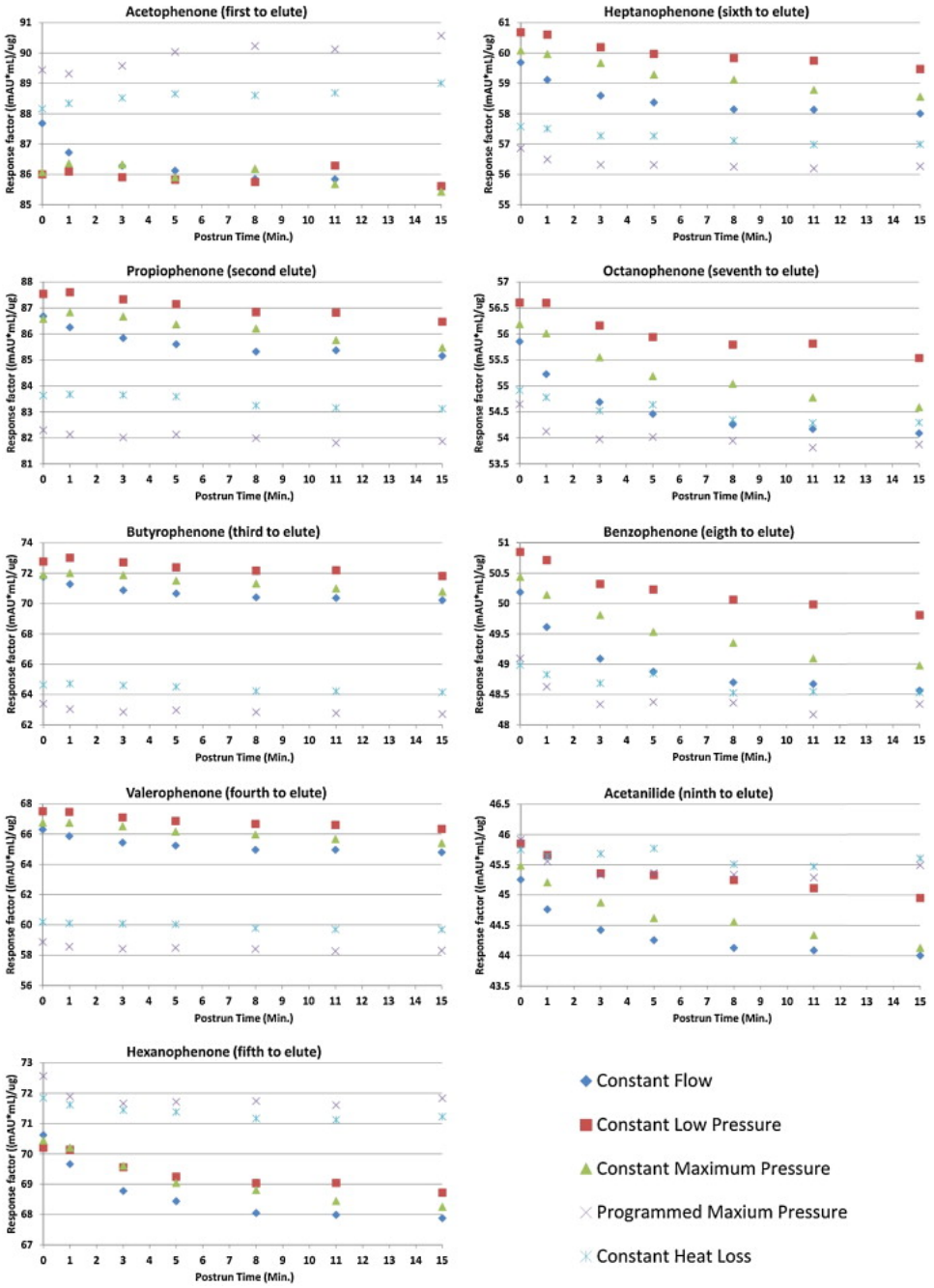

Figure 6.7: Response Factors Fully Porous Column. Response factors for the nine sample components for the fully porous column (Waters) using the discussed methods (n = 6).

The variation of the peak widths (given as the peak variance) shows how to estimate the equilibration time needed to bring the column back to its initial starting temperature. The column packed with core–shell particles requires about 1 min of post run time to generate nearly constant peak widths. The column packed with fully porous particles requires approximately 5 min of post run time to achieve constant peak widths for each consecutive injection. It is not surprising that the first column dissipates heat faster than the second one since the heat conductivity of its bed is higher [53]. This 4 min decrease in the equilibration time is important since the separation itself takes less than 3 min to perform. In a long series of repetitive analyses this gain in throughput is valuable.

Figure 6.1(C) shows the relative standard deviations of the band widths of the nine probe compounds eluted from the core–shell particle column. Figure 6.1(D) shows the same standard deviations for the peaks eluted from the fully porous particle column. The former column gives highly reproducible data after only 1 min of equilibration time and waiting 3 min between injections would improve the reproducibility of the data further but longer wait periods seem to generate less reproducible data, except for the longest wait period (15 min). The second column yields reproducible peak widths after 3 min and waiting 5 min between injections would improve the reproducibility further.

The relative standard deviations of the first moment for all chromatograms in both series of constant flow experiments were below 0.06%, as shown in Figure 6.1 (E and F) for the two columns. The data for the retention times show only minor differences for both columns.

6.4.2 Constant pressure analysis. Part 1: Equivalent analysis time as the constant flow experiments

Fig. 6.2 shows the average values of the second central moments of the nine analytes in the Agilent RPLC checkout sample for the Agilent Poroshell column

(Fig. 6.2A) and the Waters BEH column (Fig. 6.2B). The trend in both graphs is that the second moment increases with increasing equilibration time, indicating that the peaks become more diffuse. In these experiments, the net heat generated by the mobile phase stream when it flows through the column increases during the gradient separation. Longer equilibration times have a cooling effect on the column, which is why the peak variances increase. Appropriate equilibration times can be estimated for both columns operated under constant pressure based on the average values of the second moments. For the Poroshell column a 5 min post run time appears to be sufficient to bring the column to thermal equilibrium. The Waters BEH column needs longer than 5 min to reach equilibrium. The second moments of the bands keep increasing for the entire 15 min post run times. It appears that columns need longer times to dissipate heat away than to absorb heat from the mobile phase.

Fig. 6.2C and D shows the RSD for the second central moments of the bands eluted from the Agilent and Waters columns respectively. The Poroshell column gives reproducible chromatograms for all post run times. The BEH column produced highly reproducible peak variances for 3 min post time runs or more. However, a 1 min equilibration time was insufficient to achieve highly reproducible results. These graphs demonstrate also that under ambient conditions it may not be advantageous to wait for long periods of time, as shown by the 11 min post run time data for the Agilent column and the 8 min post run time for the Waters column.

Fig. 6.2E and F shows the RSD for the first moments for the two columns. Shifting from constant flow rate to constant pressure gradients caused a one order of magnitude increase in the RSD although the values do not exceed 1.2%. Both columns may yield highly reproducible retention times with equilibration times of 1 min. However, the gradual increase of the variances for both columns should not be overlooked.

6.4.3 Constant pressure analysis. Part 2: Maximum pressure

Fig. 6.3 shows the average values of the second central moments of the nine analytes in the Agilent RPLC checkout sample for the Agilent Poroshell column (Fig. 6.3A) and the Waters BEH column (Fig. 6.3B) for the experiments performed at the highest possible constant pressure. The Poroshell column gave more constant values of the second central moment and yielded peaks having a fairly steady variance even when no equilibration time was used. The BEH column requires 3 min of post run time to achieve the same degree of stability. When the post run time exceeded 8 min for the BEH column, the variance of some peaks decreased slightly, due to shifts in temperature over extended equilibration periods.

Fig. 6.3C and D shows the RSDs of the second central moments of the bands eluted from the Agilent and the Waters columns. The method used for measuring second moments has a precision of 6.08% for replicate injections of p-toluidine on a Luna C18(2) (4.6 mm × 150 mm column; 5 µm particle size) separated under isocratic conditions [22]. The precision of this method is much higher for the first moment than for the second central moments because the part of the profile that is remote from the peak center, where concentration is lowest, contributes most to that moment. The Agilent column gave RSDs of the band for variances below 1.8% for all measurements made at 510 bar, which demonstrates greater reproducibilities than in previously published work. This improvement can be attributed to several factors. In the previous work an older version of the Agilent 1290 series was used. The connections in the current system were optimized using zero void volume Viper connections while in the previous work standard metal ferrule connections were used. Metal ferrules increase band dispersion toward the base of the chromatogram, making the bounds of integration more obscure; consequently moment analysis will be less precise [11]. Additionally, lower injection volumes were used in this work and the analysis was done by solvent gradient rather than under isocratic conditions,

which typically leads to narrower peaks.

For the Waters column, a three-minute equilibration time was needed to ensure the reproducibility of consecutive separations, as indicated by the RSDs falling under 2%. The reproducibility appeared to improve slightly if a 5 min post run time was used. However the difference may be negligible between post run times of 3 and 5 min.

Fig. 6.3E and F shows the precision of the first moments of bands eluted from the Agilent and the Waters columns, respectively. The first moments of the analytes eluted from both columns are below 1.2% under high constant pressure. For both columns, the average reproducibility of the retention times of all components was best when using a 5 min equilibration time. The most significant improvement of reproducibility occurs between zero and a 1 min post run time. The Agilent column exhibited RSDs for the first moments nearly one half those recorded for the Waters column.

6.4.4 Flow programmed constant pressure analysis at maximum pressure

Fig. 6.4 shows the average values of the second central moments of the nine analytes in the Agilent RPLC checkout sample for the Agilent Poroshell column (Fig. 6.4A) and for the Waters BEH column (Fig. 6.4B) for the experiments performed with a programmed gradient that keeps the inlet pressure at approximately 510 and 550 bar, respectively. The relative standard deviations of the variances of all analytes are below 3%, regardless of the equilibration time (Fig. 6.4C and D). This method provides conditions to maintain high precision in peak width and retention time with low post run times. Programming the flow rates and the solvent compositions into the method seems to alleviate an important issue met when running gradients under constant pressure, namely the influence of the column temperature on the flow rate, which is due to the viscosity

dependence on the temperature.

Fig. 6.4C shows the second central moments for the compounds in the Agilent RPLC checkout sample when the back pressure of the Agilent column is kept at about 510 bar. The relative standard deviations of all these data are below 2% for this column, regardless of the equilibration time. Fig. 6.4D shows the same results for the Waters column. The results obtained with both columns are close, with RSDs under 3%.

The precision achieved with this method is the best provided by all methods tested using a variable flow rate. Constant flow rate analysis seems to provide more reproducible retention times when methods requiring no equilibration time are used. Programming the flow rate alleviates the issue of operating the column under constant pressure, namely the changes in the mobile phase flow rate due to the effect of the temperature on its viscosity. The relative standard deviations for the first moments were all under 0.13% as shown in Fig. 6.4E and F for the columns packed with core–shell and fully porous particles, respectively. This demonstrates that operating the instrument at the maximum possible pressure can yield highly reproducible separations that do not need any equilibration time, provided that the stationary phase has a high thermal conductivity, the radial temperature gradient in the column is minimal, and the flow rate stays constant enough to minimize the differences between successive separations.

6.4.5 Constant heat loss analysis

Fig. 6.5 shows the average values for the second central moments of the analytes eluted from the Agilent (Fig. 6.5A) and the Waters columns (Fig. 6.5B) using a method designed to keep constant the net heat loss at the column wall. Fig. 6.5C and D shows the reproducibility of the peak widths for these columns. The peak widths provided by this method are reproducible with RSDs below 5%. The key parameter in designing this method is the column

permeability, because if it changes during the course of separations, the amount of heat lost will not remain constant. This explains why there are some variations in the peak widths.

The reproducibilities of the retention times are similar to those obtained in the constant flow method. Fig. 6.5E and F shows the relative standard deviations of the retention times for the two columns. The constant heat loss method produced RSDs under 0.1% for the retention times. For separations with low post run times, the constant heat loss method appears to yield more reproducible separations than constant flow separations, however if the column permeability changes unexpectedly, the peak widths may vary (Fig. 6.5D).

6.4.6 Response factors for the five methods

Fig. 6.6 and Fig. 6.7 show the response factors for the eluted peaks of the nine analytes in the RPLC checkout sample for the two columns ($n = 6$ for every data point). The response factors provided by the different methods are not the same, which suggests that calibration for individual methods maybe necessary for some analytes. At the very least, great caution should be used before assuming that accurate quantitative results can be obtained by using a response factor calculated from the results provided by a different method. For the RPLC Checkout sample, butyrophenone (the third to elute) and valerophenone (the fourth to elute) appear to be the most sensitive compounds to changes in the flow rate and the thermal conditions of the separation. The relative standard deviation of the response factors given by different methods could be as high as 11%. Further investigations of the quantitation in methods using variable flow rate methods will be pursued.

6.5 Chapter Summary

The metrics used in this assessment are more rigorous than those employed by the majority of chromatographers; this should be taken into consideration by the reader. Many factors may impact the reproducibility of VHPLC separations,

including the mechanical stability of the column. Great effort was made to isolate the changes in response factors, peak widths, and retention times that are related to thermal effects caused by the friction of the mobile phase. The advantage of using a column packed with core–shell particles rather than one packed with fully porous particles was demonstrated by the use of moment analysis. The radial temperature gradient across the former column is lower for than that for columns packed with fully porous particles. Consequently, successive separations using columns packed with core–shell particles are more reproducible under constant flow rate, constant pressure, and programmed pressure conditions. Constant pressure gradients provide less reproducible separations than alternate methods. The precision of the first moments (the average analyte retention time) for subsequent constant pressure gradient separations is less than that of analyses made at constant flow rate. This may be accounted for by changes in the viscosity of the mobile phase since the heat produced by friction alters the temperature distribution through the column. The precision of the retention times increases five-fold when the instrument is operated under constant flow rate conditions. The potential benefit of using constant pressure and flow programmed constant pressure analysis to reduce analysis time and increase precision when successive analyses are performed was demonstrated. When the flow rate depends on the dynamic permeability of the column, the precision of the retention times decreases by a factor 5 if there is no equilibration time to bring back the column to thermal equilibrium. For these experiments, with a solvent gradient of 50–95% acetonitrile, the reduction in analysis time was 16% with respect to conventional constant flow rate analysis.

The decrease in the post run time required to bring the column back to thermal equilibrium was reduced so that for rapid separations the equilibration time required is of the same order as the analysis time. For laboratories that do many subsequent or batch separations, this benefit should not be ignored. A threefold increase in the precision of the peak width was found when a programmed

pressure gradient was used instead of a conventional constant flow rate separation. The constant heat loss method is promising, demonstrating a high precision for the values of the peak width and the retention time but the separations may suffer from unexpected changes in the peak widths if the column permeability changes (see Fig. 6.5D).

Constant pressure analysis may be more widely used if very robust columns with low radial temperature gradients become available. However, using a gradient method which simulates a constant pressure analysis, but requires the instrument to control the flow rate instead of basing the flow rate purely on the inlet pressure of the column, appears to be a more practical approach to reduce both analysis and post run equilibration times. Under the highest pressures investigated, using a column packed with core–shell particles, the precision of the first and second moments improved when there was no post run time input into the method. Difficulties were encountered when the back pressure increased by 50 bar (at the start of each of the subsequent separations) for the column packed with fully porous particles. This was alleviated by removing the inlet frit, sonicating it in tetrahydrofuran for 15 min and reassembling the column. Due to this procedure being performed on the column, the investigation of programmed constant pressure analysis and constant heat loss analysis were performed on a new column of the same type. This demonstrated that the frit was the main cause of this difficulty, even with the use of HPLC grade solvent. Cleaning the frit and filtering acetonitrile with a nylon (.45 micron) filter appeared to reduce this effect, Such considerations should be taken into account when performing separations with columns packed fine particles and frits with very small flow channels.

The response factors of analytes depend on the method used to deliver the gradient. They may change by up to 11%, suggesting that issues will be encountered when performing quantitative analysis if response factors obtained with a constant flow method are applied to analyses made with a variable flow

rate method or vice versa. Calibration using the very method selected should be done to ensure accurate results when quantitative analyses are performed using a variable flow rate method.

Using a temperature controlled oven at more than 30 ℃ could potentially reduce the heat generated by friction and make it a less critical parameter, particularly with columns packed with core–shell particles. Future work will explore this possibility.

CHAPTER VII
QUANTITATIVE ANALYSIS OF FAST GRADIENT SEPARATIONS WITHOUT POST-RUN TIMES USING FULLY POROUS PARTICES

7.1 Introduction

The need for rapid gradient separations is a driving force in the development of HPLC techniques. Continued progress and the need to improve the results obtained in very high pressure liquid chromatography (VHPLC) are generating new obstacles. Rapid analyses are made with short, efficient columns that have lower variance contributions than their longer predecessors. These contributions are small compared to the variance contributions of the tubing and connections of modern instruments, which became a nuisance for analysts working with short columns and which are now the leading cause of band spreading in VHPLC and μHPLC (micro-high performance liquid chromatography) [47].

To achieve adequate efficiency, VHPLC columns are very efficient, so short columns packed with fine particles are generally preferred. They must be operated with high back pressures. The high pressures required to run these columns at a flow rate close to optimum generate heat due to the friction of the mobile phase percolating through the tightly packed bed. This heat leads to expansion of the mobile phase and slowly diffuses to the column environment. Under isocratic conditions, a steady state is achieved and analyses are reproducible. In contrast, no steady state can take place under gradient conditions since the mobile phase composition changes, affecting flow rate and pressure. This leads to reproducibility issues if there is no sufficiently long post-run equilibration time between subsequent injections. Conventional gradient separations are run at constant flow rate, the amount of heat generated by friction decreasing during the gradient run. As a result the inlet pressure and the column temperature decrease during constant flow rate gradients. When the gradient separation is started again, the inlet pressure and the column

temperature increase, so the initial conditions are different [33,38,55]. Under constant pressure operations, the column temperature rises during the gradient run, then the column cools down until the initial gradient conditions are applied again [7]. The main advantage of using a constant pressure gradient at high flow rate is a decrease of the analysis time by about 20%. Unfortunately, during a constant pressure gradient, the mobile phase flow rate varies with the column temperature, which affects the reproducibility of analytical data (retention times and peak widths); constructing volume based chromatograms helps to correct the consequences of this effect. Verstraten et al. discuss the consequences of viscous heating and pressure effects in constant pressure gradients, using a volume based reconstructed timescale [39].

Programming the mobile phase flow rate by using the parameters that would achieve a given value of the backpressure improves the reproducibility of subsequent runs [7]. Obtaining the gradient parameters in a flow-rate programmed method can be done by exporting flow rates and gradient compositions from a constant pressure gradient method and inputting these parameters into a new flow rate controlled method. This approach uses the same set of flow rates for each separation, regardless of the current column temperature. Time-based chromatograms can be used for comparison and volume-based chromatograms can be used for quantitative analysis.

Beds of stationary phases made of fully porous particles do not dissipate heat as quickly as do beds packed with core–shell particles. When using a post-run equilibration time strategy to bring a column back to its initial temperature, columns packed with core–shell particles tend to return to their starting temperatures three times faster than columns of similar dimensions packed with fully porous particles of similar sizes [52-53,56]. Columns packed with core–shell particles can operate under significantly lower pressures as well which reduces

the magnitude of heat generated by friction [56].

The goal of this work was to investigate if a series of initial separations should be made to bring the column to a temperature that would be reproducible for all subsequent runs, with short post-run times. The first separation causes the column to heat in constant pressure operation; in constant flow operation the column cools as the gradient proceeds. The following separations would then provide reproducible measurements, provided a pseudo steady temperature could be achieved where each gradient begins at approximately the same column temperature.

Under conventional conditions, the post-run times required to bring columns packed with fully porous particles back to their initial temperature may be longer than the analysis times. Avoiding this situation is the principal motivation for this work [7,12,57-58]. Previous work demonstrated that 5 min of post-run time was required to obtain very reproducible chromatograms with the same constant flow gradient and instrumentation used in this work [7]. Sacrificing 4 min of time before a long series of runs would save both time and solvent. Finally, the achievement of reproducible quantitative determinations of the sample composition, using various gradient elution methods, conventional constant flow rate conditions, constant pressure conditions [39], and programmed flow constant pressure conditions will be discussed. An approach described earlier, to keep the net amount of heat generated at the wall of the column constant during the gradient run and to maintain isocratic conditions following the gradient run, when the column is returned to initial conditions was considered for this effort [41]. However, that method could not be applied because it was found to be sensitive to changes in pressure and the column used in this work exhibited an upward drift of its back pressure.

Isocratic conditions for the sample take in excess of 30 min with a solvent composition of water/acetonitrile (50/50, v/v). The use of a solvent gradient reduces the separation time to less than 3 min. Generally when rapid separations are required in reversed phase liquid chromatography, acetonitrile is preferred to methanol as the organic modifier. The pressures required to operate at the same flow rate are nearly twice as high when methanol is used as opposed to acetonitrile. It is notable that gradient separations involving methanol would also experience a decrease in the magnitude of heat generated under constant flow rate conditions at very high pressures. The viscosity of mixtures of methanol and water are highest (2Cp) at approximately a 50:50 %V:V (methanol:water) ratio. In comparison to mixtures of acetonitrile and water which have the highest viscosity (1.3Cp) at 20:80 %V:V (acetonitrile:water); mixtures of acetonitrile and water are significantly less viscous and therefore popular for VHPLC. The slower flow rates used in gradient separations involving methanol generally do not generate a significant amount of heat.

7.2 Materials and Methods

7.2.1 Instruments, columns, and reagents

Experiments were conducted in a 24 ℃ room, using a prototype Agilent 1290 Infinity System capable of constant pressure operation (Agilent Technologies, Waldbronn, Germany). A Thermo Viper (130 µm I.D.) column connection unit (Dionex-Fisher, Sunnyvale, CA, USA) was used to connect a Waters XBridge BEH XP C_{18} (4.6 mm × 100 mm; 2.5 µm particle size) column and a Waters XBridge BEH XP Vanguard Pre-Column (2.1 mm × 5 mm; 2.5 µm particle size) to the instrument. Fisher Scientific (Fair Lawn, NJ, USA) HPLC grade water and acetonitrile were used. The test compound for all experiments was a 1 µl sample of the Agilent RPLC checkout sample consisting of acetophenone, propiophenone, butyrophenone, valerophenone, hexanophenone, heptanophenone, octanophenone, benzophenone, and acetanilide dissolved in

water/acetonitrile (65:35, v/v) in concentrations of 100 µg/mL each (±0.5%). The Chemstation Rev. C.01.03 (37) was used for online and offline analysis.

7.3 Experimental Conditions

All experiments were performed using the shortest possible equilibration periods possible (post-run times of approximately 20 seconds) with the instrument used. Six consecutive 1 µL injections of the sample were performed for each set of experiments. For all experiments made under constant flow rate, constant pressure, and programmed flow constant pressure experiments conditions the column was insulated in several layers of cellulose sheets to buffer room temperature fluctuations and positioned horizontally. The column was operated isocratically for 15 min under the initial conditions of the forthcoming run before the first separation in each series.

7.3.1 Constant flow experiments

The inlet pressure varied while a constant gradient flow rate of 2.3 mL/min was maintained for 2.45 min with a total run-time of 2.7 min. The solvent gradient used was acetonitrile/water (50:50–95:5, v/v).

7.3.2 Constant pressure experiments

The constant pressure gradient analyses were conducted using the constant pressure interface of the prototype Agilent 1290. This instrument is equipped with a pressure controller that allows the mobile phase flow rate to be determined by the inlet column pressure. The analyst specifies the pressure of operation. The chromatogram can be displayed either in time or in volume units.

Two sets of constant pressure experiments were performed (see Table 7.1). The first set (constant pressure 1) had the inlet pressure set to 463 bar. This pressure was selected to give the same net analysis time as the constant flow experiments. The second set was run under an inlet pressure set to 580 bar

(constant high pressure). This pressure is close to the maximum pressure that the column and the instrument can provide, without damaging the column.

7.3.3 Programmed flow constant pressure experiments

Instead of letting the instrument dictate the flow rate based on the inlet pressure of the column, the flow rates and the gradient parameters were fixed. This was done by exporting the flow rates and solvent compositions from the constant high pressure experiments in 3 s increments and inputting them into the instrument method. This insured that all the flow rates would be the same regardless of the inlet column pressure. The separation pressure remained fairly constant.

7.3.4 Determination of the reproducibility and peak capacity

Moment analysis provides an accurate assessment for comparing the peaks of each analyte in the different chromatograms recorded, provided that all peaks are well resolved. In brief, the 0th moment is the peak area, the 1st moment is the true retention time for the peak (different from the time of the apex, unless the peak is symmetrical), and the 2nd central moment provides the peak variance (related to the band width) [8,59]. The peak capacity of the separations was determined by the elution time window divided by the average base width of all peaks in the chromatogram. Generally, in gradient separations, the peak capacity is more useful than the apparent efficiency.

7.3.5 Experimental conditions for quantitative analysis

The concentration of each analyte in the standard sample was 100 µg/mL (±0.5%). Triplicate injections of 2, 4, 6, and 8 µL (n = 3) of this sample were performed for each of the methods discussed. Two blank runs were conducted before acquiring data to bring the column to a pseudo stationary thermal state.

Table 7.1. Chapter 7 Experimental Summary. Summary of the experimental conditions and quantitative results.

Solvent gradient: 50–95% acetonitrile in water for all experiments				
Experiment set	Constant flow	Constant pressure 1	Constant pressure (high)	Programmed flow constant pressure (high)
Gradient time	2.45 min	2.5 min	2.0 min	2.0 min
Total time	2.7 min	2.7 min	2.15 min	2.15 min
Flow rate	2.3 mL/min	Variable	Variable	Variable
Pressure	Variable	463 bar	580 bar	≈580 bar
Retention time RSD	0.063%	0.49%	0.54%	0.11%
Peak width RSD	5.4%	3.7%	5.0%	2.3%
Retention time RSD (first separation excluded)	0.048%	0.15%	0.096%	0.028%
Peak width (first separation excluded)	2.8%	1.3%	1.6%	1.5%
Retention time RSD (first two separations excluded)	0.018%	0.17%	0.053%	0.031%
Peak width (first two separations excluded)	0.92%	1.5%	1.4%	1.6%
Peak capacity	32.9	33.1	27.8	26.4

To obtain an 8 point calibration curve, the standard mixture was diluted by mixing 1 mL of standard and 9 mL of acetonitrile/water (50:50, v/v) in a volumetric flask. Injections of 2, 4, 6, and 8 µL ($n = 3$) of the diluted sample were performed for each of the methods discussed.

In certain situations increasing injection volumes using short, narrow columns packed with core–shell particles have been found to increase the peak area abnormally [60]. Using the Agilent 1290 and relatively wide (4.6 mm) and long columns (100 mm) fully porous and core–shell columns, the errors from injection volume have been minimal (1% RDS from 2 to 10 µL injections) and do not lead to anomalous errors in peak area.

7.3.6. Determination of the response factors

Quantitation was attempted using all methods at different flow rates, because the response of the UV detector depends on the flow rate. Plotting the chromatograms in time and measuring the peak areas does not provide reliable quantitative results. Instead the chromatograms were plotted as a function of the volume eluted, via a macro written by Agilent Technologies. The macro output is the volume-based chromatogram in units of mAU s, where 1 min is equivalent to 1 mL. After integration by the Chemstation, dividing the area by 60 converts the area into mAU mL. The volume based area can be used to calculate the component response factors, using the following equation 7.1:

$$A = \frac{Sm}{F_v} \qquad \text{Eq. (7.1)}$$

where A is the peak area, S is the response factor dependent on the compound considered and the wavelength used, m is the mass injected, and Fv is the volume flow rate of the mobile phase. Other work regarding response factors can be found on Refs. [62-69].

7.4 Results and Discussion

7.4.1 Constant flow rate analysis

Fig. 7.1 shows the chromatograms and pressure curves for the constant flow rate separations. The results of the constant flow experiments showed that two consecutive gradient separations brought the column to a pseudo stationary thermal state. The greatest difference between the different pressure curves is between the first and second separations. As subsequent separations are performed, the column cools progressively, leading to increased retention of the analytes. If consecutive separations are performed with brief post-run times, a steady state is achieved after two separations. The following chromatograms in the series are highly reproducible, as long as the back pressure of the column does not increase. The net peak capacity of these experiments was 32.9, the second highest of the tested methods.

As the mobile phase viscosity decreases, the amount of heat produced by friction decreases, causing the column temperature to drop when operating the column at constant flow rate, which explains why the pressure curves become higher. Moment analysis demonstrated the data to be highly reproducible. The relative standard deviations of the first moment (average retention time) for the six replicate separations were 0.063%. The second central moment (band variance) was 5.4% RSD. If the first chromatogram is removed from this series and used strictly for column equilibration, not for analytical purposes, these values drop to 0.048% and 2.8% RSD, respectively. If the second chromatogram is also used for column conditioning, the retention times and band variances improve further to 0.018% and 0.92% RSD, respectively.

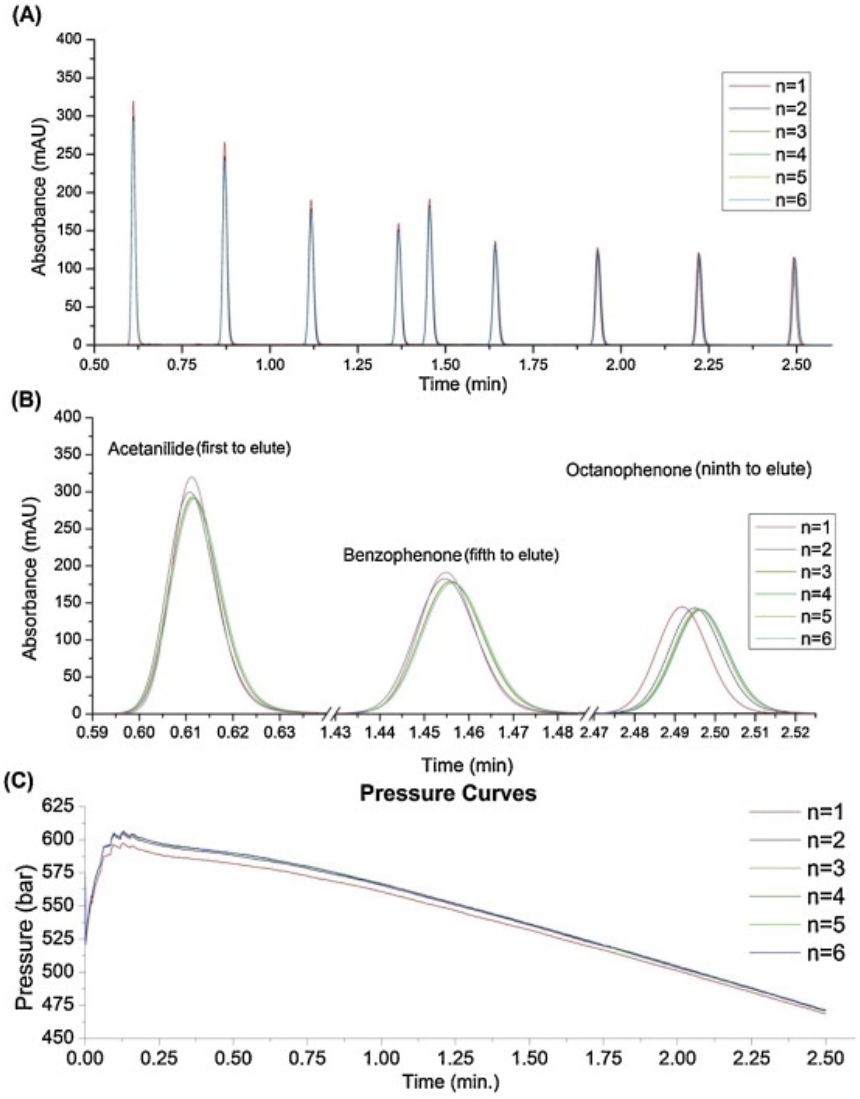

Figure 7.1. Chromatograms and Pressure Curves (Cf – Fully Porous). Constant flow rate (2.3 mL/min). (A) The overlaid chromatograms obtained for constant flow rate experiments. (B) An enlarged view of the peaks of the first, fifth, and ninth sample components. (C) The variations of the pressure during each separation.

7.4.2 Constant pressure analysis. Part 1: analysis time equivalent to the constant flow experiments

Figure 7.2 shows the chromatograms and flow curves for the 1st set of constant pressure separations. It is difficult to achieve reproducible time-based chromatograms under constant pressure conditions since the column temperature rises and falls depending on the value of the inlet pressure applied. The flow rate under constant pressure operation depends directly on the column temperature, so a reproducible thermal steady-state is difficult to achieve. The first separation takes place at a temperature lower than the subsequent separations. The temperatures of the second and third separations in the series keep increasing and the retention times of the sample components decrease. After the fourth separation is performed, the column temperature begins to decrease and it continues to decrease for further separations.

The standard deviation of the pressure in constant pressure operation is 0.55 bar across this method. After an injection the instrument takes 3 s to reach a stable pressure, after that 3 s period the standard deviation of the pressure is approximately 0.12 bar.

Moment analysis showed that the average precision for the first and second central moments were 0.49% and 3.7% RSD, respectively. If the first run is discarded, these values are reduced to 0.15% and 1.3% RSD, respectively. If the first and second runs are also removed, the RSDs of the peak width and the retention times increase, demonstrating that thermal effects are poorly reproducible.

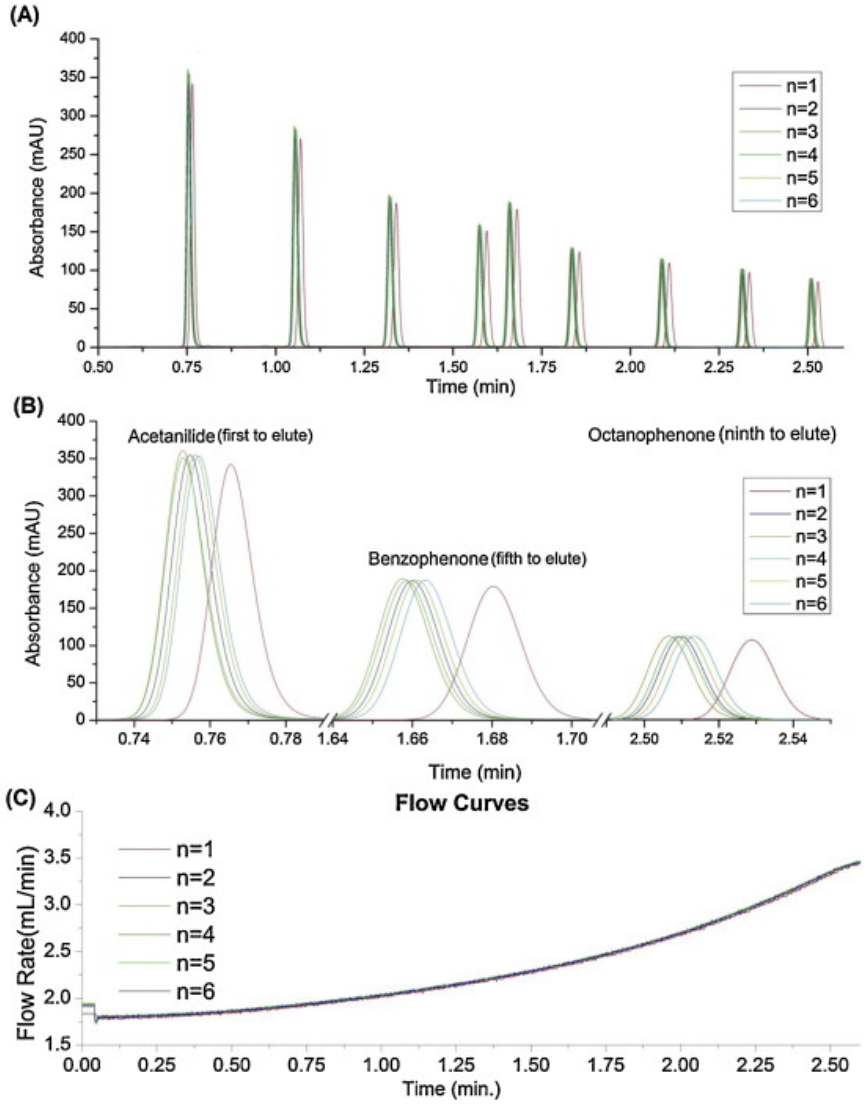

Figure 7.2. Chromatograms and Pressure Curves (Cp 1 – Fully Porous). Constant pressure part 1 (463 bar). (A) The overlaid chromatograms obtained for constant pressure experiments made under a pressure that provides the same net analysis time as the constant flow rate experiments. (B) An enlarged view of the peaks of the first, fifth, and ninth sample components. (C) The variations of the pressure during each separation.

The first moment RSD under constant pressure operation was nearly an order of magnitude higher than under constant flow rate separations. In contrast, the reproducibility of the band variance under constant pressure gradients was found to be more reproducible than under constant flow rate operation, suggesting the radial temperature difference taking place during the separation is less important than under constant flow rate operations. The variation of retention times demonstrates why the use of volume-based chromatograms is necessary for routine analyses performed under constant pressure. Plotting volume-based chromatograms can correct for differences in the flow rates but cannot correct for differing retention times due to an increase in temperature.

The net peak capacity of this approach was 33.1, slightly higher than with the constant flow experiments, which is in agreement to previously published results [61].

7.4.3 Constant pressure analysis. Part 2: operation at high pressure

Fig. 7.3 shows the chromatograms and flow curves for the 2nd set of constant pressure separations. During high constant pressure experiments, the first three separations showed that the column exhibited the same heating trend as during the lower pressure experiments when the separations took place at average temperatures alternating between cooler and warmer values.

The average precisions of the first and second moments were 0.54% and 5.0% RSD, respectively. These two values drop to 0.096% and 1.6% RSD, respectively, if the first separation is discarded as used only to condition the column. If the first two separations also are discarded for the same reason, the precision improves further to 0.053% and 1.4% RSD, respectively.

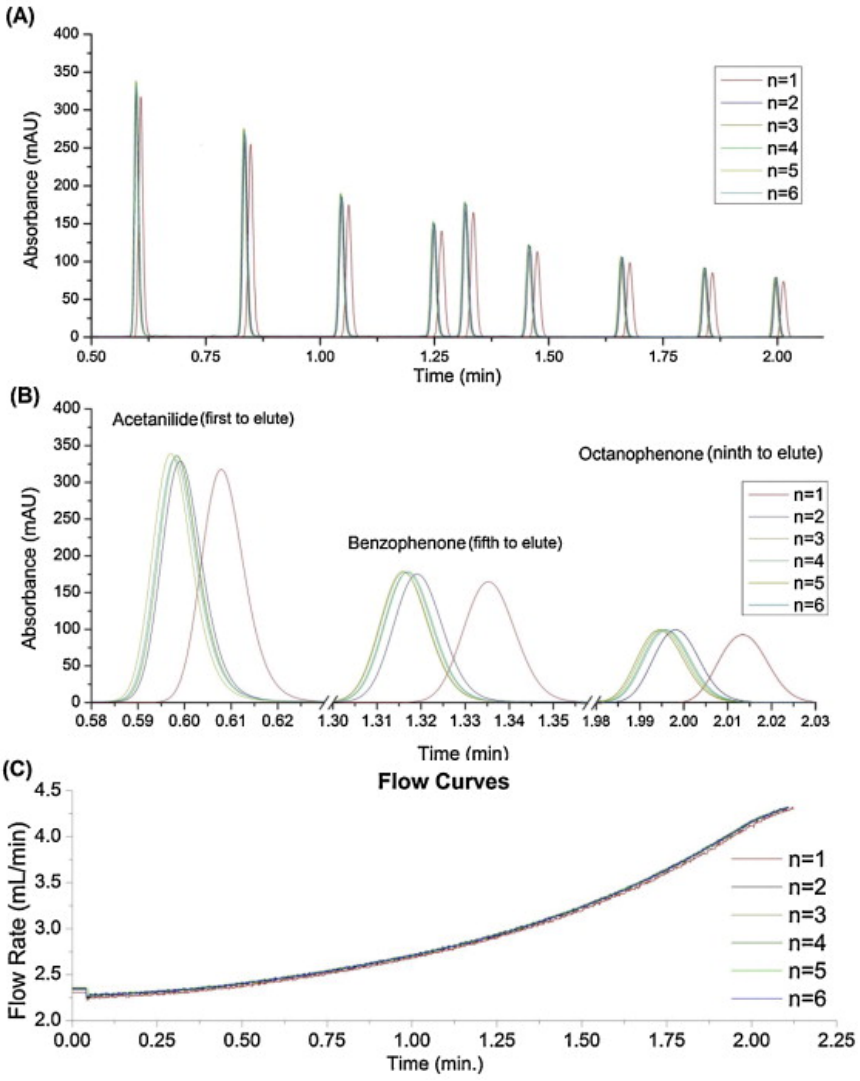

Figure 7.3. Chromatograms and Pressure Curves (Cp 2 – Fully Porous). Constant pressure part 2 (580 bar). (A) The overlaid chromatograms obtained for constant pressure experiments made under the maximum possible inlet pressure. (B) An enlarged view of the peaks of the first, fifth, and ninth sample components. (C) The variations of the pressure during each separation.

The net peak capacity of very high constant pressure operation was 27.8, lower than the one observed under constant flow rate conditions. The analysis time was 20.4% shorter than under constant flow rate conditions.

7.4.4 Programmed flow constant pressure analysis at high pressure

Figure 7.4 shows the chromatograms, pressure curves, and flow curves for the programmed flow constant pressure separations. The standard deviation of the pressure in programmed constant pressure operation is 4.4 bar across this method. After an injection the instrument takes 3 s to reach a stable pressure, after that 3 s period the standard deviation of the pressure is approximately 1.2 bar. Programming the flow rate to keep the pressure constant during gradient separations improved the RSDs of the average retention times by a factor 5 and of the peak widths by a factor 2 over the reproducibilities provided by high constant pressure operations. Discarding the first run of the series for column conditioning improved the precision of the retention times from 0.11% to 0.028% RSD and the precision of the peak widths improved from 2.3% to 1.5% RSD. Removing the second separation results from the series did not improve these results.

The net peak capacity of this method was 26.4, the lowest value of this series of experiments. Moment analysis confirmed that bands are more dispersed for programmed constant pressure than for true constant pressure gradient operations.

7.4.5 Benchmarks of reproducibility from previous work

A report was made on the wait time between injections needed to bring a fully porous and core–shell column back to their initial starting temperature after a gradient separation was performed [7]. The same gradient was applied as in this work and the same RPLC checkout sample was used.

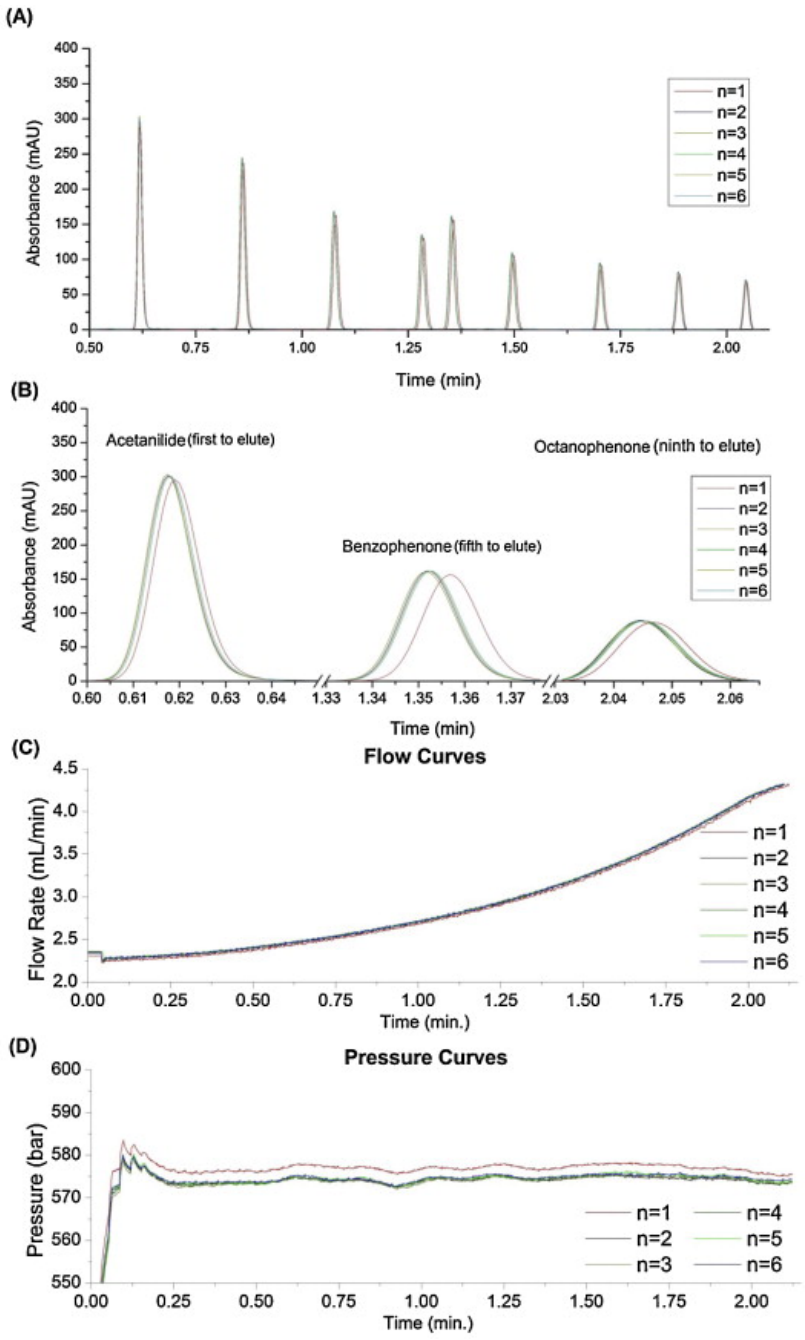

Figure 7.4. Chromatograms and Pressure Curves (CPp – Fully Porous). Constant programmed pressure (≈580 bar). (A) The overlaid chromatograms obtained for the constant programmed pressure experiments made at the maximum possible pressure. (B) An enlarged view of the peaks of the first, fifth, and ninth sample components. (C and D) The flow and pressure variations

curves of each separation.

Constant flow rate separations (n = 6) were under <2.0 RSD for the peak width and <0.060% RSD for retention times when post-run times were above 3 min. Operating the instrument in constant pressure mode (n = 6) the RSD for the peak width was <2.0% and <0.40% for the retention times of injections with post-run times above 3 min. Using programmed flow methods above 500 bar the chromatograms (n = 6) had RSDs of <2.0% for the peak width and <0.070% for the retention times if post-run times exceeded 1 min.

7.4.6 Data for quantitative analysis

Based on the exported volume-based integration values provided by the Chemstation software and the Agilent macro, the response factors for each of the nine analytes were calculated from the chromatograms provided by the triplicate injection of the following masses of the sample: 0.02, 0.04, 0.06, 0.08, 0.2, 0.4, 0.6, and 0.8 µg.

Fluctuations of two parameters may cause errors in quantitation made in the methods discussed. The first source of error may occur if a compound is eluted when the eluent composition during the gradient is different from the one expected because, due to frictional heat, the column temperature deviates from one method to the other. Changes in this temperature affect retention of analytes. If a compound elutes at different times during the gradient the detector response may change. The second potential source of error is when compounds elute at different temperatures in each method. This could also affect the detector response, since the extinction coefficient may be affected by the temperature [70].

Table 7.2 lists the average response factors calculated from the volume-based chromatograms provided by the four methods. The relative standard deviations

of these factors are also listed. The response factors decrease with increasing flow rate. Table 7.3 lists the average relative errors in calculated compound mass made in the constant pressure and the constant programmed pressure methods when assuming that the response factors measured in constant flow rate operations are correct. Some individual calculated masses are between 5 and 6% in error, suggesting that calibration is necessary for an analyst to achieve higher accuracy.

7.5 Chapter Summary

Four different approaches to deliver the mobile phase in VHPLC gradients were explored for a column packed with fully porous particles. The approaches providing the best reproducibility of the average retention times and band dispersions are constant flow rate and constant programmed pressure operations. Each method has its own specific benefits. Constant programmed pressure operation may prove the most useful for analysts concerned with achieving rapid yet highly reproducible separations. Using gradients performed under high constant pressure and under constant programmed pressure give shorter analysis times than the other two, by about 20% in this work. However, fast methods yield lower peak capacities, 16% lower with high constant pressure and 20% lower with constant programmed pressure compared to conventional constant flow rate methods.

Table 7.2. Response Factors Averaged Across Two Orders of Magnitude.

Average response factors [(mAU mL)/µg] and RSDs				
Compound	Constant flow	Constant pressure 1	Constant pressure max.	Programmed flow
Acetanilide	88.4/0.61%	88.6/1.06%	87.9/1.01%	88.1/0.89%
Acetophenone	92.6/0.75%	92.7/0.88%	91.3/0.82%	91.2/0.77%
Propiophenone	77.1/0.70%	77.3/0.56%	75.6/0.77%	75.5/0.65%
Butyrophenone	71.8/0.70%	71.9/0.74%	70.1/0.97%	70.1/0.81%
Benzophenone	74.6/2.90%	73.9/1.35%	73.3/0.96%	73.3/0.87%
Valerophenone	64.6/0.70%	64.5/0.61%	62.8/0.72%	62.8/0.67%
Hexanophenone	61.3/1.46%	60.9/0.52%	59.3/0.76%	59.0/0.56%
Heptanophenone	56.3/2.23%	55.8/0.89%	54.4/1.16%	54.1/0.72%
Octanophenone	50.9/2.84%	50.0/1.19%	49.0/1.25%	48.7/0.99%
Average percent error vs. constant flow		0.57%	2.35%	2.53%

Table 7.3 Relative Errors in Calculated Masses. Average relative error made on masses calculated when using response factors obtained from constant flow rate analyses.

Relative Errors in Calculated Masses			
Compound	Constant pressure 1	Constant pressure max.	Programmed pressure
Acetanilide	0.86%	0.83%	0.74%
Acetophenone	0.76%	1.39%	1.43%
Propiophenone	0.53%	1.98%	2.05%
Butyrophenone	0.61%	2.34%	2.37%
Benzophenone	1.33%	1.82%	1.82%
Valerophenone	0.56%	2.85%	2.85%
Hexanophenone	0.67%	3.17%	3.70%
Heptanophenone	1.02%	3.30%	3.92%
Octanophenone	1.59%	3.66%	4.26%

The method with the highest peak capacity was found in constant low pressure operation (33.1), followed by constant flow rate (32.9), constant high pressure (27.8), and programmed constant high pressure (26.4). Increasing the speed of the separation by 20% drops the net peak capacity by 20% for these methods. There is only a marginal gain by using constant pressure methods with the same analysis time. Previous work also shows that switching to a programmed flow constant pressure method results in a small loss in peak capacity.

The reproducibility of the retention time for the constant flow rate method improves when two separations are conducted. The precision of the retention times improve from 0.063% RSD to 0.048% RSD (if one separation is used to condition the column) to 0.018% RSD (if two separations are used to condition the column). A similar trend is observed with constant high pressure operation where the precision of the retention time improves from 0.54% RSD to 0.096% to 0.053%, respectively. Under constant high pressure and constant low pressure operation there is no significant improvement in precision if more than one separation is used to thermally condition the column. This suggests that a pseudo-steady state temperate can be achieved more rapidly in these methods.

There is no significant benefit in terms of data reproducibility in performing separations under moderate constant pressures. Constant pressure methods may have the slight advantage of increasing the peak capacity and giving peaks that tend to be less dispersed when using beds packed with fully porous particles.

Using constant pressure methods at moderate pressures may aid analysts in performing accurate quantitation, when response factors are measured using such methods. Errors made on the calculated masses were found to be as high as 6% when the response factors that had been obtained from constant flow rate operations were used to quantitate the results of high constant pressure gradients and programmed constant pressure experiments. When these same response factors were used to calculate the masses from chromatograms recorded during analyses made by constant flow rate separations run under moderate pressures, the errors did not exceed 3.3% for individual injections. The analyte response factors used for any specific method should be obtained in a way ensuring that errors made in quantitative analyses are minimal, especially for analyses that demand a high accuracy.

Previous work had demonstrated an average precision for the retention times of 37 analytes (n = 5) of approximately 0.045% RSD using an HP 1100 liquid chromatograph with a Symmetry C18 column (150 mm × 3.9 mm; particle size 5 μm) separated in isocratic analyses made at 25.0 °C [71]. The net time of these separations ranged from 15 to 35 min. In this work we presented rapid gradient separations using programmed flow constant pressure gradient with retention times RSDs (n = 5), that are about 1.6 times lower, provided that the first separation be used to bring the column to a pseudo-stationary initial temperature. Also, that previous work did not have to address possible changes in column temperature, which can shift retention times. This increase in reproducibility can be attributed to recent improvements in modern instrumentation and injection technology.

CHAPTER VIII
QUANTITATIVE ANALYSIS OF FAST GRADIENT SEPARATIONS WITHOUT POST-RUN TIMES USING CORE-SHELL PARTICLES

8.1 Introduction

Over time and particularly over the last ten years, manufacturers of chromatographic instruments and columns have considerably improved technology. Shorter columns are packed with finer particles and are operated at higher velocities than they were ten years ago, providing higher column efficiencies, which reduce the analysis times. These trends persisted for fifty years but are now reaching a limit. The permeability of columns packed with fine particles decreases rapidly with decreasing particle size; these columns need to be operated with high inlet pressures to achieve high column efficiency. This leads to a new source of difficulties due to mobile phase expansion and its friction against the column bed. These effects generate heat that diffuses along and across the column, affecting the temperature distribution through the column bed. While still negligible for 20 cm long columns packed with 5 µm particles and eluted under an inlet pressure of a few hundred bars, this heat is considerable for 5 cm long columns packed with 1.7 µm particles and eluted under an inlet pressure of 1000 bar [33,38,55,72-77]. The column is no longer isothermal, the mobile phase viscosity, the analyte diffusion coefficients, and the analyte retention factors are no longer constant along and across the column. For analyses carried out under isocratic conditions, the heat exchanges between the bed and the column environment may be limited by keeping the column in a still air enclosure. Then, the temperature gradient is radially isothermal, which minimizes the radial gradients of mobile phase viscosity and velocity, and of analyte retention factors. However, analysts experience the consequences of

axial gradients of these properties.

During gradient analyses, the mobile phase composition varies; its viscosity and the relevant analyte properties change as well. Accordingly, the heat power generated by the percolation of the mobile phase stream varies during the analysis and its distribution across the column changes depending on the delay between successive analyses. Reproducible results can be achieved when the frequency of analyses is sufficiently low to allow the column to return to thermal equilibrium between successive analyses.

The analysis time and the delay between injections contribute to the throughput [12,57-58], so increasing the equilibration time is inconsistent with the purpose of achieving fast analyses. Decreasing analysis times by increasing the flow rate beyond the optimal flow rate of the column decreases the net peak capacity and increases the frictional heat power of the mobile phase stream. Better solutions are needed.

While gradient separations are traditionally carried out at a constant flow rate, several alternate approaches were recently proposed to accelerate these separations in VHPLC. Constant pressure gradient [39] and constant temperature at the column wall [41] were suggested. Based on the theoretical and potential advantages of gradient separations performed under steady state temperature, our goal is to explore and compare several approaches to optimize separation throughputs in VHPLC and to determine the reproducibility of the results.

8.2 Material and Methods

8.2.1 Instruments, columns, and reagents

Experiments were conducted in a 24 °C room using a prototype Agilent 1290 infinity system capable of constant pressure operations and equipped with a low

volume (600 nL) detector flow cell (Agilent Technologies, Waldbronn, Germany). Two thermo viper (130 µm I.D., 250 mm long) column connection units (Thermo Fisher, Waltham, MA, USA) were used, one to connect the column to the injector, and the other to connect the column to the detector. A 4.6 × 100 mm Agilent technology column packed with Poroshell 120 EC-C18 particles (2.7 µm size) was used for all experiments.

Fisher scientific (Fair Lawn, NJ, USA) HPLC grade water and acetonitrile were used. The test mixture was composed of (in order of elution) acetanilide, acetophenone, propiophenone, butyrophenone, benzophenone, valerophenone, hexanophenone, heptanophenone, and octanophenone, all at 100 µg/mL (±0.5%) (RPLC checkout sample Agilent Technologies P/N 5188-6529) in a solution of acetonitrile/water (65:35 v/v). 1 µL was injected for the performance evaluation.

8.3 Experimental Conditions

All the experiments were performed using the briefest equilibration periods (post-run times) that the instrument would allow. Six consecutive 1 µL injections of the standard solution were performed for each set of experiments. For the constant flow, constant pressure, and programmed flow constant pressure experiments, the column was positioned horizontally and insulated in several layers of cellulose sheets to buffer the changes in room temperature due to the heating/cooling system in the room. For the constant heat loss experiments, the column was positioned in the oven, with the door removed. Exposure to open air is necessary for constant wall heat experiments; the equations used to derive the appropriate conditions taking into account the diffusion of heat into open air. The column was operated for 15 min before the first separation was made in each series.

Constant flow experiments were input into the ChemStation software in the conventional way. Constant pressure operation is controlled by the instrument pumping system, based on the inlet pressure of the column throughout the gradient. The time of the gradient is based on the net volume eluted, lower pressures would elute the mobile phase at a slower rate and therefore the net time required would be greater than under a higher pressure. Programmed constant pressure operation is based on the values of the flow rate and the gradient composition each 3 s increments derived from the constant pressure operation (at 510 bar). In programmed constant pressure operation the instrument controls the flow rate and gradient compositions based on inputs set by the operator in 3 s increments, regardless of the actual inlet pressure of the column. The constant heat loss gradient is operated in a similar manor where the results of several equations are used to generate a gradient which should keep the net heat dissipated by the column's wall constant, as is discussed in greater detail in a following section. Time based chromatograms are recorded and shown in this work.

8.3.1 Constant flow rate experiments

Pressure varied while a constant gradient flow rate of 2.8 mL/min was maintained for 2.1 min with a total runtime of 2.25 min (Table 8.1). The constant flow rate gradient was input into the ChemStation software in conventional operation.

8.3.2 Constant pressure experiments

Constant pressure experiments were conducted using the constant pressure interface of the Agilent 1290 that controls the mobile phase flow rate based on the inlet pressure set by the operator. For the constant pressure experiments the instrument uses a volume based gradient, so the net volume of solvent eluted for all separations are the same. This volume based gradient is based on the constant flow conditions, where the constant flow method is converted to a constant pressure method by use of an instrument macro. The macro instructs

the instrument to change the solvent composition of the mobile phase as a function of net volume of solvent eluted for the constant pressure methods.

Table 8.1. Summary of Experimental Conditions and Peak Information.

Solvent gradient 50–95% acetonitrile in water for all experiments					
Experiment set	Constant flow	Constant pressure 1	Constant pressure max.	Programmed flow constant pressure max.	Constant wall heat
Gradient time	2.1 min	2.15 min	1.85 min	1.85 min	1.7 min
Total time	2.25 min	2.25 min	1.9 min	1.9 min	2.25 min
Flow rate	2.8 mL/min	Variable	Variable	Variable	Variable
Pressure	Variable	435 bar	510 bar	≈510 bar	Variable
Retention time RSD	0.029%	0.32%	0.35%	0.057%	0.029%
Peak width RSD	2.9%	0.69%	0.88%	0.89%	2.0%
Retention time RSD (first separation excluded)	0.018%	0.099%	0.060%	0.026%	0.027%
Peak width (first separation excluded)	0.97%	0.66%	0.69%	0.55%	1.79%
Peak capacity	31.4	25.9	28.0	29.2	23.2
Peak capacity per min of total run time	14.0 (peaks/min)	11.5 (peaks/min)	14.7 (peaks/min)	15.4 (peaks/min)	10.4 (peaks/min)

For the constant pressure and programmed constant pressure experiments the variable is how the volumetric gradient is delivered,either by instrument controlled pressure, or manual input of the gradient steps in the instrument software.

Two series of constant pressure experiments were performed (see Table 8.1). The first one (constant pressure 1) had the inlet pressure set to 435 bar. This pressure was selected to give the same net analysis time as the constant flow experiments. After one constant pressure method had been run, Eq. (8.1) can be used to obtain an exact net analysis time by calculating the pressure needed.

$$T_{Experimental} * P_{Experimental} = T_{Desired} * P_{Required} \quad \text{Eq. (8.1)}$$

where, $T_{\text{Experimental}}$ is the net analysis time of one separation, $P_{\text{Experimental}}$ is the inlet pressure of the separation, T_{Desired} is the target net analysis time, P_{Required} is the inlet pressure that will yield close to the target net analysis time. Generally, using this calculation yields analysis times that are within seconds of the target analysis time. This method will be accurate as long as the column's permeability has not changed markedly and the same volume based gradient is used from the experimental run to the target run.

The second series had an inlet pressure set to 510 bar (constant pressure max). This pressure is close to the maximum pressure that the column can endure and instrument can provide. Operating at high pressures with the Agilent column brought the flow rate to around 5 mL/min, the instrument maximum.

8.3.3 Programmed flow constant pressure experiments

Instead of having the instrument control the flow rate based on the column inlet pressure, the flow rates and gradient parameters were manually set using the flow rates and solvent compositions recorded during the constant pressure max

experiments with the values taken at every 3 s increment and put into the instrument method. To account for rapidly changing flow rates in the constant pressure method, five flow rates were averaged for each incremental step. This ensured that all the flow rates are the same regardless of the column inlet pressure and that the pressure under which the separation takes place stays fairly constant. This process could be automated to reduce the time required to write a flow controlled constant pressure method.

8.3.4 Constant heat loss experiments

The flow rates and gradient parameters were determined using an Excel program that calculates the gradient curve and flow rates required to keep the heat loss of the column wall constant. The program takes into account the column inner and outer radii, the temperature of the mobile phase at the column inlet and outlet, the column permeability, the dwell volume, the column hold-up volume, various physico-chemical properties (viscosity, density, and expansion coefficient) of the eluent mixture that are functions of its composition, and the ambient temperature of the room. The analyst inputs the desired initial flow rate and the spreadsheet calculates the gradient curve and flow rates incrementally in 38 steps for the gradient, and 38 steps for post analysis equilibration. The data station can accept only a finite number of gradient steps, so a total of 42 steps were used for both the gradient and the equilibration. These equilibration steps cause the gradient to be returned to the initial eluent composition while maintaining the net loss of column heat constant. Details on the principles and implementation of this technique can be found in reference [41]. For the constant heat loss experiment, the column must be kept in still air, which is one of the properties taken into consideration in the calculation of the gradient parameters. This method minimizes the change in the temperature distribution across the column.

8.3.5 Determination of the reproducibility and peak capacity

Moment analysis provides accurate information on the retention times and the peak widths. The 0th moment is the peak area, the 1st moment is the true

retention time of the peak (different from the time of its apex, unless the peak is symmetrical), and the 2nd central moment is the band variance (related to the peak width) [8,16]. The peak capacity for the separations was determined by the time window for elution divided by the average base width of all the peaks in the chromatogram. In gradient separations, the peak capacity is of greater interest than the apparent efficiency.

8.3.6 Experimental conditions for quantitative analysis

The concentration of each analyte in the sample was 100 µg/mL (±0.5%). The Agilent RPLC checkout sample was used as such and diluted 1:10 in acetonitrile/water (50:50 v/v) with a volumetric flask.

The gradient methods were used to obtain quantitative data with no post run times. A blank run was conducted to bring the column to a pseudo-stationary thermal state. To obtain a calibration curve for all the gradient methods, the following amounts of the diluted sample (n = 3): 2, 4, 6, and 8 µL and of the pure RPLC standard were injected (n = 3): 2, 4, 6, and 8 µL.

8.3.7 Determination of the response factors

The use of gradient methods during which the flow rate changes raises an important challenge when quantitative analyses are performed. Plotting chromatograms in time units and comparing the peak areas yields reliable quantitative results only when the variations of the mass flow rate are taken into account during the elution of the compounds. To simplify this problem, the chromatograms were plotted as functions of the volume of mobile phase eluted. This is accomplished using a macro run by the ChemStation of the instrument, which generates a volume based chromatogram from the flow rate data and the detector signal. When the volume based chromatogram is integrated by the ChemStation, peak areas are expressed in mAU min (milliabsorbance units min), but can be converted to mAU mL by dividing the area by 60. The peak areas are expressed as [mAU mL] instead of [mAU s] and plotted against the mass of

compound injected. For this work, the response factors obtained in the separations are examined for a straightforward comparison of the methods.

8.4 Results and Discussion

8.4.1 Constant flow rate analysis

Fig. 8.1 shows the chromatograms and pressure curves for the constant flow rate separations. The effects of performing subsequent gradient separations under constant flow rate conditions are most clearly seen in the pressure curves (Fig. 8.1C). As the viscosity of the mobile phase decreases, the amount of heat produced decreases, causing the column temperature to drop. This explains why the pressure curves progressively increase. The greatest difference in the pressure curves is between the first and second separations. As subsequent separations are performed, the column cools, leading to an increased retention of analytes. As long as consecutive separations are performed with the same short equilibration time, a steady state is achieved after a few separations, yielding very reproducible separations. The net peak capacity of these experiments was 31.4, the highest of all tested methods.

Moment analysis demonstrated a high degree of reproducibility of the data. The relative standard deviation of the first moment (average retention time) for the six replicate separations was 0.029% with a RSD of 2.9% for the second central moment (band variance). If the first chromatogram is removed from this series and used strictly as a step toward column thermal equilibration, the RSDs of the first and second moments drop to 0.018 and 0.97% respectively. The process of disregarding the first chromatogram in a series is feasible, and could be done in a laboratory that must analyze many samples daily.

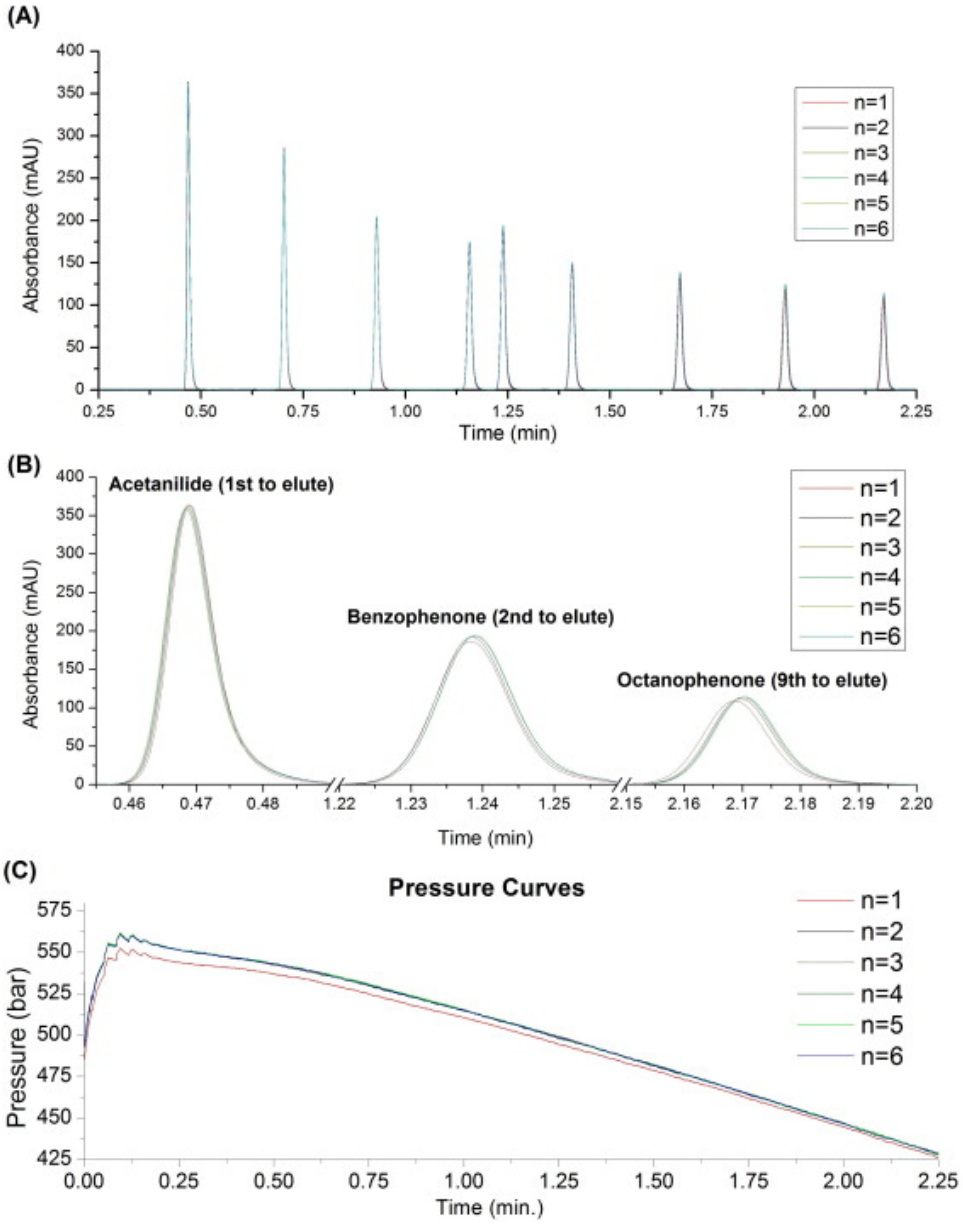

Figure 8.1. Chromatograms and Pressure Curves (Cf – Core-Shell). Constant flow (2.8 mL/min). (A) shows the overlaid chromatograms ($n = 6$) for constant flow rate experiments. Part (B) shows an enlarged view of the profiles of the first, fifth, and ninth sample components eluted. Part (C) shows the pressure curves for each separation.

8.4.2 Constant pressure analysis part 1: Analysis time equivalent to the constant flow experiments

Figure 8.2 shows the chromatograms and flow curves for the first set of constant pressure separations. In constant pressure operation, the column temperature rises and falls depending on the inlet pressure being applied. The flow rate in constant pressure operation depends directly on the column temperature, but thermal equilibrium is difficult to achieve, since as the flow rate changes, the amount of heat produced also changes. Furthermore, the retentions of the sample components depend also on the temperature of the separation, which further decreases the reproducibility. As in constant flow rate experiments, the greatest difference in reproducibilities occurs between the first and second separations in the series. The first gradient causes the column to heat. After that, subsequent separations produce less frictional heat since the flow rate drops slightly. For this reason, the column cools after the second separation and thermal equilibrium takes a long time to achieve. Among possible remedies, the post run time may be increased so that the column can return to its initial temperature or many more separations ($n > 6$) may be performed, using the same post-run time to attempt to reach thermal equilibrium.

The average RSD for the first moments was 0.32% and the one for the second central moments was 0.69%. If the first run is disregarded, these values decrease to 0.099 and 0.66%, respectively. The first moment under constant pressure operation was one order of magnitude higher than for constant flow rate separations. The band variances were found to be more reproducible under constant pressure than under constant flow rate operations, suggesting that the radial temperature gradient across the column was smaller under constant pressure than under constant flow rate operations. Volume based chromatograms are necessary for routine analyses, since this approach corrects for differences in the flow rate. However, it cannot correct for errors in retention.

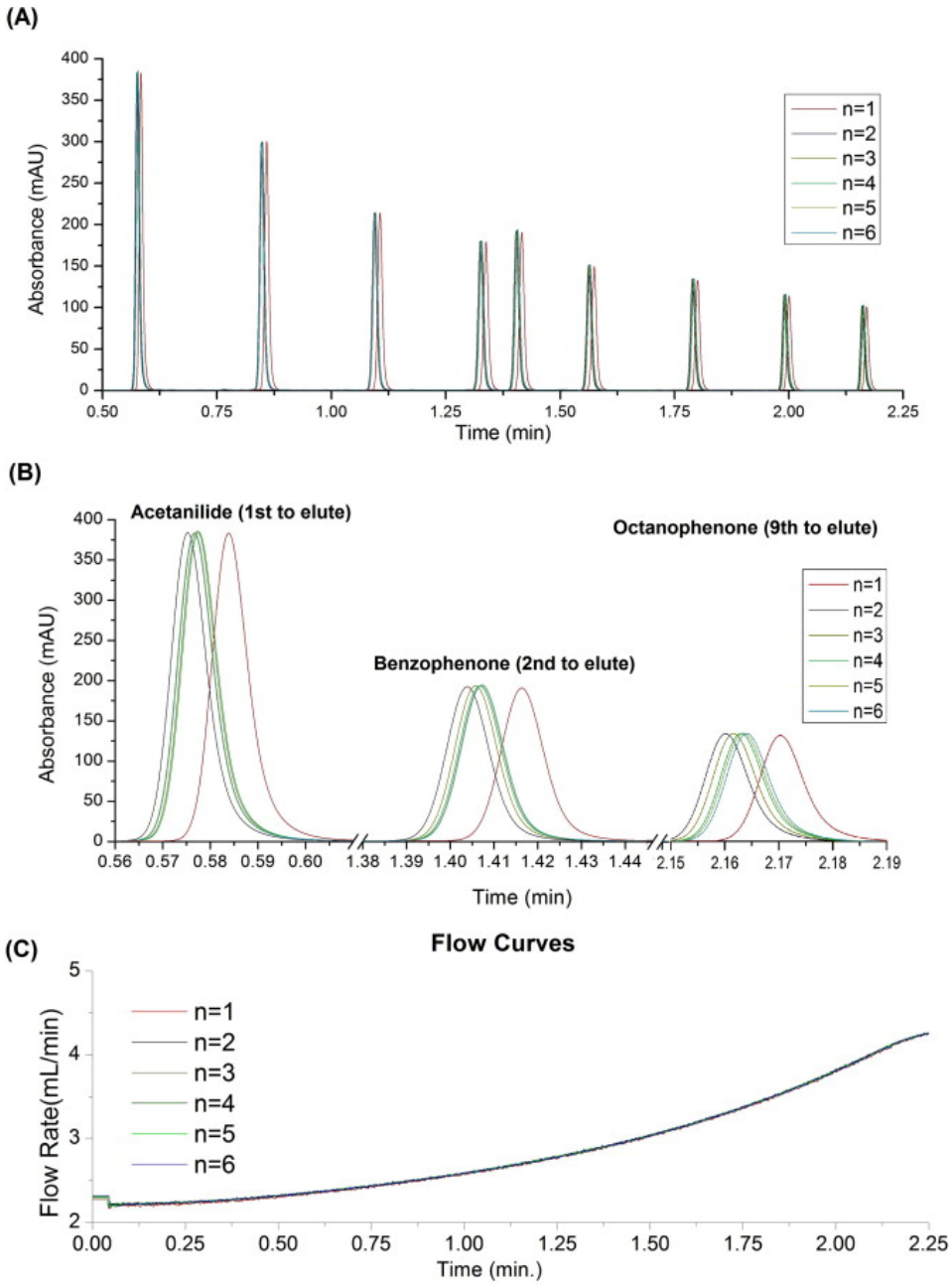

Figure 8.2. Chromatograms and Pressure Curves (Cp 1– Core-Shell). Constant pressure part 1(435 bar). (A) shows the overlaid chromatograms ($n = 6$) for constant pressure experiments that have the same analysis time as the constant flow experiments. Part (B) shows an enlarged view of the profiles of the first, fifth, and ninth sample components. Part (C) shows the flow curves for the separations.

The net peak capacity of this approach was 25.9, slightly lower than under constant flow rate. Other work has shown that there is only a small change in the peak capacity when separations are conducted under constant pressure instead of under constant flow rate conditions [59]. For this reason and for other issues with reproducibility, there appears to be no direct advantage to operate gradient separations under low constant pressures.

8.4.3 Constant pressure analysis part 2: Operation at high pressure

Figure 8.3 shows the chromatograms and flow curves for the second set of constant pressure separations. Results show that separations performed under constant high pressures and low pressure are similar. Operating at very high pressures causes the production of a higher heat power, which is why three or more successive separations are required for the column to reach a fairly stable temperature. The benefit of very high constant pressure operations is that the separation is rapid, 16% faster than for constant flow rate analyses. The drawback is a lower reproducibility, with respect to constant flow rate separations.

Moment analysis of chromatograms recorded under high constant pressure provides results similar to those of the previous series of constant pressure experiments. The average RSDs for the first and second moments were 0.35 and 0.88%, respectively. These values drop to 0.060 and 0.69%, respectively, if the first separation is used to equilibrate the column. The band variances were more reproducible under constant high pressure conditions than under constant flow rate operations, but slightly less so than under the constant lower pressure. The first moment, for constant high pressure operations, was an order of magnitude higher than for the constant flow rate separations. The net peak capacity under constant high pressure operations was 28.0, not much lower than that observed for constant flow rate operation (31.4).

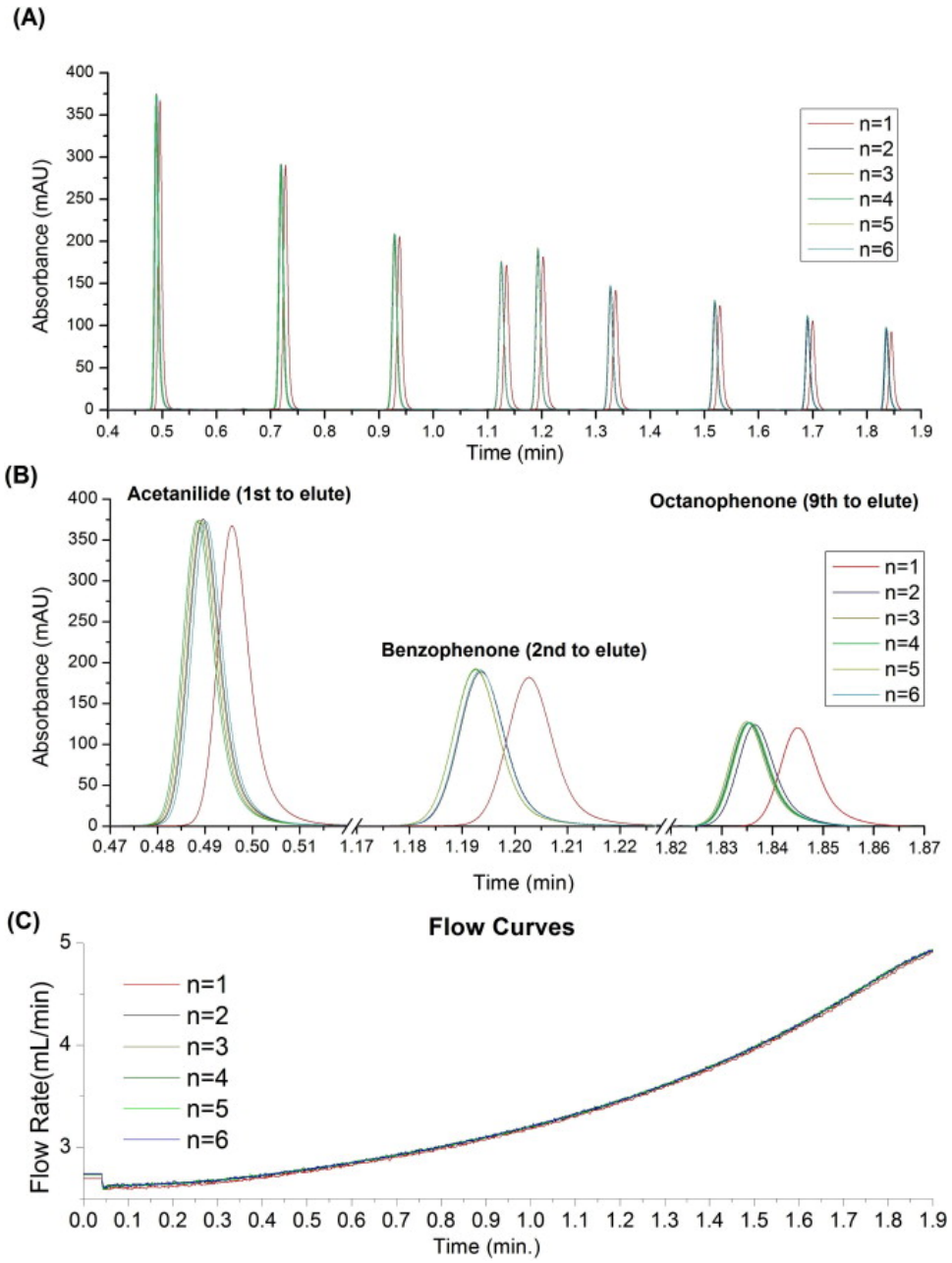

Figure 8.3. Chromatograms and Pressure Curves (Cp 2 – Core-Shell). Constant pressure part 2 (510 bar). (A) shows the overlaid chromatograms ($n = 6$) for constant pressure experiments at the maximum possible pressure. Part (B) shows an enlarged view of the profiles of the first, fifth, and ninth sample components. Part (C) shows the flow curves for each separation.

8.4.4 Programmed flow constant pressure analysis at high pressure

Figure 8.4 shows the chromatograms and flow curves for the programmed flow constant pressure separations. Programming the flow rates at which separations are carried out improved their reproducibility. These separations were set to mimic high constant pressure analyses although flow rates and gradient parameters were input into the data station so that the flow rate of each analysis is independent of the operating pressure. The pressure curve was nearly linear close to 510 bar. Fig 4 (B and D) shows that the first separation deviates from the others. The retention times in the first chromatogram are slightly longer and the pressure is higher. As in constant pressure experiments, the first separation heats the column and the following separations occur at a higher temperature. The RSD of the first moments in programmed flow constant pressure experiments was 0.057%, twice the RSD for constant flow rate experiments (0.029%). The RSD of the second central moments for programmed flow constant pressure experiments was 0.89%, a band variance three times smaller than for constant flow rate analyses.

If the first chromatogram of the series is discarded as an equilibration step, the RSDs of the first and second central moments decrease to 0.026 and 0.55%, respectively. These values are close to those obtained in constant flow rate operations (0.018 and 0.97%, respectively). This demonstrates how reproducibility could be improved by using a semi-constant pressure approach in VHPLC, which reduces the time of analysis by 16%. The net peak capacity was 29.2, nearly equivalent to the peak capacity at constant flow rate.

8.4.5 Constant column heat loss analysis

Fig. 8.5 shows the chromatograms, flow curves, and pressure curves for the constant column heat loss separations. The results of the separations made under constant heat loss conditions show good reproducibility.

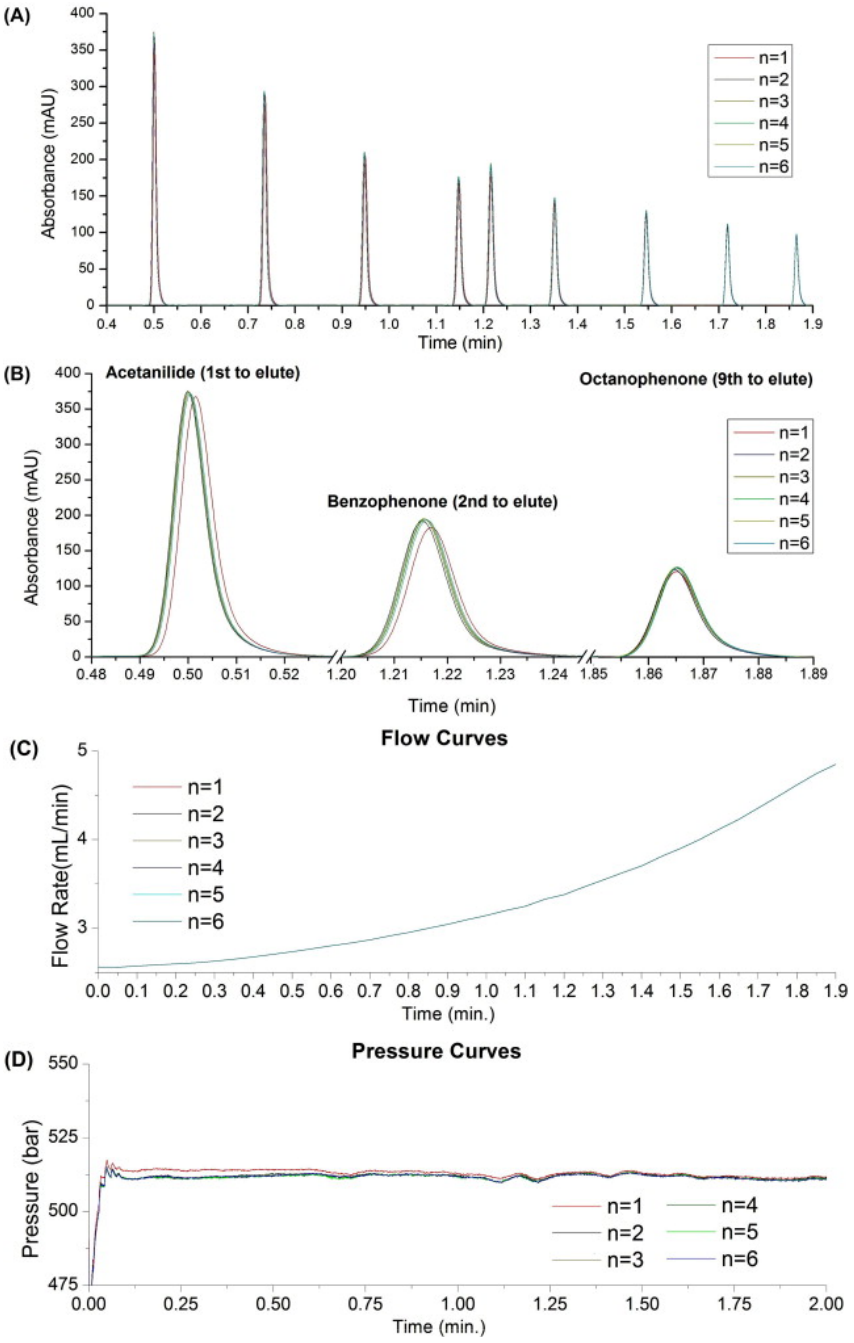

Figure 8.4. Chromatograms and Pressure Curves (CPp – Core-Shell). Programmed flow constant pressure (≈510 bar). (A) shows the overlaid chromatograms ($n = 6$) for programmed flow constant pressure experiments at the maximum possible pressure. Part (B) shows an enlarged view of the profiles of the first, fifth, and ninth sample components. Parts (C) and (D) show the flow and pressure curves for these separations.

This method keeps the heat lost through the column wall constant but the temperature distribution across the column still changes. This explains subtle differences in both the average retention times and the band variances. This method provides the fastest analyses, all components eluting in 1.75 min, with a total analysis time of 2.25 min due to the post-analysis time (see Fig. 8.5(C and D)) of 0.5 min required to keep the column wall temperature constant. During this period, the gradient returns progressively to its starting conditions, a return process that is different from a post-run time, which is isocratic and done at constant flow rate.

Moment analysis gave RSDs of the first and second central moments of the constant wall heat experiments of 0.029 and 2.0%, respectively; equivalent to the values found for constant flow rate experiments. If the first chromatogram is used for column equilibration, the RSDs for the first and second central moments are 0.027 and 1.7%, respectively while constant flow rate analyses yielded RSDs of 0.018 and 0.97%.

The reproducibility of separations is not improved by making them at constant wall heat lost. The peak capacity of constant wall heat experiments was 23.2, the lowest of all the experiments discussed. This can be due to the small elution time window and to band dispersion caused by a flow rate above the optimal one.

8.4.6 Quantitative results

Using volume-based integration provided by the ChemStation and the Agilent macro, the response factors for the analytes were calculated from the chromatograms provided by triplicate injections of the following sample masses: 0.02, 0.04, 0.06, 0.08, 0.2, 0.4, 0.6, and 0.8 µg.

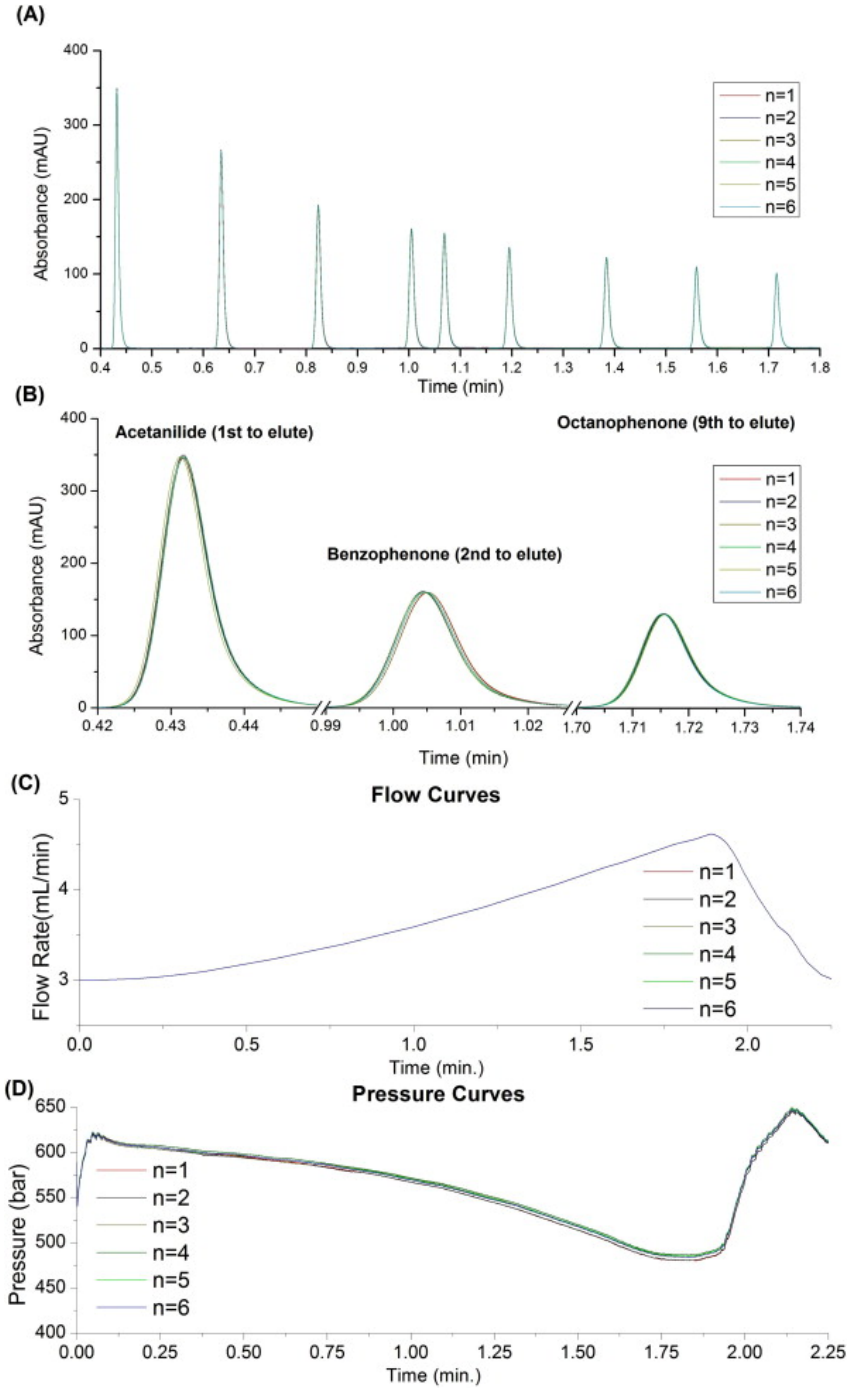

Figure 8.5. Chromatograms and Pressure Curves (CHL – Core-Shell). (A) shows the overlaid chromatograms ($n = 6$) for constant heat loss experiments at the maximum possible speeds. Part (B) shows an enlarged view of the profiles of the first, fifth, and ninth sample components. Parts (C) and (D) show the flow and pressure curves for these separations.

Table 8.2 lists the average response factors calculated from the volume-based chromatograms provided by the four gradient methods and their RSDs. Table 8.3 lists the average relative errors in the calculated compound masses using the four gradient methods when the response factors measured in constant flow rate operation are assumed to have the correct values. The errors in quantitative analyses made when using the response factors derived from constant flow rate analyses with a column packed with core-shell particles and applying them to variable flow rate methods are less than 3%. Previous work found that these errors were 6% when the same method was used with a column packed with fully porous particles [78]. The explanation for this increase in accuracy is that columns packed with core-shell particles dissipate heat faster than columns packed with fully porous particles. It can be concluded that across methods the thermal conditions inside columns packed with core-shell particles are relatively similar, whereas columns packed with fully porous particles appear to have greater temperature variations across methods. The temperature at which analytes are eluted can lead to changes in the response factors.

8.5 Chapter Summary

Five different strategies for delivering the mobile phase in VHPLC gradient analysis were explored. When a column packed with core-shell particles was used, the response factors measured for the gradient methods discussed differ by less than 3% one from the other. In contrast, previous work showed that columns packed with fully porous particles might cause larger errors if calibration was not done for each method [78]. Analyses times obtained under constant pressure or flow programmed constant pressure methods were 16% shorter than those obtained under constant flow rate conditions. The peak capacity was 11% less with a high constant pressure method than with a constant flow rate method. For all the methods discussed, using a first separation to approach thermal equilibrium of the column improved the reproducibility for all the discussed

metrics. Previous work with a column packed with fully porous particles showed that discarding two previous separations was beneficial to condition the column before a long series of subsequent analyses [78].

Table 8.2. Accuracy of the discussed methods with respect to constant flow.

Average response factors [(mAU mL)/µg] and RSDs					
Compound	Constant flow (%)	Constant pressure 1 (%)	Constant pressure max. (%)	Programmed flow constant pressure max. (%)	Constant wall heat (%)
Acetanilide	87.7/0.61	88.9/0.77	88.3/0.72	88.0/0.63	88.9/0.77
Acetophenone	90.7/0.52	89.8/0.68	90.3/0.67	90.9/0.54	89.8/0.68
Propiophenone	76.0/0.62	73.7/0.55	75.4/0.71	76.2/0.57	73.7/0.55
Butyrophenone	70.7/0.77	69.4/0.69	70.1/0.94	70.9/0.73	69.4/0.69
Benzophenone	73.1/0.49	73.6/0.48	73.4/0.65	73.3/0.44	73.6/0.47
Valerophenone	63.4/0.82	62.4/0.73	62.9/1.00	63.4/0.79	62.4/0.73
Hexanophenone	59.5/0.74	58.6/0.67	59.0/0.94	59.4/0.76	58.6/0.67
Heptanophenone	53.5/0.69	52.9/0.83	53.2/1.12	53.5/0.85	52.9/0.83
Octanophenone	48.4/0.82	47.8/0.78	48.2/0.90	48.4/0.75	47.8/0.78
Average percent error vs. constant flow	–	1.51	0.66	0.17	1.06

Table 8.3. Average Relative Error. Average relative error for masses calculated using response factors obtained from constant flow rate analyses.

Average Relative Error				
Compound	Constant pressure 1 (%)	Constant pressure max. (%)	Programmed flow constant pressure max. (%)	Constant wall heat (%)
Acetanilide	1.40	0.74	0.57	0.66
Acetophenone	1.01	0.62	0.48	0.80
Propiophenone	1.71	0.84	0.51	1.27
Butyrophenone	1.82	0.86	0.63	1.45
Benzophenone	0.67	0.74	0.39	0.51
Valerophenone	1.53	0.78	0.66	1.50
Hexanophenone	1.54	0.75	0.59	1.46
Heptanophenone	1.24	0.79	0.54	1.26
Octanophenone	1.36	0.64	0.66	1.22

Columns packed with core-shell particles seem to be more suitable for constant pressure methods than those packed with fully porous particles. They demonstrate good reproducibility of the response factors, the peak widths, and the retention times. Analysts using constant pressure methods will find columns packed with core-shell particles useful in improving the reproducibility of quantitative analyses.

Ultimately there is a relatively minor gain when the throughput (number of peaks eluted per minute) is compared across the discussed methods. The peak capacity decreases as the total time decreases (Table 8.1: Peak capacity per minute of total time) the number of peaks eluted per minute increases by approximately 7% for the high constant pressure method and the programmed flow method which mimics the high constant pressure method. This may not be enough to warrant many labs to adopt alternative methods of delivering the gradient. In certain situations where the reproducibility of the peak area can be an important factor, such as in proteomics, there may be a benefit in adopting these rapid techniques. Later work will discuss the reproducibility of volume based chromatograms in constant pressure operation used to correct for changes in the flow rate from separation to separation.

CHAPTER IX
Volume Based and Time Based Chromatograms

9.1 Introduction

The desire to accelerate chromatographic separations caused scientists to conduct constant pressure operations in which separation speed is increased by operating the instrument and the column under the highest pressure that they can withstand. The revival of the use of constant pressure gradients was recently suggested [21-23,79]. Previous work confirmed the advantages of constant pressure techniques [7,61,80-82]. However, if the column permeability changes during a series of analyses due to deterioration of the packed beds or to a poor control of the eluent temperature, the instrument will perform operations at flow rates that will fluctuate. Experiments are needed to better understand the constant pressure process, the performance of different column packing materials under different separation conditions, the way different means of delivering the gradient affects on the reproducibility of chromatograms, and what errors may be encountered in quantitation using ultra-violet detection.

In theory if there is neither appreciable frictional heating during the separation nor change of the eluent density along the column, the time-based chromatogram should be as reproducible as volume-based ones under constant flow rate separations. When the temperature distribution across and along the column is neither uniform nor stationary, time-based and volume-based chromatograms cannot be as reproducible due to the uncontrollable fluctuations in the retention of the analytes. Constant pressure operation in Very High Pressure Liquid Chromatography (VHPLC) exhibit lower reproducibility of retention times when time-based chromatograms are used to compare methods in which the flow rates are input into the instrument by the analyst [7,61,81-82]. Lack of reproducibility occurs under very high pressures due to the heating caused by friction affecting

the mobile phase viscosity and density, and may take place at low pressures when the column permeability changes between runs. The goal of this work was to determine how much volume-based chromatograms correct for undesirable but unavoidable fluctuations in flow rate and thermal environment.

Frictional heating in chromatographic columns is a well-known physical phenomenon, which affects retention and band broadening in liquid chromatography [33,38,41,55,72-77,83]. In general, the heat power generated by friction of the mobile phase percolating through the column increases with decreasing average size of the particles in the column packing material and with increasing the flow rate. This is not of great concern in isocratic separations since the mobile phase viscosity and its thermal conductivity do not change over time. In gradient separations, these parameters vary during a run and during the isocratic periods preceding or following each analysis [38,61]. There are two potential remedies for this situation. First, an adequate post-run time after each separation allows the column to return to the same starting temperature after each analysis [7]. Second, a very brief post-run time is used, and after one or two separations a reproducible starting temperature is achieved for subsequent separations [81-82]. The first separation(s) are used strictly for column equilibration, and the following runs are excellent reproducibility. For many practitioners this is a reasonable solution to quickly achieve highly reproducible separations.

To evaluate the volume based chromatograms generated by Agilent ChemStation Rev. C.01.03, a column packed with fully porous particles was selected because such columns do not dissipate heat as quickly as those packed with core-shell particles [84-85] and thus their use permits a more rigorous assessment of the software generating the volume-based chromatograms in the ChemStation. Both time-based and volume-based chromatograms were integrated and the response factors for each method compared.

Nine gradient elution methods were used to test various experimental conditions including two sets of constant flow rate separations, four sets of constant pressure separations, two sets of programmed flow constant pressure experiments, and one set of experiments involving experimental conditions which should produce a constant amount of heat at the column wall. Details of these methods are discussed in the next sections.

9.2 Materials and Methods

9.2.1 Instruments, columns, and reagents

Experiments were conducted in a 24°C room, using a prototype Agilent 1290 Infinity System capable of constant pressure operations (Agilent Technologies, Waldbroen, Germany). A Thermo Viper (130µm I.D.) column connection unit (Dionex-Fisher, Sunnyvale, CA, USA) was used to connect a Waters XBridge BEH XP C_{18} (4.6x100mm; 2.5 µm particle size) column and a Waters XBridge BEH XP Vanguard Pre-Column (2.1x5mm; 2.5 µm particle size) to the instrument. Fisher Scientific (Fair Lawn, NJ, USA) HPLC grade water and acetonitrile were used. The test mixture for all the experiments was a 2 µl sample of the Agilent RPLC checkout sample consisting of (in order of elution) acetophenone, propiophenone, butyrophenone, valerophenone, hexanophenone, heptanophenone, octanophenone, benzophenone, and acetanilide dissolved in water/acetonitrile (65:35 v/v) in concentrations of 100µg/mL each (+/- 0.5%). Chemstation Rev. C.01.03(37) was used for online and offline analyses.

9.2.2 Experimental conditions

The instrument was set to provide the briefest possible equilibration periods (post-run times) allowable by the software. Eight consecutive 2 µl injections of the sample were performed for all experiments. The column was insulated in a one inch thick layer of Styrofoam insulation. In previous work [7,81], the column was left in open air for constant heat loss experiments. It was determined that a

marginal difference between constant heat loss experiments took place whether the column was insulated or exposed to open air, as long as an adequate time allowed temperature to equilibrate across the column and between column and Styrofoam insulation before a new separation was performed. For separations made with an inlet column pressure less than 300 bar, the frictional heat generated by the mobile phase is small and separations should be highly reproducible. To ensure that the column temperature was stable for each set of separations, the mobile phase was flowed through the column for 10 min before each series of runs . A 50 to 95% gradient of acetonitrile in water was used for all experiments. Table 9.1 gives a quick reference to the experimental conditions. It lists the method parameters for the low pressure experiments. Table 9.2 lists the method parameters for the high flow experiments.

9.2.3 Constant flow rate experiments

The parameters of constant flow rate experiments were input into the instrument software in the conventional way. The first set of constant flow rate experiments was conducted at a flow rate of 0.5 mL/min, with a starting inlet pressure of approximately 141 bar and a total run time of 11.4 minutes; this generated an average of 0.84 W/meter of heat inside the column. The second set of constant flow rate separations was conducted at 2.25 mL/min and a total runtime of 2.55 min with a starting inlet pressure of approximately 600 bar generating an average of 16.99 W/m of heat inside the column.

9.2.4 Constant pressure experiments part 1

Both constant pressure experiments were based on the volumetric flow profile from the constant flow rate experiments using the macro provided by the manufacturer. The ChemStation takes the constant flow rate method and creates a volume based method operating under constant inlet pressure. The mobile phase composition is dictated by the net volume of solvent eluted under constant pressure operation.

Table 9.1. Summary of Experimental Conditions and Results at Low Pressures.

Solvent Gradient 50% to 95% Acetonitrile in Water for All Experiments				
Experiment Set	Constant Flow	Constant Pressure 1	Constant Pressure 2	Programmed Flow Constant Pressure
Gradient Time	10.0 min	10.3 min	7.6 min	7.6 min
Total Time	11.4 min	11.2 min	8.3 min	8.3 min
Flow Rate	0.5mL/min	Variable	Variable	Variable
Pressure	Variable	105.5 bar	141 bar	≈ 141 bar
Retention Time RSD (Time Chromatogram)	0.029%	0.15%	0.15%	0.021%
Retention Time RSD (Volume Chromatogram)	0.026%	0.034%	0.078%	0.026%
Peak Width RSD (Time Chromatogram)	0.56%	0.56%	0.95%	0.62%
Peak Width (Volume Chromatogram)	0.57%	0.41%	0.84%	0.68%

Four sets of constant pressure experiments were performed, two at low operating pressures and two at high operating pressures.

The first series of separations was performed at 105.5 bar, yielding separations nearly as long as the constant flow rate separations (11.4 minutes); this method generated an average of 0.89 W/meter of heat inside the column. The second set of separations was performed at 141 bar (the maximum pressure reached during the 0.5 mL/min constant flow separations) with an average total runtime of 8.26 minutes. The average amount of heat generated by the method was 1.62 W/meter inside the column. Increasing the operating pressure by 35.5 bar nearly doubled the amount of heat generated.

Table 9.2. Summary of the Experimental Conditions and Results at High Pressures.

Solvent Gradient 50% to 95% Acetonitrile in Water for All Experiments					
Experiment Set	**Constant Flow**	**Constant Pressure 3**	**Constant Pressure 4**	**Programmed Flow Constant Pressure**	**Constant Heat Loss**
Gradient Time	2.25 min	2.30 min	1.78 min	1.80 min	2.05 min
Total Time	2.55 min	2.53 min	1.93 min	1.94 min	3.13 min
Flow Rate	2.25mL/min	Variable	Variable	Variable	Variable
Pressure	Variable	462 bar	600 bar	≈ 600 bar	Variable
Retention Time RSD (Time Chromatogram)	0.12%	0.50%	0.52%	0.085%	0.040%
Retention Time RSD (Volume Chromatogram)	0.12%	0.15%	0.12%	0.10%	0.044%
Peak Width RSD (Time Chromatogram)	7.3%	2.2%	4.3%	2.6%	2.0%
Peak Width (Volume Chromatogram)	7.3%	2.0%	3.8%	2.6%	1.9%
Retention Time RSD (Time Chromatogram First separation excluded)	0.092%	0.13%	0.15%	0.018%	0.042%
Retention Time RSD (Volume Chromatogram First separation excluded)	0.093%	0.030%	0.037%	0.022%	0.047%
Peak Width RSD (Time Chromatogram First separation excluded)	3.9%	1.1%	1.2%	2.1%	1.9%
Peak Width (Volume Chromatogram First separation excluded)	3.8%	1.1%	1.0%	2.0%	1.9%

The third and fourth series of constant pressure runs were conducted at higher pressures. The third series was performed at 462 bar, with an average total runtime of 2.5 min, close to the total runtime as the constant flow rate separations at 2.25 ml/min. The 462 bar constant pressure method generated an average 17.46 W/meter of heat inside the column. The last series of constant pressure separations was run at 600 bar, close to the maximum inlet pressure that the column can stand, with a total runtime of 1.91 min. The 600 bar constant pressure method generated an average of 29.63 W/meter of heat inside the column.

9.2.5 Constant pressure experiments part 2

This method delivers a series of separations all made at the same flow rate, regardless of changes in the inlet pressure. Two sets of programed constant pressure experiments were performed. The first series of separations was based on the constant pressure separations obtained using 141 bar with a total runtime of 8.28 minutes. For the 141 bar separations at ten second increments in the flow rate profile, seven data points were averaged and manually input into a flow controlled method in the ChemStation. This method produced an average of 1.64 W/meter of heat inside the column.

The second series was based on the constant pressure separations obtained using 600 bar. For these experiments the flow rates and gradient parameters were taken from the constant pressure experiments and entered into the Excel program. For the 600 bar separations at three second increments in the flow rate profile, seven data points were averaged and manually input into a flow controlled method in ChemStation. The 600 bar programmed constant pressure method generated an average of 30.16 W/meter of heat inside the column.

9.2.6 Constant wall heat experiments

An Excel program was used to calculate the flow rates and the gradient profiles intended to yield a constant amount of heat generated at the column wall [86].

The equations used take into account many factors including the physico-chemical properties of the eluent mixture (viscosity, density, and expansion coefficient) as functions of its composition, the column inner and outer radii, the temperature of the mobile phase at the column inlet and outlet, the permeability of the column, the dwell volume, the column hold-up volume, and the ambient temperature in the room. The desired initial flow rate input into the program provides the gradient and the flow rates for 38 incremental steps of the separation. An additional 38 steps bring the mobile phase composition back to the initial isocratic conditions, without any marked change in the column temperature. The ChemStation allows a maximum of 42 steps for each method; 16 steps were used for the gradient separation and 16 steps to return the mobile phase to the initial conditions. Details on this method are in reference [86]. For the method used in this work a starting flow rate of 2.20 mL/min was used. Table 3 lists the input parameters for the constant heat loss method.

9.2.7 Determination of the Reproducibility (RSDs)

Moment analysis was used to assess the sizes and widths of the selected peaks in the chromatograms and their reproducibilities. In general, moment analysis provides an accurate assessment to compare chromatograms, provided that all the peaks are completely resolved. The 0^{th} moment gives the peak area, the 1^{st} moment gives the true retention time of the peak (it is different from the time of the apex, unless the peak is symmetrical), and the 2^{nd} central moment provides the peak variance (related to the band width) [59]. There were 8 injections performed for each method, with the RSD's calculated and averaged for each of 1^{st} and 2^{nd} central moments for all the analytes in the sample.

9.3 Results and Discussion

The goal of this study was to compare the reproducibility of time-based and volume-based chromatograms. This issue is discussed in the next sections. The peak capacity of a separation is the same if it is plotted in either time-based or volume-based chromatograms.

9.3.1 Constant flow rate analysis

Figure 9.1 shows the 1st, 5th, and 9th peaks of the test sample eluted with two constant flow rate methods, displayed as time-based and volume based chromatograms. In terms of reproducibility, there should be no significant changes when a time-based chromatogram obtained using a constant flow rate method is converted into a volume-based chromatogram. This was the case, the first and second moments provided by both chromatograms are very close, the reproducibility of the peak widths and retention times are the same for both low and high pressure separations, as shown in Tables 9.1 and 9.2. The differences in retention times observed for both low pressure separations gave a 0.003% RSD discrepancy between time- and volume-based chromatograms. The most likely cause of this effect is in the different sampling rates of the time-based (160hz) and the volume-based chromatograms (83.3 hz). The manipulation of the chromatographic data does not alter the reproducibility of the data obtained for constant flow rate separations; it rather demonstrates that the macro works as intended.

9.3.2 Constant pressure analysis

A notable result of this work is that the volume-based transformation affects the reproducibility of separations performed under constant pressure is shown in Figure 9.2. Constant pressure separations are less reproducible when plotted as time-based chromatograms. When constant pressure chromatograms are plotted as functions of the eluent volume eluted, the reproducibility of retention times and peak widths improves drastically. For the constant pressure separations having the same analysis time as the constant flow separations, the RSD of the retention time and peak width (under an inlet pressure of 105.5 bar) were 0.034 and 0.41% for volume-based chromatograms. For the time-based chromatograms of separations run under constant flow rate at the same analysis time, the RSD of the retention time and the peak width were 0.029 and 0.56%.

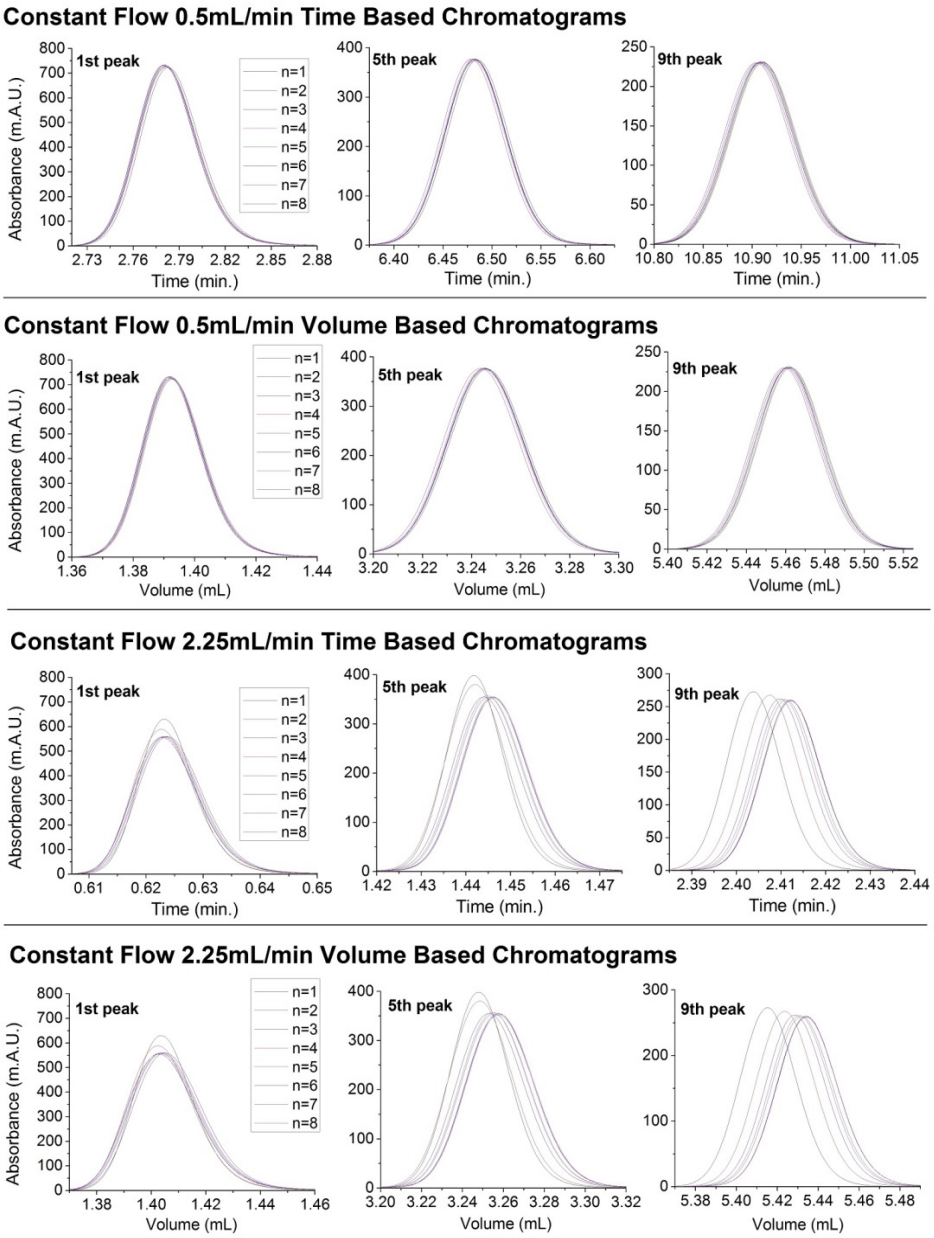

Figure 9.1. Chromatograms (Cf). Shows enlarged views of the 1st, 5th, and 9th compounds of the RPLC checkout sample (acetophenone, hexanophenone, and acetanilide) displayed in time and volume units, as eluted during eight successive runs with the constant flow rate methods discussed.

A second series of constant pressure separations was run at 141 bar. The reproducibility of the volume-based chromatograms fell by nearly a factor of two for both retention times and peak widths (see Table 2). This precision level, with a RSD below 0.8% for retention time and 1% for peak width, is still acceptable. The reproducibility of chromatograms depends on the flow rate(s) and the operating pressure(s), which seems to be the case for all methods explored so far. This would also be the same situation under isothermal and non-isothermal conditions.

Figure 9.3 shows the 1st, 5th, and 9th peaks of the RPLC checkout sample displayed in time and volume units for the two constant pressure methods run under high pressures. Using the first run of the gradient series to achieve thermal equilibrium across the column, improves reproducibility of volume-based chromatograms by a factor of 5 for experiments run at 462 bar and a factor of 3 for those run at 600 bar. Using a constant high pressure method rather than a constant flow rate one (run at high flow rate) improves the precision of the retention times by a factor of 3 and that of the peak widths by nearly a factor of 4. This improvement is very promising. More investigations are needed to assess the long term reproducibility of this method.

For constant pressure separations reported as volume-based chromatograms, a high degree of reproducibility was obtained under isothermal and non-isothermal conditions, providing a considerable improvement over time-based chromatograms.

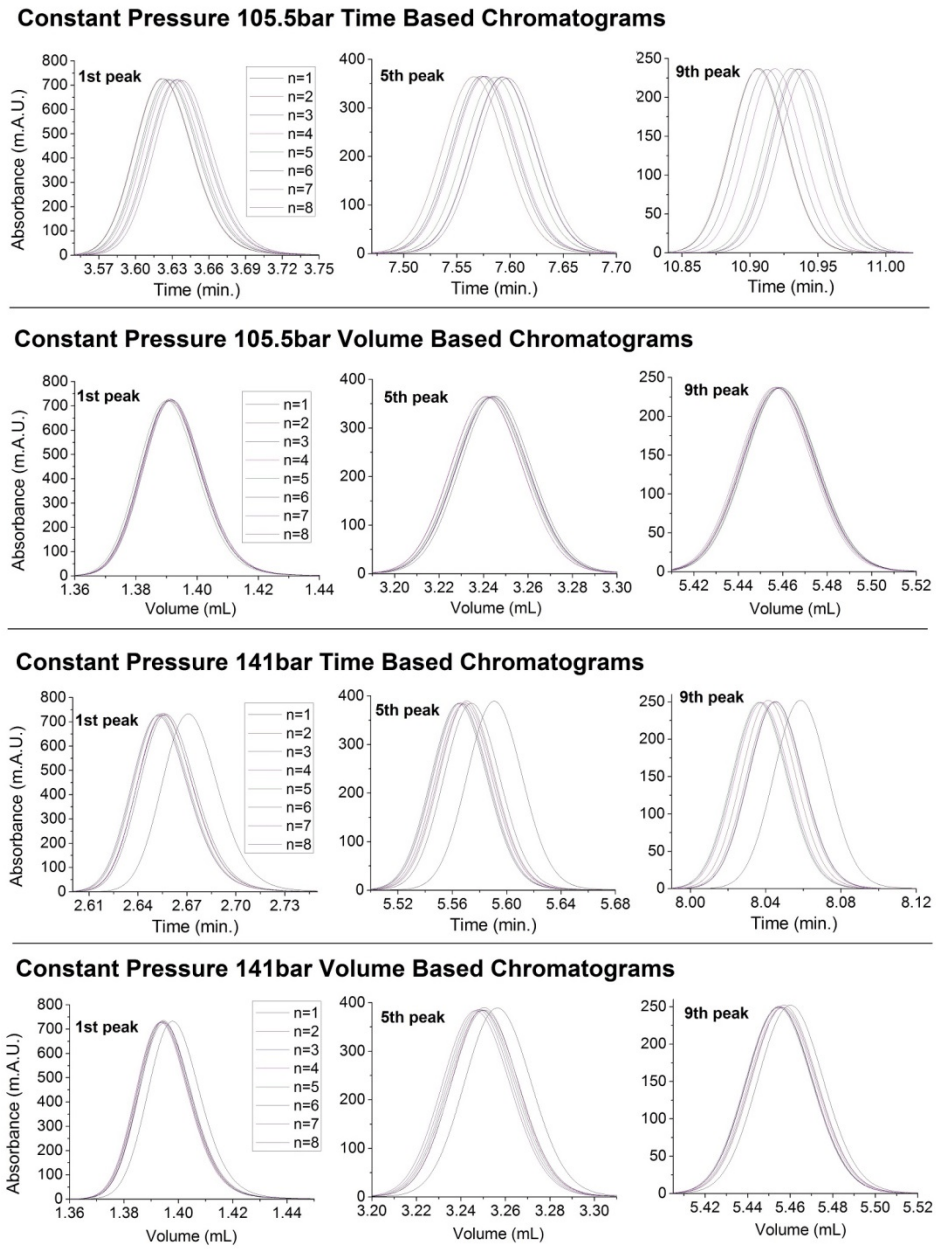

Figure 9.2. Chromatograms (Cp1). Shows enlarged views of the 1st, 5th, and 9th compounds of the RPLC checkout sample (acetophenone, hexanophenone, and acetanilide) displayed in time and volume units, as eluted during eight successive runs with the two constant low pressure methods.

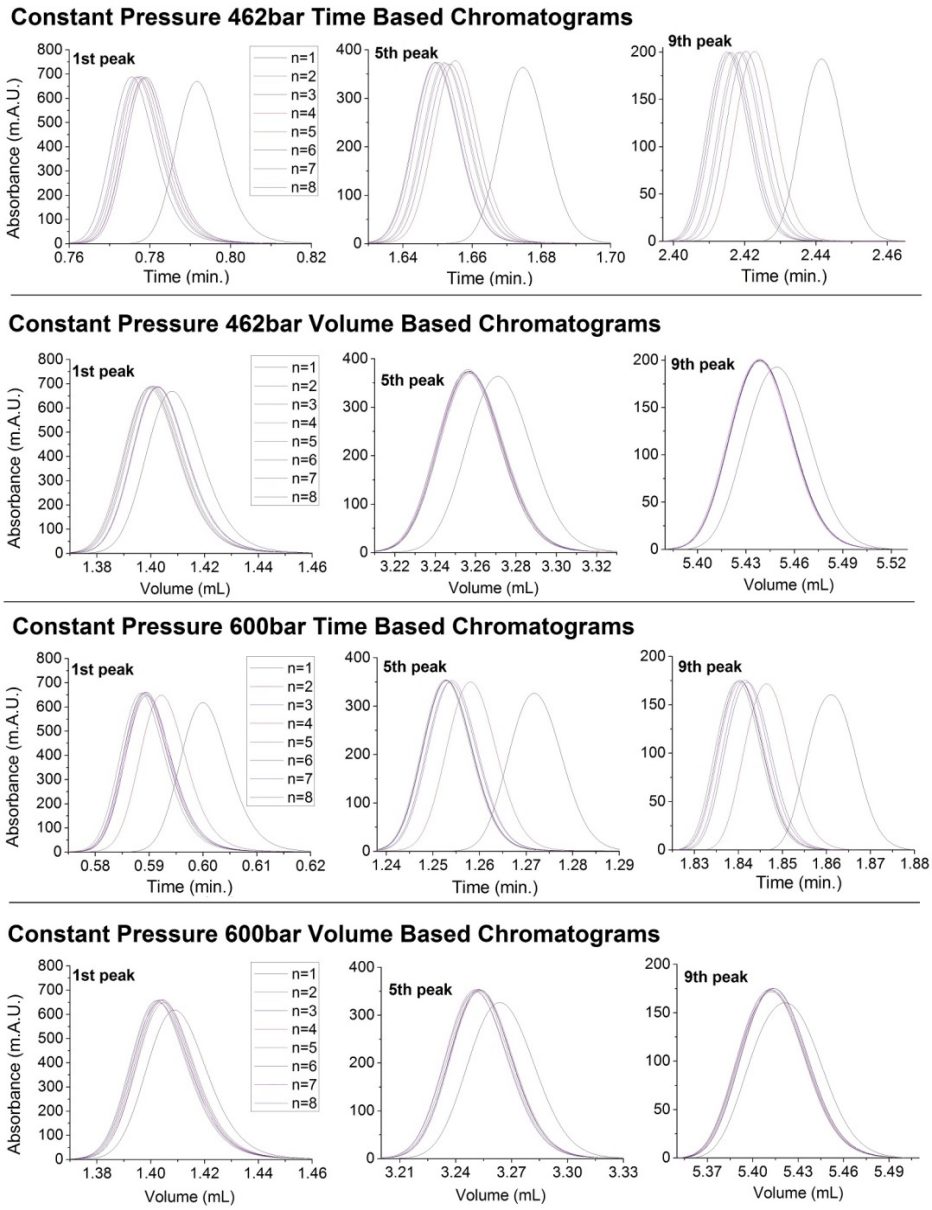

Figure 9.3. Chromatograms (CP 2). Shows enlarged views of the 1st, 5th, and 9th compounds of the RPLC checkout sample (acetophenone, hexanophenone, and acetanilide) displayed in time and volume units, as eluted during eight successive runs with the two constant pressure methods operated at high pressures.

9.3.3 Programmed constant pressure analysis

In programmed constant pressure experiments, the flow rates and gradient curves are input into the instrument method, so the flow rate remains independent of the column inlet pressure. Figure 9.4 shows the 1st, 5th, and 9th peaks of the RPLC checkout sample displayed in time and volume units, as eluted during eight successive runs with the two programmed flow rate under constant pressure methods discussed. Clearly, viscous heating affects the retention during the first run in the series run at 600 bar. The reproducibilities of retention times in time-based and volume-based chromatograms are different. The differences are minor when pressures are low and the column isothermal, the RSD of the retention times being 0.021 (time-based chromatograms) and 0.026% (volume-based chromatograms). For peak widths, the reproducibility shifts from 0.62% (time-based) to 0.68% (volume-based). A slightly larger difference in reproducibility was found when the first separation was excluded, giving a retention time RSD of 0.018% for time-based and 0.047% for volume-based chromatograms. With this method and the constant flow method, time-based provide more reproducible results than volume-based chromatograms. Performing high pressure separations under programmed constant pressure yields more reproducible retention time data than other methods under non-isothermal conditions when the first run of a series is used for column conditioning. Programmed flow constant pressure methods appear to give four times more precise retention times and twice as precise peak widths as those obtained using constant flow rate methods at 2.25 mL/min.

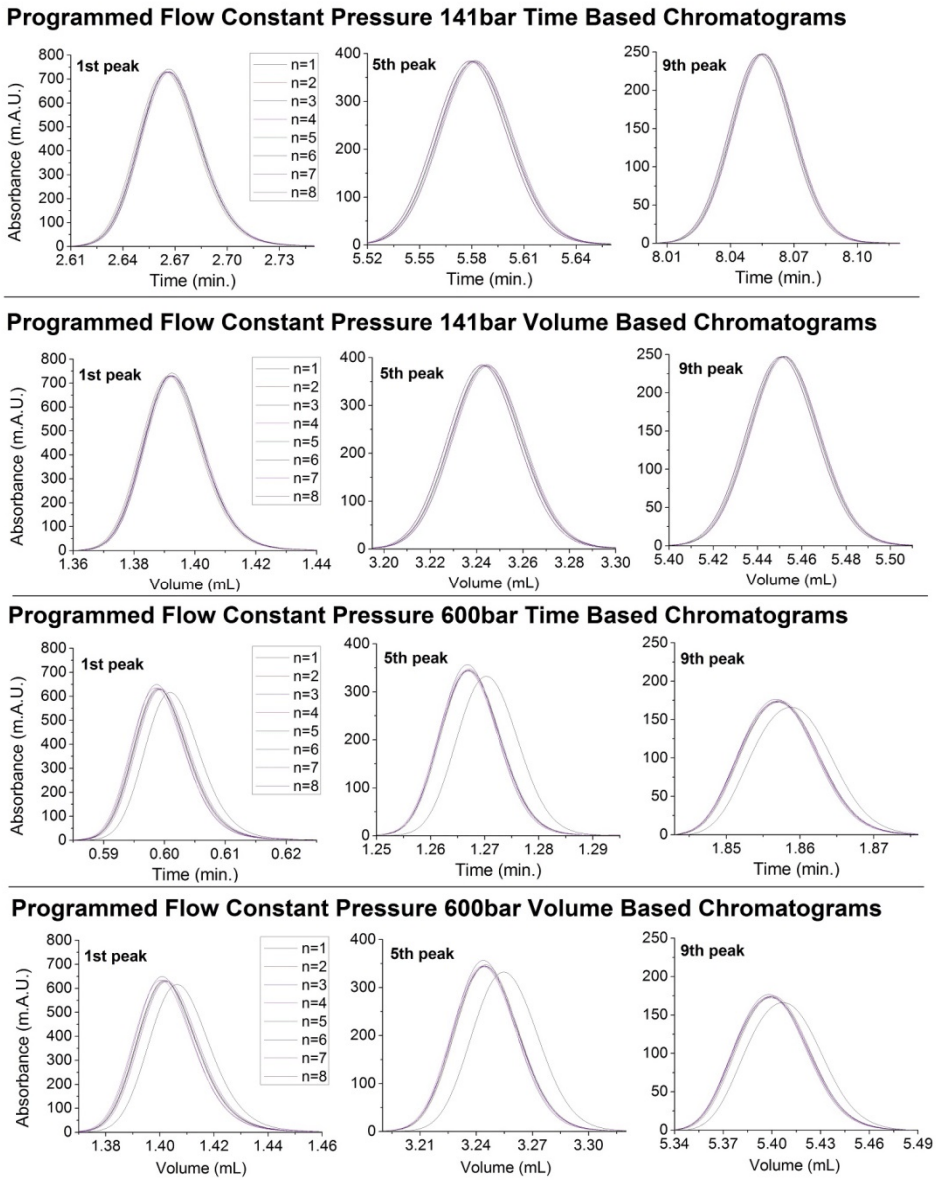

Figure 9.4. Chromatograms (CHL). Shows enlarged views of the 1st, 5th, and 9th compounds of the RPLC checkout sample (acetophenone, hexanophenone, and acetanilide) displayed in time and volume units, as eluted during eight successive runs with the two programmed flow rate under constant pressure methods discussed.

9.3.4 Constant heat loss analysis

Only one series of constant heat loss separations was performed, at the maximum pressure that the column could withstand. Figure 9.5 shows the 1st, 5th, and 9th peaks displayed in time and volume units, as eluted during eight successive runs with this method. There would be no advantage in performing this method under low pressures, since gradient runs do not cause any significant temperature rise inside the column. The data in Table 9.2 suggests that there is a minor benefit in plotting time-based rather than volume-based chromatograms. In agreement with the results of previous work [81], there is very little benefit in using the first gradient run to equilibrate the column with this method since its motivation is to improve data reproducibility without needing to use the first run of a series to condition the column. However, the column still needs to be equilibrated under isocratic conditions for at least 5 minutes to achieve thermal stability before the start of the analyses.

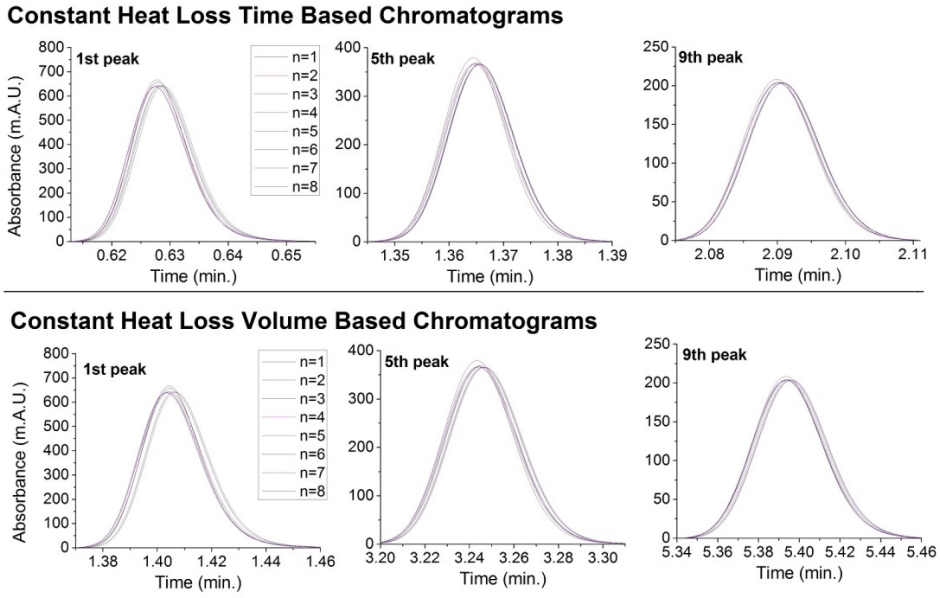

Figure 9.5 shows enlarged views of the 1st, 5th, and 9th compounds of the RPLC checkout sample (acetophenone, hexanophenone, and acetanilide) displayed in time and volume units, as eluted during eight successive runs with the constant heat loss method.

9.4 Summary of Findings

Figure 9.6 shows the retention time RSDs for time and volume based chromatograms in the discussed methods. Plotting chromatograms for constant pressure separations as a function of volume eluted, as opposed to functions of time elapsed, improves the reproducibility of the retention time by an average factor of 3.7 and brings them much closer to the values obtained in flow controlled methods. Flow controlled methods (constant flow, programmed constant pressure, and constant wall heat) were more reproducible when the first separation was included in the calculation of the RSD for the retention times of eluted compounds with respect to constant pressure approaches.

Figure 9.7 shows the retention time RSDs for the time and volume based chromatograms in the discussed methods, with the first separation in the series excluded as a column equilibration step. If one gradient run is used to bring the column to a relatively stable temperature, constant pressure separations have a factor of 3 times better reproducibility of retention time with respect to constant flow rate gradient separations. These differences are marginal for the majority of practitioners, especially when operating at very high operating pressures.

9.5 Chapter Summary

Nine gradient methods were used to determine the difference between the volume-based and time-based chromatograms generated by the ChemStation Rev. C.01.03(37). The volume-based chromatograms improve the retention time reproducibilities of the four constant pressure methods by a factor of 3.7 on average. The data indicates that the reproducibilities of the retention times and peak widths are better with constant pressure than constant flow rate methods, if a first gradient is run before a long series of separations and discarded from data analysis.

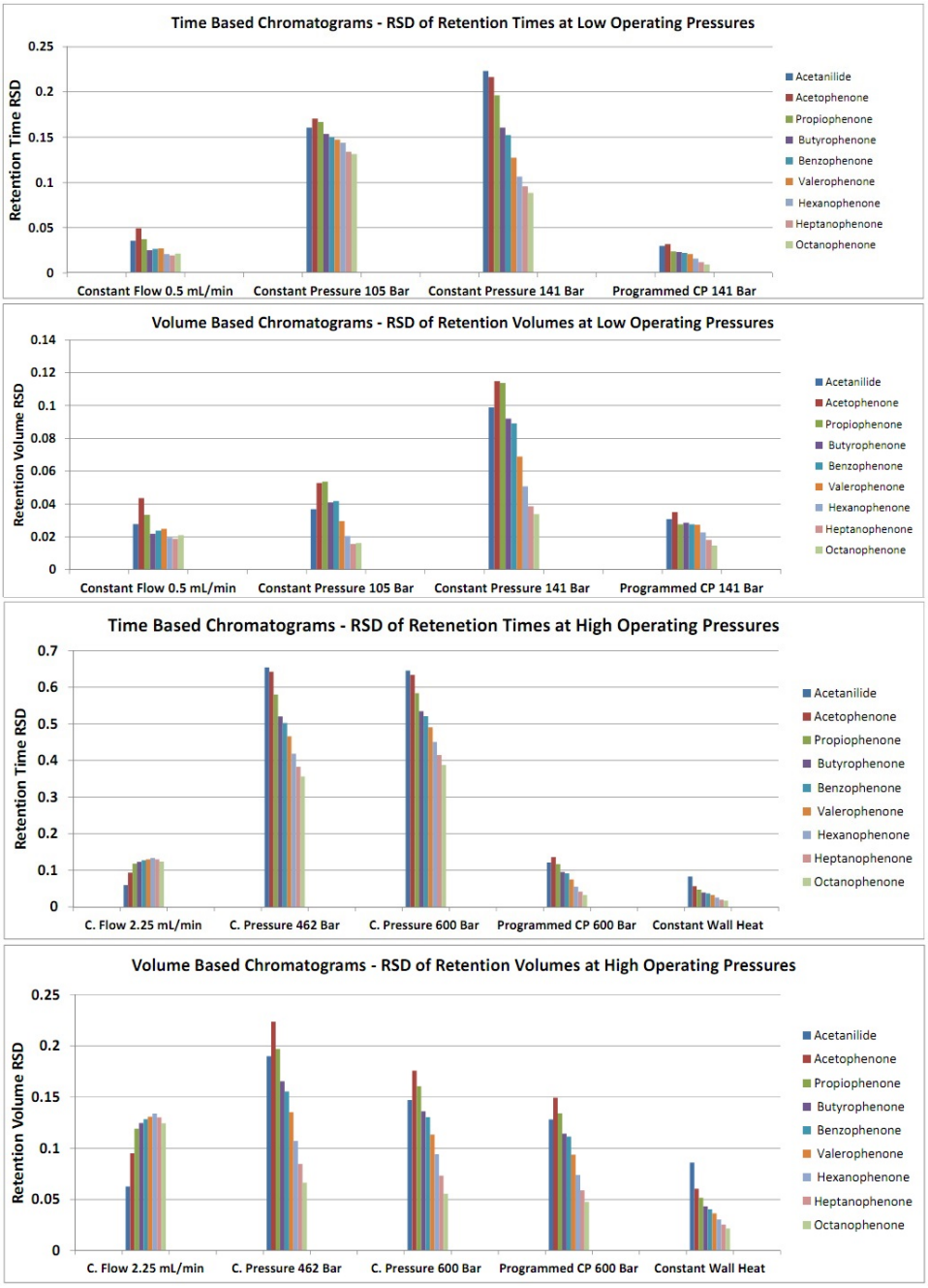

Figure 9.6. Relative Standard Deviations. Displays the RSDs (n=8) for all the compounds in the sample for time and volume based chromatograms.

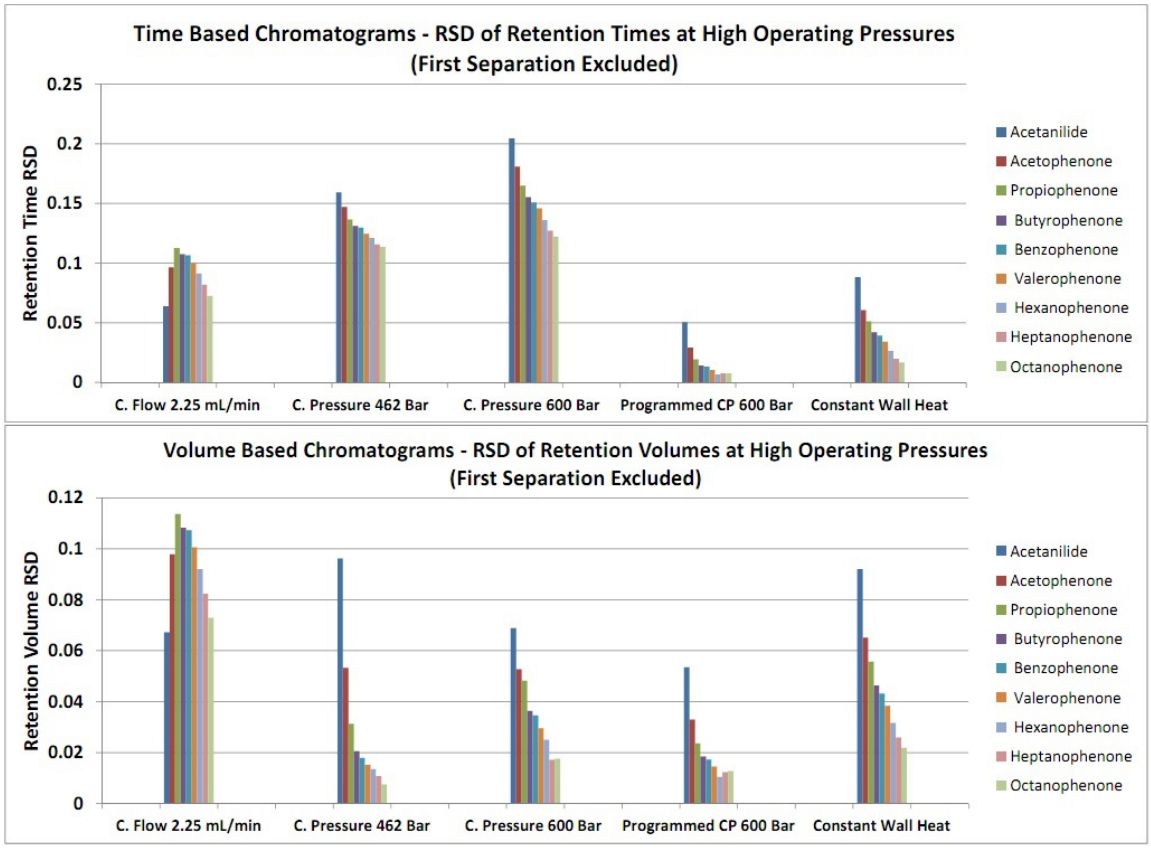

Figure 9.7. Relative Standard Deviations (1st Sepataion Exluded). Displays the RSDs (n=7) for all the compounds in the sample for time and volume based chromatograms. The first separation in the series is used to bring the column to a relatively stable temperature.

Volume-based chromatograms have little effect on the reproducibilities of peak widths and retention times provided by methods that use controlled flow rate. Volume-based chromatograms are useful only with constant pressure methods; they do not affect the peak capacities of the methods. The shift from time-based to volume-based chromatograms cannot account for retention changes that take place at high or low column temperature, but do correct for the variances in flow rates from constant pressure methods. Care should be taken to ensure that separations begin at the same initial temperature to achieve the most

reproducible separations possible. Programming a flow rate controlled constant pressure method provides retention times that are more reproducible than constant flow rate and constant pressure separations. However the precision of peak widths is two times lower that of pressure controlled methods. When a high degree of reproducibility is required constant pressure methods and programmed constant pressure methods appear to be useful in high throughput applications.

CHAPTER X
CONCLUSIONS AND RECOMMENDATIONS

The practical limits of linear chromatographic systems are quickly being reached. Decreasing separation time, while maintaining separation efficiency, is no longer a function of decreasing the particle size and packing shorter columns. In linear systems there are thermal effects which can affect the retention time and peak width of eluted compounds. If the operator does not take precautions to account for the change in column temperature caused by changing gradient conditions, the reproducibility of the data obtained will be in question.

The possibility of using a constant pressure approach to increases the throughput of liquid phase chromatography has been demonstrated. Such methods can also be used to eliminate the need for post-run times using reversed phase liquid chromatography and the techniques discussed in this manuscript.

There are many practical concerns with downscaling chromatographic systems. As the column size decreases, the systems volume becomes the largest contributing factor to band broadening. Part of this task falls on the manufacturer; the other part of this task must be performed by the analyst to ensure that proper connections and proper pluming is used with VHPLC instruments.

LIST OF REFERENCES

[1] F. F. Runge, Farenchemie III, Berlin, (1850) 15.
[2] B. Spangenberg, C. F. Poole, C. Weins, Quantitative Thin-Layer Chromatography : A Practical Survey; Springer (2010).
[3] C. H. Horvath, B. A. Preiss, S. R. Lipsky, Anal. Chem. 39 (1967) 1422.
[4] F. Gritti, G. Guiochon, J. Chromatography A, 1228 (2011) 2.
[5] G. Guiochon, J. Chromatogr. A, 1168 (2007) 101.
[6] F. Gritti, C. A. Sanchez, T. Farkas, G. Guiochon, J. Chromatogr. A, 1217 (2010) 3000.
[7] J. J. Stankovich, F. Gritti, L. A. Beaver, P. G. Stevenson, G. Guiochon, J. Chromatogr. A, 1318 (2013) 122.
[8] P. G. Stevenson, F. Gritti, G. Guiochon, J. Chromatogr. A, 1218 (2011) 8255.
[9] S. N. Chesler, S. P. Cram, Anal. Chem., 43 (1971) 1922.
[10] D. J. Anderson, R. R. Walters, J. Chromatogr. Sci. 8 (1984) 353.
[11] K. Miyabe, G. Guiochon, J. Sep. Sci. 26 (2003) 155.
[12] M. Squillacote, J. Chen, A. Seibert, Chromatographia 69 (2009) 771.
[13] R. W. Dwyer, H. A. Hartung, J. Chromatogr. 72 (1972) 384.
[14]] D. Ishii, K. Asai, K. Hibi, T. Jonokuchi, M. Nagaya, J.; Chromatogr. 144 (1977) 157.
[15] G. Gritti, G. Guiochon, J. Chromatogr. 1218 (2011) 4452.
[16] P. Jandera, J. Churacek Gradient Elution in Column Liquid Chromatography—Theory and Practice, Elsevier, Amsterdam (1985).
[17] L. Snyder, J. Dolan High Performance Gradient Elution—The Practical Application of the Linear-Solvent-Strength Model Wiley, Hoboken (2007).
[18] U.D. Neue, J. Chromatogr. A, 1079 (2005) 153.
[19] U.D. Neue, J. Chromatogr. A, 1184 (2008) 107.
[20] F. Gritti, G. Guiochon J. Chromatogr. A, 1217 (2010) 1604.
[21] M. Verstraeten, K. Broeckhoven, M. Dittmann, K. Choikhet, K. Witt, G. Desmet J. Chromatogr. A, 1218 (2012) 65.
[22] M. Verstraeten, K. Broeckhoven, M. Dittmann, K. Choikhet, K. Witt, G. Desmet J. Chromatogr. A, 1218 (2011) 1170.

[23] K. Broeckhoven, M. Verstraeten, K. Choikhet, M. Dittmann, K. Witt, G. Desmet J. Chromatogr. A, 1218 (2011) 1153.
[24] F. Gritti, G. Guiochon J. Chromatogr. A, 1253 (2012) 71.
[25] F. Gritti, G. Guiochon, J. Chromatogr. A 1253 (2012) 31.
[26] S. Khirevich, A. Daneyko, A. Höltzel, A. Seidel-Morgenstern, U. Tallarek, J. Chromatogr. A, 1217 (2010) 4713.
[27] A. Daneyko, S. Khirevich, A. Höltzel, A. Seidel-Morgenstern, U. Tallarek J. Chromatogr. A, 1218 (2011) 8231.
[28] F. Gritti, G. Guiochon LC–GC N. Am., 30 (2012) 586.
[29] F. Gritti; G. Guiochon; AIChE J., 57 (2011) 333.
[30] L. Pismen Chem. Eng. Sci., 29 (1974) 1227.
[31] L. Pismen Chem. Eng. Sci., 29 (1974) 1227.
[32] F. Gritti; G. Guiochon; J. Chromatogr. A, 1131 (2006) 151.
[33] F. Gritti; G. Guiochon; J. Chromatogr. A, 1216 (2009) 1353.
[34] F. Gritti; G. Guiochon; J. Chromatogr. A, 1155 (2007) 85.
[35] F. Gritti, Y. Kazakevich, G. Guiochon J. Chromatogr. A, 1169 (2007) 111.
[36] F. Gritti, G. Guiochon J. Chromatogr. A, 1145 (2007) 67.
[37] F. Gritti, G. Guiochon J. Chromatogr. A, 1070 (2005) 1.
[38] F. Gritti; G. Guiochon; Anal. Chem. 80 (2008) 6488.
[39] M. Verstraeten, K. Broeckhoven, F. Lynen, K. Choikhet, M. Dittmann, K. Witt, P. Sandra, G. Desmet, J. Chromatogr. A, 1232 (2012) 65.
[40] F. Gritti, G. Guiochon, J. Chromatogr. A, 1289 (2013) 1.
[41] F. Gritti, G. Guiochon, J. Chromatogr. A, 1291 (2013) 104.
[42] G. Guiochon, D. G. Shirazi, A. Felinger, A. M. Katti, Fundamentals of Preparative and Non-Linear Chromatography, Academic Press, Boston, 2006.
[43] D. Cabooter, S. Heinisch, J. L. Rocca, D. Clicq, G. Desmet, J. Chromatogr. A, 1143 (2007) 121.
[44] D. Clicq, S. Heinisch, J. L. Rocca, D. Cabooter, P. Gzil, G. Desmet, J. Chromatogr. A, 1146 (2007) 193.
[45] A. P. Schellinger, D. R. Stoll, P.W. Carr, J. Chromatogr. A, 1192 (2008) 41.

[46] A. P. Schellinger, D. R. Stoll, P.W. Carr, J. Chromatogr. A, 1192 (2008) 54.
[47] J. J. Stankovich, F. Gritti, P. G. Stevenson, G. Guiochon, J. Sep Sci. 36 (2013) 2709.
[48] I. Halasz, Anal. Chem. 36 (1964) 1428.
[49] M. Dimbat, P.E. Porter, F.H. Stross, Anal. Chem. 28 (1956) 290.
[50] G. Guiochon, J. Chromatogr. 14 (1964) 378.
[51] G. Guiochon, C. Guillemin, Modeling for Preparative Chromatography, Elsevier, Amsterdam, 2003.
[52] F. Gritti, G. Guiochon, Chem. Eng. Sci. 65 (2010) 6310.
[53] F. Gritti, G. Guiochon, J. Chromatogr. A 1217 (2010) 5069.
[54] F. Gritti, G. Guiochon, J. Chromatogr. A 1221 (2012) 2.
[55] F. Gritti, G. Guiochon, Anal. Chem., 80 (2008) 5009.
[56] J. J. Kirkland, S. A. Schuster, W. L. Johnson, B. E. Boyes, J. Pharm. Anal., 3 (2013) 303.
[57] R. W. Dwyer, H. A. Hartung, J. Chromatogr., 72 (1972) 384.
[58] D. Ishii, K. Asai, K. Hibi, T. Jonokuchi, M. Nagaya, J. Chromatogr., 144 (1977) 157.
[59] H. Gao, X. Wu, L. Bingchang, J. Chromatogr. Sci., 48 (2010) 742.
[60] J. Boonen, M. D'hondt, L. Veryser, K. Peremans, C. Burvenich, B. De Spinegeleer, J. Pharm. Anal., 5 (2013) 330.
[61] F. Gritti, J. J. Stankovich, G. Guiochon, J. Chromatogr. A, 1263 (2012) 51.
[62] P. Sun, X. Wang, L. Alquier, C. A. Maryanoff, J. Chromatogr. A, 1177 (2008) 87.
[63] T. L. Ramus, S. J. Hein, L. C. Thomas, J. Chromatogr., 314 (1984) 243.
[64] L. Gonzales-Bravo, D. Marrero-Delange, J. L. Gonzales-Guevara, J. Chromatogr. A, 888 (2000) 159.
[65] J. Bongers, T. K. Chen, J. Liq. Chromatogr. Rel. Technol., 23 (2000) 925.
[66] J. P. Mercier, C. Elfakir, M. Dreux, S. Lazar, M. E. Haddad, M. Akssira, J. Liq. Chromatogr. Rel. Technol., 23 (2000) 2345.
[67] H. S. Park, C. K. Rhee J. Chromatogr. A, 1046 (2004) 289.

[68] R. Schultz, H. Engelhardt, Chromatographia, 29 (1990) 517.
[69] T. H. Mourey, L. E. Oppenheimer, Anal. Chem., 56 (1984) 2427.
[70] A. K. Bhattacharya, N. R. Dhar, J. Phys. Chem., 35 (1930) 653.
[71] M. Kele, G. Guiochon, J. Chromatogr. A, 830 (1999) 41.
[72] L. Novakova, J. L. Veuthey, D. Guillarme, J. Chromatogr. A 1218 (2011) 7971.
[73] M. M. Fallas, M. R. Hadley, D. V. McCalley, J. Chromatogr. A 1216 (2009) 3961.
[74] A. de Villiers, H. Lauer, R. Roman, S. Goodall, P. Sandra, J. Chromatogr. A 1113 (2006) 84.
[75] L. A. Colon, J. M. Cintron, J. A. Anspach, A. M. Fermier, K. A. Swinney, Analyst 129 (2004) 503.
[76] I. Halasz, R. Endele, J. Asshauer, J. Chromatogr. A 112 (1975) 37.
[77] H. Lin, S. Horvath, Chem. Eng. Sci. 36 (1981) 47.
[78] J. J. Stankovich, F. Gritti, L. A. Beaver, P. G. Stevenson, G. Guiochon, J. Chromatogr. A, 1324 (2014) 155.
[79] M. Verstraeten, K. Broeckhoven, F. Lynen, K. Choikhet, M. Dittmann, K. Witt, P. Sandra, G. Desmet, J. Chromatogr. A. 1232 (2012) 65.
[80] F. Gritti, G. Guiochon, J. Chromatogr. A 1253 (2012) 71.
[81] J. J. Stankovich, F. Gritti, L. A. Beaver, P. G. Stevenson, G. Guiochon, J. Chromatog. A 1325 (2013) 99.
[82] J. J. Stankovich, F. Gritti, L. A. Beaver, P. G. Stevenson, G. Guiochon, J. Chromatogr. A 1324 (2013) 155.
83] M. Kele, U. Neue, J. Chromatogr. A 1149 (2007) 236.
[84] F. Gritti, G. Guiochon, Anal. Chem. 81 (2009) 2723.
[85] F. Gritti, G. Guiochon, Chem. Eng. Sci. 65 (2010) 6310.
[86] F. Gritti, G. Guiochon, J. Chromatogr. A 1187 (2008) 165.

VITA

Joseph J. Stankovich was born in Northwest Indiana. He was raised by his father, mother, grandmother, great-grandmother, and grandfather. He received a Catholic Education from kindergarten to the 8th grade. He attended High School in Highland Indiana. His undergraduate degree was achieved at Purdue University Calumet in Northwest Indiana. He attended the University of Tennessee in Knoxville where he wrote this dissertation and graduated under the mentoring of Dr. Georges Guiochon.